INFORMATION TO USERS

This manuscript has been reproduced from the microfilm master. UMI films the text directly from the original or copy submitted. Thus, some thesis and dissertation copies are in typewriter face, while others may be from any type of computer printer.

The quality of this reproduction is dependent upon the quality of the copy submitted. Broken or indistinct print, colored or poor quality illustrations and photographs, print bleedthrough, substandard margins, and improper alignment can adversely affect reproduction.

In the unlikely event that the author did not send UMI a complete manuscript and there are missing pages, these will be noted. Also, if unauthorized copyright material had to be removed, a note will indicate the deletion.

Oversize materials (e.g., maps, drawings, charts) are reproduced by sectioning the original, beginning at the upper left-hand corner and continuing from left to right in equal sections with small overlaps.

Photographs included in the original manuscript have been reproduced xerographically in this copy. Higher quality 6" x 9" black and white photographic prints are available for any photographs or illustrations appearing in this copy for an additional charge. Contact UMI directly to order.

Bell & Howell Information and Learning
300 North Zeeb Road, Ann Arbor, MI 48106-1346 USA

UMI®
800-521-0600

Downloaded from SHAREOK. Persistent Handle URL: https://hdl.handle.net/11244/5887

NOTE TO USERS

This reproduction is the best copy available.

UMI

UNIVERSITY OF OKLAHOMA

GRADUATE COLLEGE

Ferric Enterobactin Transport Through FepA in *Escherichia coli:* From Hydrophobic Stacking to Charge Interactions

A Dissertation

SUBMITTED TO THE GRADUATE FACULTY

in partial fulfillment of the requirements for the

degree of

Doctor of Philosophy

By

Zhenghua Cao
Norman, Oklahoma
1999

UMI Number: 9949713

UMI®

UMI Microform 9949713
Copyright 2000 by Bell & Howell Information and Learning Company.
All rights reserved. This microform edition is protected against
unauthorized copying under Title 17, United States Code.

Bell & Howell Information and Learning Company
300 North Zeeb Road
P.O. Box 1346
Ann Arbor, MI 48106-1346

© Copyright by Zhenghua Cao 1999
All Rights Reserved.

Ferric Enterobactin Transport Through FepA in *Escherichia coli:* From Hydrophobic Stacking to Charge Interactions

A Dissertation APPROVED FOR THE
DEPARTMENT OF CHEMISTRY AND BIOCHEMISTRY

BY

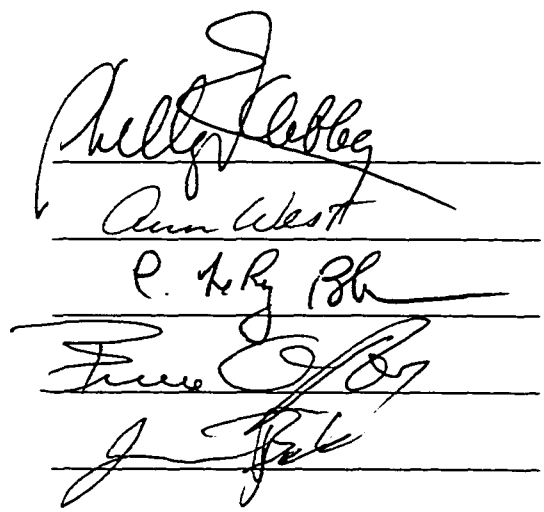

This dissertation is dedicated to

Lulin, my wife, Grace, my daughter, and Sean, my son.

Acknowledgements

I would like to thank my research advisor, Dr. Phillip Klebba, for all his guidance and training for the last five and half years. His pursuit of research excellence has always been an inspiration for me to continue my research when facing hard times.

I would also like to thank the members of my research advisory committee, Drs. Jimmy D. Ballard, C. LeRoy Blank, Paul F. Cook, Daniel L. Riggs, Bruce A. Roe, and Ann H. West, for their advice and time.

Many thanks to Drs. Sally Newton and Marvin Payne for their unselfish and unfailing help. I am very grateful to them for training me in the use of various techniques. Thanks to Marjorie Montague for her wonderful technical support.

Special thanks to Cathy Sprencel for spending many long hours to assist me in analyzing the mutants. Without Cathy, the data collection would be miserable, and this research would be almost impossible.

I am deeply grateful to many members of our research group. Some of them are Matt Bauler, John Igo, Dr. Xunqing Jiang, Zengbiao Qi, Danny Scott, and Paul Warfel. Many thanks for their input and for the conversations we had throughout the long journey.

This research would be impossible if not for the generous financial support from the Department of Chemistry and Biochemistry and Dr. P. E. Klebba.

Finally, and most importantly, I would like to thank my dad and my mom for their encouragement and unfailing love.

Table of Contents

List of Tables.....ix
List of Illustrations.....x
Abstract.....xii

I. INTRODUCTION 1

Ferric Enterobactin Transport System 6

Positively Charged Residues in FepA and Their Functions 16

Aromatic Features of FepA and Their Functions 17
Structural functions of aromatic residues 17
Ligand interaction involvement of the aromatic residues 19
Aromatic-aromatic interactions 19
Cation-π interactions 20

What Are the Important Aromatic Residues Involved? 22
Site directed mutagenesis 22
Methods for mutant analysis 23

What Are the Components of the Biphasic Binding between FeEnt and FepA? 26
Fluorescence 28
CPM and binding site 30
IAF and binding interaction 32
IAEDANS and environmental change..... 34

II. EXPERIMENTAL PROCEDURES

Materials, Strains and Plasmids 36
Strains and plasmids 36
Media 37
Ferric enterobactin 38
Colicins B, D and colicin B-Sepharose resin 39

Site-Directed Mutagenesis 39
Sequence comparisons 39
Site-directed mutagenesis 40
Preparation of uracylated template for mutagenesis 40

Phosphorylation of mutagenesis primers 41
In vitro mutagenesis reaction 41
Mutant selection 42
Transformation of the mutant DNA into the expression vector .. 43

FepA Mutant Phenotypic Analysis 44
FepA mutant expression 44
Colicin killing 45
Siderophore nutrition assay 45
Siderophore binding affinities and their screening 46
Siderophore uptake capabilities and their screening 47
Data analysis 48

Polyclonal Antibodies Against Fluorescent Probes 49
Preparation of fluorescent probes 49
Preparation of antigens for immunization 50
Generation of polyclonal antibodies 50
Polyclonal antibody analysis 51

Preparation of Fluorescent FepA Mutant Proteins 51
Purification of FepA wild type and mutant proteins 51
Protein concentration determinations 52
Labeling FepA proteins with IAEDANS and 5-IAF 52
Fluorescent labeling specificity 53

Fluorescent Measurements 53
CPM time-course labeling of purified proteins 53
Emission scan and labeling specificity 54
Fluorescent quenching by ferric enterobactin and determination of K_d 55
Epitope proximity 55
Antibody competition 56
FeEnt binding time-course 56

III. RESULTS

The Aromatic Component 58
Experimental strategies 58
Candidates of the aromatic component 59
Site-directed mutagenesis 61
Optimization of siderophore binding and transport assays 63
Aromatic residues important in siderophore binding 63

Effect of aromatic residue replacement on siderophore binding 67
Effect of aromatic residue replacement on siderophore transport 71
Effect of aromatic residue replacement on colicin sensitivities 77

The Aromatic and Positively Charged Components 79
Experimental strategies 79
Candidates of the positively charged component.....79
Site-directed mutagenesis.....80
The alteration of siderophore binding due to aromatic/charge replacement 80
Effect of aromatic/charge replacement on siderophore uptake 85
Effect of aromatic/charge replacement on colicin sensitivities 88

The Structural Information Conveyed in the Disulfide Bond 89
Experimental strategies 89
Site-directed mutagenesis 90
Effect of disulfide bond removal on siderophore binding 90
Effect of disulfide bond removal on siderophore transport 90
Effect of disulfide bond removal on colicin sensitivities 91

Biphasic Binding Between FepA and Ferric Enterobactin 94
Experimental strategies.....94
What does the crystal structure tell us?.....95
What do the previous data tell us?.....95
Why was E280C introduced?.....97
Generation of polyclonal antibodies 98
E280C can be specifically labeled by fluorescent probes.....102
Ferric enterobactin binding changes the environmental accessibility of E280C site 106
E280C can be quenched dynamically and statically.....106
Antibodies can block the binding of ferric enterobactin to E280C.... 109
Antibodies can compete off the ferric enterobactin bound.....113
Biphasic binding between FepA and ferric enterobactin..... 115

IV. DISCUSSIONS 118

REFERENCES 131

List of Tables

Table 2-1. Bacterial strains, plasmid and phage 37
Table 2-2. Media and references 38
Table 2-3. Primers for site-directed mutagenesis in the structural gene of FepA..... 42

Table 3-1. Phenotypic properties of FepA aromatic substitution mutants 70
Table 3-2. Phenotypic properties of FepA aromatic/charge substitution mutants.....84
Table 3-3. Phenotypic properties of FepA cysteine substitution mutants.....93

List of Illustrations

Figure 1-1. Structure of ferric enterobactin 9
Figure 1-2. CPM structure and its reaction mechanism 31
Figure 1-3. 5-IAF structure and its reaction mechanism 33
Figure 1-4. IAEDANS structure and its reaction mechanism 35

Figure 3-1. FepA secondary structure and the central region sequence alignment 60
Figure 3-2. Expression of FepA aromatic mutants.....62
Figure 3-3. Siderophore binding screening at wild type K_d FeEnt concentration.....65
Figure 3-4. Siderophore binding abilities of Y260A series compared with wt FepA at 20nM substrate concentration.....66
Figure 3-5. Concentration dependence of ferric enterobactin binding by single aromatic replacement mutants.....68
Figure 3-6. Concentration dependence of ferric enterobactin binding by double aromatic substitution mutants.....69
Figure 3-7. Siderophore uptake screening at wild type K_d FeEnt concentration.....73
Figure 3-8. Siderophore uptake screening for Y260A mutant series.....74
Figure 3-9. Siderophore uptake screening for F329A series.....75
Figure 3-10. Concentration dependence of ferric enterobactin uptake by single aromatic replacement mutants.....76
Figure 3-11. Concentration dependence of ferric enterobactin uptake by double aromatic substitution mutants.....78
Figure 3-12. Expression of FepA aromatic/charge mutants.....81
Figure 3-13. Concentration dependence of ferric enterobactin binding by aromatic/charge substitution mutants.....83
Figure 3-14. Concentration dependence of ferric enterobactin uptake by aromatic/charge substitution mutants.....86
Figure 3-15. Concentration dependence of ferric enterobactin uptake by aromatic and aromatic/charge substitution mutants 87
Figure 3-16. Expression of FepA cysteine mutants.....92
Figure 3-17. The crystal structure of FepA showing the locations of Y260, Y272 and R316.....96
Figure 3-18. Sephadex G-50 column separation of free fluorescent probes from the BSA conjugation.....99
Figure 3-19. Western blot analysis for polyclonal antisera against fluorescent probes.....100
Figure 3-20. ELISA analysis for polyclonal antiserum against BSA-CPM.....101
Figure 3-21. Labeling specificity of CPM to the E280C cysteine under denatured conditions.....103
Figure 3-22. Labeling specificity of 5-IAF to thiol group in E280C FepA..... 104
Figure 3-23. Labeling specificity of IAEDANS to thiol group in E280C FepA..... 105

Figure 3-24. The inhibition of E280C FepA labeling by CPM upon ferric enterobactin treatment..... 107
Figure 3-25. E280C-IAF was quenched by NaI..... 108
Figure 3-26. Titration of E280C-IAF with ferric enterobactin.....110
Figure 3-27. Effect of monoclonal antibodies against FepA on ferric enterobactin binding.....112
Figure 3-28. Competition of monoclonal antibodies against ferric enterobactin..... 114
Figure 3-29. Time course of ferric enterobactin binding to mutant FepA..... 117

Figure 4-1. The location of E280 residue in the crystal structure.....128

Abstract

In gram-negative bacteria, the uptake of ferric enterobactin is achieved by a ferric siderophore transport system. Enterobactin, one of the native siderophores synthesized in *Escherichia coli*, functions as an iron carrier, by forming ferric enterobactin, to supply iron through the ferric enterobactin transport system. FepA is the outer membrane receptor protein for ferric enterobactin. The chemical features of ferric enterobactin indicate that the aromatic and positively charged residues in its receptor might be important in ferric enterobactin absorption.

The site-directed alanine substitution studies revealed that three aromatic residues in the central region of FepA, Y260, Y272, and F329, are involved in the binding and transport of ferric enterobactin. A significant decrease was observed for Y260A, while only slight or no changes were found in Y272A and F329A. In any of the double mutant combinations, however, dramatic decreases were detected.

To demonstrate that the decreased functionality in the double combinations did not result from the conformational change due to the removal of aromatic stacking interactions, the single aromatic substitution mutants were combined with R316A, a positively charged mutant found to be essential in previous studies. The double mutations thus proved that any combination of two independent essential residues resulted in a dramatic decrease in receptor functionality. Furthermore, the binding and transport analysis revealed that Y260 and Y272 are important in ligand binding, while R316 and F329 contribute to both ferric enterobactin binding and transport.

The crystal structure of FepA showed that Y272 and F329 were located at the surface of FepA, while Y260 and R316 were found at the hinge of the surface loops and the β-barrel domain. Fluorescent studies indicated that Y272 and F329 are involved in the initial binding, on the other hand, Y260 and R316 are responsible for the subsequent absorption.

CHAPTER I

INTRODUCTION

In gram-negative bacteria, the outer membrane functions as a barrier to toxic molecules, such as detergents, bacterial toxins, and harmful chemicals, entering the cell from the environment. Such a barrier, meanwhile, presents a problem for the bacteria to efficiently absorb nutrients from the environment and to excrete the waste from inside the cells. To solve this dilemma, the bacteria utilize very sophisticated systems in which outer membrane proteins play an important role.

Since the first structural model for a bacteriorhodopsin integral membrane protein appeared in 1975 (Henderson and Unwin, 1975), researchers have had a much better understanding of how the cell membrane functions as a toxin barrier while remaining nutrient permeable. The understanding of outer membrane transport systems has provided potential targets for humans in the fight against various

bacterial infections.

Current research indicates that outer membrane and inner membrane proteins have very different structural features. All the inner membrane proteins studied so far carry alpha-helical structures, with the bacterial photosynthetic reaction center as the prototype (Deisenhofer *et al.*, 1985), while all the outer membrane proteins have a beta-barrel architecture, with outer membrane porins as the prototype (Cowan *et al.*, 1992). The up-to-date results demonstrated that the outer membrane protein functions are determined by the structure of each specific protein. Crystal structure studies showed that the outer membrane proteins can be categorized into four groups, and each group of outer membrane proteins have the same number of beta-sheets.

8-stranded non-porin outer membrane proteins. Outer membrane protein A (OmpA), an outer membrane monomer (Sugawara and Nikaido, 1992), has an 8-stranded β-transmembrane domain while the remaining residues are supposed to interact with periplasmic peptidoglycan. Even though previous studies indicated that OmpA had some porin-like features (Sugawara and Nikaido, 1992; Saint *et al.*, 1993; Sugawara and Nikaido, 1994), the recently solved crystal structure of the transmembrane domain suggested that OmpA does not function as a porin, which lies in the fact that even molecules as small as water cannot pass the barrel (Pautsch and Schulz, 1998). Instead, the barrel acts as an outer membrane anchor to the carboxyl terminal exposing to the periplasmic space and the scaffold for the extracellular loops of the protein (Pautsch and Schulz, 1998; Gouaux, 1998). Although such an

amphiphilic transmembrane anchor is energetically costly compared with the non-polar α-helical transmembrane anchor widely found in the inner membranes, the outer membrane protein needs to remain as a barrel for its proper function.

16-stranded general porins. Striking structural and functional similarities between *Rhodobacter capsulatus* porin (Weiss *et al.*, 1991a; Weiss *et al.*, 1991b; Weiss and Schulz, 1992) and *E. coli* OmpF and PhoE porins (Cowan *et al.*, 1992) remain. They mainly function as general diffusion channels with the same linear diffusion rate at various substrate concentrations (Nikaido, 1992) although PhoE is more specific to anionic substrates while OmpF is more cation selective (Cowan *et al.*, 1992; Cowan, 1993). So far all general porins with the structure determined are trimers.

18-stranded specific channels. LamB, a trimeric beta-barrel, is a typical 18-stranded outer membrane protein (Schirmer and Cowan, 1993), with specific activities for lamda phage (Randall and Schwartz, 1973) and maltodextrin (Szmelcman and Hofnung, 1975). Specific channels, usually, retain general diffusion characteristics (Schulein *et al.*, 1991).

The specific channels are different from general diffusion porins in many ways. Structurally, the pore is restricted by an inwardly folded loop about half way through the channel as in the case of LamB (Schirmer *et al.*, 1995). Genetically, the expression of the maltose transport system is controlled by several regulatory circuits, stimulated and repressed under different mechanisms (Boos and Shuman, 1998).

The LamB transport system has been widely studied because of the importance of the understanding of the special regulation mechanisms (Boos and Shuman, 1998). Crystal structures have been solved for both LamB (Schirmer *et al.*, 1995) and its periplasmic binding protein MalE, or MBP (Shilton *et al.*, 1996). Structures of LamB complexed with disaccharides sucrose, trehalose and melibiose (Wang *et al.*, 1997; Dutzler *et al.*, 1996) are also available for exploring the binding and transport mechanisms. This system has been the prototype of research on many other outer membrane proteins due to the existence of a large amount of data.

22-stranded energy dependent ligand-gated active transporters. This structure of β-barrels is found in FepA (Buchanan *et al.*, 1999) and FhuA (Ferguson *et al.*, 1998; Locher *et al.*, 1998), the two TonB-dependent energy-dependent ferric siderophore active transporters (Rutz *et al.*, 1992). Although previous models predicted that FepA (Murphy *et al.*, 1990) and FhuA (Koebnik and Braun, 1993) had 29 and 32 anti-parallel β-transmembrane sheets, respectively, the recently solved crystal structures (Buchanan *et al.*, 1999; Ferguson *et al.*, 1998; Locher *et al.*, 1998) indicated that both of them are 22-stranded, with the N-terminal regions functioning as plugs or corks. Similar structures and absorption mechanisms were observed in the studies of these two siderophore receptors (Buchanan *et al.*, 1999; Ferguson *et al.*, 1998; Locher *et al.*, 1998).

The data on the solved crystal structures reveal that: (1) the important structural features are retained in all the outer membrane proteins, no matter how different their

functions are. These important features include the anti-parallel beta-sheet structure, amino acid compositions of the beta-transmembrane strands, charge distributions, large surface loops, and small periplasmic turns; (2) all the outer membrane proteins with the same pore function have the same structural features also, such as the cell surface loop structure and the N-terminal plug structure; (3) with the increase of the number of the anti-parallel beta-strands, the function of the outer membrane changes accordingly, from the 16-stranded general diffusion porins, to the 18-stranded specific channels and the 22-stranded TonB-dependent transporters; (4) the energy requirement is different. Active transporters with 22 β-strands require not only proton gradient as the energy source but also TonB as the possible energy transducer; (5) the affinities of the specific channels and the active transporters are quite different. The receptor in the active transport system binds the ligand much more strongly than that in the specific channel system, which is consistent with the function of the active transporter to avidly absorb very low concentrations of substrate in the environment and transport against a reverse substrate gradient.

One of the 22-stranded outer membrane proteins, as shown above, is FepA (Buchanan *et al.*, 1999), the cell-surface receptor for ferric enterobactin made in *E. coli* bacteria. Iron transport systems have proven to be important. For example, (1) iron metabolism is essential in bacterial infection; and (2) current research advances have made it possible to use the iron transport system as antibiotic carriers to provide clinical applications. In this research, we studied ferric enterobactin binding and

transport mechanisms, especially, the aromatic component of FepA.

Ferric Enterobactin Transport System

Iron plays a very important role in prokaryotic and eukaryotic cell metabolisms. All the organisms studied so far, except *Lactobacillus spp.* (Archibald, 1983), need to have iron. Iron is involved in various essential processes inside cells (Earhart, 1996). For example, (1) heme-containing proteins participate in electron transport chain reactions (cytochromes); (2) iron-sulfur proteins play roles in the tricarboxylic acid (TCA) cycle (aconitase, succinate dehydrogenase); (3) non-heme, non-iron-sulfur proteins involve in the DNA synthesis (ribonucleotide reductase). Iron's importance in cell metabolism lies in the fact of the wide range of redox potentials of Fe^{3+}/Fe^{2+}, varying from +300 mV in a-type cytochromes to -490 mV in certain iron-sulfur proteins (Guerinot, 1994), which makes it a perfect element in various kinds of reduction-oxidation reactions.

The free iron concentration is too low in aquatic or terrestrial environments or in animal hosts to meet the growth requirement for bacteria. In mammalian hosts, iron exists as hemes, iron-sulfur proteins, and the iron storage compound ferritin intracellularly. Extracellularly, it is contained in iron-carrying glycoproteins such as transferrin in serum and lactoferrin in secretory fluids (Griffiths, 1991). Although free Fe^{2+} is soluble to as high as 100 mM at neutral pH (Neilands, 1991), it can easily be oxidized to Fe^{3+} under aerobic environment. The latter has extremely low solubility

(about 10^{-18} M) under physiological conditions (Raymond and Carrano, 1979). It is only under certain circumstances that iron can be obtained directly (Braun and Killmann, 1999): anaerobic bacteria can obtain enough Fe^{2+} due to the high concentration of ferrous iron available under anaerobic conditions; certain acid-tolerant bacteria might acquire sufficient ferric iron which has a relatively higher solubility at a lower pH (10^{-8} M for the ferric iron solubility at pH 3).

To overcome the iron limitations of the living environment, bacteria have developed different strategies to acquire iron to suffice their growth. One of the strategies is to generate certain iron chelators, called siderophores, to compete for iron from other iron complexes. Meanwhile, the bacteria have highly specific transport systems to absorb the ferric siderophore. Such a strategy is common not only in prokaryotic bacteria but also among eukaryotic fungi and monocotyledonous plants.

Enterobactin: the native siderophore produced in E. coli

Enterobactin (Neilands, 1973) is the native siderophore produced in wild type *E. coli* strains. It binds ferric iron (Figure 1-1) with an extremely high affinity (the formation constant of ferric enterobactin is 10^{52} M^{-1}; Avdeef *et al.*, 1978), which derives from both the characteristics of Fe^{3+} and the structural features of enterobactin. The important characteristics of ferric iron, such as the hardness, size, d^5 electron configuration, charge, and electronegativity, causes ferric iron to tend to form stable high-spin complexes with hard O donor containing siderophores. Also the

electrostatic interaction between the positive charge (+3) of ferric iron and the negative charge of O stabilizes the ferric enterobactin complex. The macrocyclic effect (Constable, 1999) of enterobactin further strengthens the binding affinity.

There are two possible enantiomers for enterobactin, a right-handed propeller configuration (Δ-configuration) and a left-handed configuration (Λ-configuration). The Δ-configuration is one that exists in nature. In 1970, enterobactin was purified from *E. coli* and *Aerobacter aerogenes* (O'Brien and Gibson, 1970) and from *Salmonella typhimurium* (Pollack and Neilands, 1970). Enterobactin was first synthesized in 1977 (Corey and Bhattacharyya, 1977), and enantioenterobactin in 1981 (Rastetter *et al.*, 1981).

The structure of ferric enterobactin determines its thermodynamic and kinetic chemistry. Ferric enterobactin is a six-coordinate, right handed octahedral complex with three identical catechol groups surrounding the central iron. Previous studies indicated that alteration of the aromatic catechols may dramatically impair the recognition of the ligand by its receptor (Thulasiraman *et al.*, 1998), and also, the positively charged residues of the receptor play an important role in the absorption of the ligand (*Newton et al.*, 1997), indicating the importance of the net negative charge of ferric enterobactin.

FepA: the receptor for ferric enterobactin

FepA, a 723 amino acid outer membrane protein, is the receptor for ferric

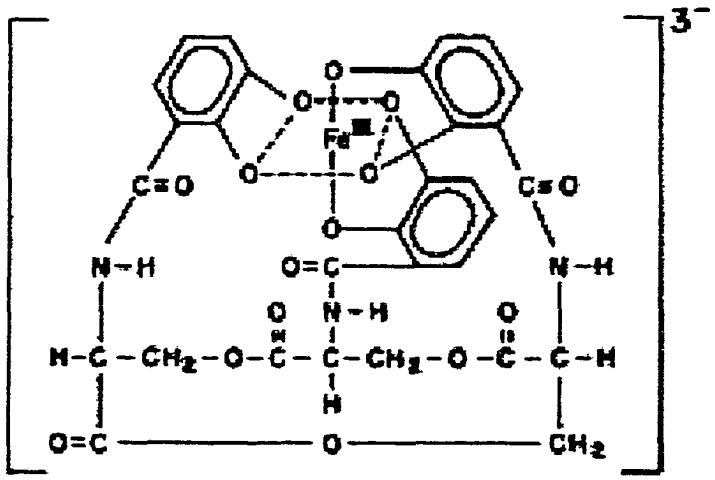

Figure 1-1. Structure of ferric enterobactin.

enterobactin (Pugsley and Reeves, 1977a). With a size of 719 Da, ferric enterobactin is too large to pass the general porins which allow the passive diffusion of substrates smaller than 600 Da. Therefore, gram-negative bacteria acquire iron via ferric enterobactin, using a ligand-gated TonB-dependent transport system (Rutz *et al.*, 1992, Jiang *et al.*, 1997). FepA binds ferric enterobactin avidly in a TonB-independent manner (Payne *et al.*, 1997), with an affinity of Kd < 0.2 nM (Newton *et al.*, 1999), at the same level as other TonB-dependent transport systems like BtuB (Bradbeer *et al.*, 1976). FepA loop deletion mutagenesis studies showed that the interaction between ferric enterobactin and its receptor is so avid that FepA can tolerate the removal of many of the individual cell-surface loops (Newton *et al.*, 1999).

FepA: the receptor for colicins B and D

The FepA transport system is multifunctional. While FepA is the receptor for ferric enterobactin, it also serves as the receptor for colicins B and D (Guterman, 1971; Guterman, 1973; Davies and Reeves, 1975; Wayne *et al.*, 1976; Pugsley and Reeves, 1976), two bacterial toxins made by plasmids carrying the respective structural genes. Colicins penetrate the outer membrane of the sensitive bacteria via their specific receptors and kill the target cells. Although they both kill bacteria which do not make the immunity protein, colicin B and colicin D act quite differently: while colicin B kills by forming a pore in the cytoplasmic membrane, colicin D

functions as a ribonuclease in the cytoplasm.

The process by which ferric enterobactin is transported through the ligand gated TonB-dependent channel is highly selective and directional. Such a system, instead of a general porin design, is necessary in the fact that a diffusion channel large enough to compromise the uptake of ferric enterobactin would pose a threat to the cells because of the capability of such a pore to allow the traverse of detergents, antibiotics, and other toxic molecules. Furthermore, the uptake would be thermodynamically and kinetically unfavorable if a general porin system is utilized for the fact that the substrate concentration in the environment is very low, and the uptake has to overcome the concentration gradient to aggregate inside the bacteria to support the growth.

The ferric enterobactin transport system is ligand gated in the sense that the ligand binding to the receptor causes a conformational change in the receptor (Rutz *et al.*, 1992; Jiang *et al.*, 1997; Buchanan *et al.*, 1999) and induces the subsequent uptake of the ligand (Jiang *et al.*, 1997). The same effect is observed and postulated for the system of FhuA (Killmann *et al.*, 1993; Killmann *et al,* 1996; Locher *et al.*, 1998; Ferguson, *et al.*, 1998). Phage T5 binds to FhuA and releases its DNA into the host bacteria in a TonB independent manner without energy requirement although little is known about the mechanism. Electrophysiological studies indicated that upon phage T5 binding, FhuA opens its channel, and the size of the channel is large enough

for the phage DNA to enter the channel (Bonhivers *et al.*, 1996), indicating that FhuA contains a closed channel which opens upon phage T5 binding, which then induces the release and entry of the phage DNA. In particular, the fact that the deletion of the proposed cell-surface loops turned FepA (Rutz *et al.*, 1992) and FhuA (Killmann *et al.*, 1993) into passive diffusion porins, allowing the non-specific uptake of the ligands, SDS, and antibiotics, demonstrated that the surface-loops of the ligand gated channels act as the sensors of the ligand availability for the transport system.

The crystal structures of FepA (Buchanan *et al.*, 1999) and FhuA (Ferguson *et al.*, 1998; Locher *et al.*, 1998) showed that both FepA and FhuA are monomers, which is different from the typical trimeric structure of all the other solved general porins and specific channels (Cowan, 1993). But several lines of evidence indicated that the purified proteins might have different structures from those in outer membranes: first, Locher and Rosenbusch (1997) indicated that oligomeric FhuA states exist, and the cross-linking reactions revealed the existence of possible dimeric and trimeric FhuA species; second, a recently published 2-dimentional 8-Å projected structure of FhuA from electron crystallography (Lambert *et al.*, 1999) showed that the molecules of FhuA crystallize within the membrane as dimers, and their X-ray electron density suggested that a lipopolysaccharide (LPS) molecule (Ferguson *et al.*, 1998; Lambert *et al.*, 1999) was located between two FhuA monomers (Lambert *et al.*, 1999). Since the crystal structures obtained from electron crystallography are closer to the actual structures in the membrane environment, the 2-dimentional

structure of FhuA presents a challenge to the present monomeric structure model. Furthermore, the non-denaturing SDS-PAGE revealed a high-molecular-weight oligomer band of the size of trimeric FepA (Liu *et al.*, 1993); the purified protein binds ferric enterobactin at a lower affinity (15nM; Payne *et al.*, 1997); the thermodynamic and kinetic studies on FepA-ligand interactions showed that the ligand colicin D might bind to a trimeric FepA while colicin B and FeEnt bind to monomers (Payne *et al.*, 1997); and a FeTRANCAM molecule, a synthetic analog of FeEnt, is possibly absorbed by a FepA trimer while a FeEnt molecule binds to a FepA monomer (Thulasiraman *et al.*, 1998). All these results dispute the idea that FepA or FhuA are monomers. Further reliable methods performed under a native membrane environment will be necessary either to exclude the possibility of a trimeric structure or to prove an oligomeric construction. One thing for certain is that if FepA or FhuA is a trimer, it is much less stable than the passive porin or specific channel trimers.

Another structural feature observed in ligand-gated TonB-dependent transporters is the N-terminal plug (Buchanan *et al.*, 1999; Ferguson *et al.*, 1998; Locher *et al.*, 1998), which was not found in any of the other solved general porin or specific channel structures (Cowan *et al.*, 1992; Wang *et al.*, 1997). The N-terminal residues of 1-153 of FepA (Buchanan *et al.*, 1999) or 1-160 of FhuA (Ferguson *et al.*, 1998; Locher *et al.*, 1998) fold into the interior of the beta-barrel domain to form the plug to sterically occlude most of the cross section of the barrel (Ferguson *et al.*, 1998). The plug separates the entire barrel into a two-pocket structure: the pocket

exposed to the extracellular space where the ligands first contact the long surface loops and the pocket facing the periplasmic space where only small β-sheet reverse turns reside.

The prevailing model for the ligand binding and transport mechanisms in the ligand-gated TonB-dependent systems is that upon ligand binding to the receptor, minor conformational changes occur within the surface-loops which in turn transform into much more significant conformational changes at the other side the membrane, and most importantly, the structural alteration results in the change of the noncovalent bonds of the plug domain, particularly, the unwinding of the helical structure in FhuA (Ferguson *et al.*, 1998). The change of the plug domain structure is proposed to be the switch of the energy transduction via TonB (Ferguson *et al.*, 1998; Locher *et al.*, 1998).

The role TonB plays in the ferric enterobactin transport system is still subject to debate (Klebba *et al.*, 1993; Klebba and Newton, 1998). The favored current model for the TonB function is that TonB couples the energy transduction between the outer membrane receptor and the cytoplasmic energy gradient by interacting directly with the TonB box of the receptor upon ligand induction at the surface loops of the receptor protein (Kadner, 1990; Hannavy and Haggins, 1991; Letain and Postle, 1997; Braun *et al.*, 1994). The existence and importance of the above direct interaction were initially derived from the finding that the mutations in TonB suppressed the deficiencies of ligand uptake via vitamin (Gudmundsdottir *et al.*, 1989) with

mutations in their respective TonB boxes (Heller *et al.*, 1988; Bell *et al.*, 1990). Most recently, Cadieux and Kadner (1999) reported that site-directed disulfide bondings were observed in the BtuB system when cysteines were introduced to both the TonB box and its proposed reaction site on TonB, which reveals an interaction site between the proposed energy coupling protein TonB and BtuB. FepA (Buchanan *et al.*, 1999) and FhuA (Ferguson *et al.*, 1998; Locher *et al.*, 1998) crystal structures indicated that the N-terminals of both FepA and FhuA do not form part of the transmembrane domain, but instead, function as a plug to control the influx of the ligand to the periplasmic side of the receptor (Buchanan *et al.*, 1999). Although the finding that the TonB box is part of the plug favors the possible direct interaction between the TonB box and TonB, recent discoveries on the plug-free FhuA mutant (Braun *et al.*, 1999) showed that FhuAΔ5-160 turned the receptor into a non-specific diffusion channel in a TonB-independent manner, but meanwhile, the beta-barrel domain of FhuA remained close to wild type TonB-dependent FhuA activities, i.e., turning the receptor into a non-specific diffusion channel does not change the role TonB plays in the transport system. Therefore, the interaction between TonB and TonB box, if it does exist, does not seem to be essential in the sequence of reactions for the ligand to pass the outer membrane.

This research was aimed at finding the important ligand binding/transport components of FepA. In particular, the focus was on the charge and aromatic features

of the ferric enterobactin ligand, from which the importance of the charged and aromatic residues was proposed. Although positively charged residues have been studied before, this research intended to investigate the ligand interaction from a different point of view.

Positively Charged Residues in FepA and Their Functions

As mentioned above, outer membrane β-barrels have some structural features in common, one of which is the appearance of charged residues at both sides of the transmembrane domain (Cowan *et al.*, 1992; Buchanan *et al.*, 1999; Locher *et al.*, 1998; Ferguson *et al.*, 1998). Although general porins are diffusion controlled, the charged residues have been shown to play an important role in the charge selectivity of general porins (Bauer *et al.*, 1989).

The net negative charge distribution of the FeEnt macrocyclic molecule had been the subject of previous research (Newton *et al.*, 1997) by studying the receptors with the positively charged residues removed. Newton *et al.* (1997) showed that among the five positively charged residues in the proposed central region of FepA, designated as PL5 previously (Murphy *et al.*, 1990), but L3, L4 and the transmembrane strands between these two loops in the crystal structure (Buchanan *et al.*, 1999), arginines 286 and 316 are critical for both siderophore and colicin recognition. Newton *et al.* concluded that charge-charge interactions are essential in ferric enterobactin absorption.

Aromatic Features of FepA and Their Functions

Another important feature of ferric enterobactin is the aromaticity of the three catechol rings. It has been confirmed that it is very important to keep the catechol structure intact to maintain the ligand uptake capability (Thulasiraman *et al.*, 1998). Therefore, the aromaticity of the ligands, and most likely, the interaction between the aromatic component of the ligand and the aromatic residues in FepA are critical.

The abundant existence of aromatic residues in membrane proteins is well-known. Surprisingly, the aromatic residues in receptor proteins are important in various systems, including both aromatic (Befort *et al.*, 1996) and non-aromatic (Charbit *et al.*, 1998) ligands. The interaction was observed in both helical structured membrane proteins (Kasahara and Kasahara, 1998) and beta-barrels (Charbit *et al.*, 1998).

Structural functions of the aromatic residues

One of the important structural features found in all the membrane protein crystal structures is that there are two rings of aromatic residues, one at each side of the membrane flanking membrane spanning segments (Cowan, 1993). The two rings of aromatic residues mark the boundaries of the extracellular and periplasmic domains of transmembrane proteins (Sakai and Tsukihara, 1998). This feature is found in bacterial reaction centers (Deisenhofer *et al.*, 1985), eukaryotic membrane proteins (Xia *et al.*, 1997), bacterial general porins (Cowan *et al.*, 1992), bacterial

specific transport channels (Schirmer *et al.*, 1995), and bacterial and fungal active iron transporters (Buchanan *et al.*, 1999; Ferguson *et al.*, 1998; Locher *et al.*, 1999). Therefore, this structural attribute dominates not only in β-barrels, no matter trimeric (Cowan *et al.*, 1992) or monomeric (Buchanan *et al.*, 1999), but also in transmembrane α-helical structures (Doyle *et al.*, 1998). The abundant existence of aromatic residues is mostly found at the central + 10-15 Å regions (Sakai and Tsukihara, 1998).

Several structural functions have been proposed for these two aromatic rings: First, they are supposed to position the membrane proteins with regard to the membrane bilayer (Schiffer *et al.*, 1992). This function is probably more important in locking the cell surface loops for the two iron transporters because they feature short periplasmic turns and long surface-located loops (Buchanan *et al.*, 1999; Locher *et al.*, 1998).

Second, they are proposed to seal the membrane leakage by providing a strong interaction between the aromatic residues and the hydrophobic components of the membrane, such as lipid fatty acids (Cowan *et al.*, 1992). With the existence of the aromatic girdle and the strong hydrophobic van der Waals interaction, the two rings of aromatic residues are apparently favored in this region.

Third, they are suggested to prevent any conformational damage of membrane proteins due to mechanical movements in the membrane (Schulz, 1994). Whenever a damaging movement occurs, the C_α-C_β rotation shields the respective surfaces by

counterparting the tension caused by the damaging movement.

The interaction between macromolecules is a delicate balance of various interactions. Therefore, any proposed functions are just a subtle part of their overall interactions. From the structure alone, it is hard to decide the exact roles of the aromatic girdle, not to mention the structural function of each aromatic residue. It would also not be a good subject for mutagenesis study due to the existence of a large amount of aromatic residues in the girdles. Structural functions probably will not be changed even when the important residues are removed because a subtle difference in the structure or function cannot be revealed by the assays available.

Ligand interaction involvement of the aromatic residues

A ligand interacts with its receptor through various delicate interactions, including H-bonds, hydrophobic effects, and salt bridges. For the interaction between a substrate and its macromolecular protein receptor, the structural features of the ligand play a fundamental role in the recognition of the ligand by the receptor. Here, we are interested in the interaction with aromatic components of FepA.

Aromatic-aromatic interactions

The aromatic-aromatic ring interaction is one of the most common interactions between macromolecules due to the fact that the aromaticity is one of the most common features of the macromolecules. In double stranded DNA, the aromatic rings

were found to stack against each other (Dickerson *et al.*, 1982), and therefore, the aromatic ring interaction is best known as the aromatic ring stacking interaction or π-stacking interaction. In most cases, however, it is not as straight forward as in the case of DNA. Based on the significant amount of studies on protein interactions, two kinds of structures between aromatic ring interactions were classified (McGaughey *et al.*, 1998): the off-centered parallel displaced structure (or offset-stacked arrangement, Samanta *et al.*, 1999) and the T-shape structure (or edge-to-face motif, Samanta *et al.*, 1999). Researchers have tried to find out which of the above structures is predominant in the aromatic-aromatic ring interactions (McGaughey *et al.*, 1998; Samanta *et al.*, 1999 and the references therein), and very different results were reported from different labs. Recently, Samanta *et al.* (1999) reported that by studying the packing of aromatic rings (phenylalanine, tyrosine, tryptophan, and histidine) against tryptophan residues in proteins, the parallel stacking was only found to be dominant in Trp-His pairs.

Cation-π interactions

One of the interactions that might not have caught much attention in the aromatic interactions is the cation-π interaction. Cell surface exposed H-bonds and ion-pair formation do not contribute significantly to the protein stability (Dougherty, 1996). This is due to the fact that to form the non-covalent bonds in biological aqueous media, the two parties of a non-covalent bond have to overcome the

solvation energies of each species. The non-covalent bond formation, such as the hydrogen bond and ion pair, will not be sufficient to compensate the solvation energy loss, which then results in the "desolvation energy penalty" (Sun *et al.*, 1991). Therefore, in protein structures, the above non-covalent bonds are usually accompanied by other folding pattern changes to pay for the energy penalty (Dougherty, 1996).

In small ligand interactions, however, such a "desolvation penalty" of small ligands cannot be overcome, which then results in the importance of another group of interactions, the cation-π interaction (Dougherty, 1996; Gallivan and Dougherty, 1999; Scrutton and Raine, 1996). A unique feature about this interaction is the combination of a hydrophobic aromatic ring and a hydrophilic ion which are usually considered exclusive of each other. Such a unique feature is also revealed in the structure of aromatic rings: while aromatic residues are highly nonpolar due to their bulk hydrophobic rings, they are also considered to be highly polar - quadrupolar, however, not dipolar (Dougherty, 1996). Therefore, such cation-π interactions can be of special importance in some favorable biological systems.

A study of the structures in the Protein Data Bank revealed that the cation-π interaction is common among protein interactions (Gallivan and Dougherty, 1999). A positive charge interacts with the π face of an aromatic system, and the eletrostatic interactions between the positive charge and the quadruple charge distribution of the aromatic are of prime importance (Dougherty, 1996). Among the positively charged

residues, lysine and arginine can be the two residues which participate as cations, where arginine is more likely to be involved than lysine. The aromatic side chains of phenylalanine, tyrosine, or tryptophan participate in the cation-π interaction.

Although the above research was performed in protein systems, it is reasonable to extend the above results to the ligand-receptor interaction where "desolvation penalty" is stronger than in protein-protein interactions. The roles played by the ligand and its receptor are determined by the structural features of each molecule. In the ferric enterobactin system, the ligand is an anion. Therefore, the only possible cation-π interaction is between the positively charged residues within FepA and the aromatic rings in ferric enterobactin.

What Are the Important Aromatic Residues Involved?

Protein crystallization studies provided a very important tool to study the ligand-receptor interaction. But due to the existence of the large amount of aromatic residues in membrane proteins and the difficulties to have stable ligand-receptor crystals, it is usually not easy to determine the essential aromatic residues in the ligand-receptor interaction. Therefore, site-directed mutagenesis has been widely used in various systems for ligand-receptor interaction studies.

Site directed mutagenesis

Site-directed mutagenesis studies have been commonly used in molecular

biology systems. Among the significant amount of research performed, cysteine scanning, alanine scanning, and deletion mutagenesis were of special interest in various applications. The deletion mutagenesis was used to locate ligand binding domains and transport components in the FepA system (Rutz *et al.*, 1992; Newton *et al.*, 1999) and the FhuA system (Killman and Braun, 1993). Cysteine scanning (Frillingos *et al.*, 1998) was successfully used to study the secondary structures of membrane proteins by introducing cysteines at various sites of membrane proteins and characterizing the ESR (Klug *et al.*, 1997; Oh *et al.*, 1999; Altenbach *et al.*, 1999; Steinhoff *et al.*, 1994) or fluorescent (Wu *et al.*, 1995) probes attached to the cysteine site. It was also used to study the interaction between different proteins by investigating their cysteine cross-linking patterns (Wu *et al.*, 1999; Cadieux and Kadner, 1999). Alanine scanning, on the other hand, found its general applications in locating the important residues in various systems (Newton *et al.*, 1997), due to the fact that alanine could be an amino acid in any of the secondary structures. Therefore, the introduction of alanine usually would not change the global structure of proteins.

Methods for mutant analysis

Several traditional methods have been developed to examine substrate uptake and ligand binding in specific channel and active transporter systems. Some of the methods are: (1) the binding and uptake of radioactively labeled ligands, such as ^{59}ferric enterobactin in siderophore uptake systems (Rutz *et al.*, 1992; Newton *et al.*,

1997) and ^{125}I ColB/D used for colicin binding to FepA (Payne *et al.*, 1997); (2) the growth of host bacteria upon utilizing the substrate, for instance, the nutrition assay for the ferric enterobactin transport system (Liu *et al.*, 1993); (3) the susceptibility of host bacteria to bacteriotoxins (Newton *et al.*, 1997).

Among these methods, binding and transport assays using radioactively labeled substrates is the most sensitive and accurate method which yields quantitative thermodynamic and kinetic parameters. This method, however, determines the uptake rate of the rate-limiting step of the complicated multicomponent system. Therefore, only when the uptake of the substrate via the membrane receptor step is rate-limiting can this method be accurately used. Also, this method is quite time consuming and laborious. In this research, modifications to previous assays were used to screen a large amount of mutant receptors to examine their activities compared to the wild type receptor instead of determining all mutant thermodynamic and kinetic parameters. Such an assay strategy minimizes the time required for the assays without sacrificing the use of a quantitative method.

The other analysis methods mentioned above can be used to see if certain substrates can permeate the host cell outer membrane. These methods are quite sensitive to the variations of the porin structures. For instance, the colicin susceptibility method successfully located the FepA R316A single charge mutant with decreased sensitivities for both colicins B and D (Newton *et al.*, 1997), and nutrition assays for FepA deletion mutants provided different uptake patterns for the

determination of receptor functionality (Newton *et al.*, 1999).

Several biophysical methods have been successfully used in some membrane systems by attaching reporter probes to specific sites of outer membrane proteins. Site-directed spin labeling (SDSL) was performed by Jiang *et al.* (1997) to study the FepA-ligand interaction in live cells by conjugating Electron Spin Resonance (ESR) probes to the receptor protein. This method successfully monitored the channel opening and closing of FepA upon ligand absorption. Fluorescent labeling of FhuA (Bos *et al.*, 1998) was also reported, but unfortunately, the specific labeling of FhuA receptor could not be achieved. Therefore, it was not very useful for the determination of the receptor activity. This lack of usefulness is probably related to the relatively bulky structure of most of the fluorescent probes and their hydrophobicity. Only in very special systems, where labeling specificity was not required as strictly as in other systems, was the fluorescent labeling utilized successfully (Mannuzzu *et al.*, 1996).

Other cell based methods have also found their specific purposes in cell membrane studies. The cytofluorimetric method (Newton *et al.*, 1999) and the ELISA assay are the two widely used methods to determine the cell-surface loop exposure of receptor proteins. These methods, combined with protein expression level determination, can be used to determine quantitatively if the cell-surface loops are localized at the right positions.

Specific channels can be converted into non-specific porins by site-directed mutagenesis. Therefore, the following cell based diffusion analyses for non-specific

porins can be used in the study of specific channels and active transporters: 1) the analysis of the periplasmic space located beta-lactomase activities (Zimmermann and Rosselet, 1977; Sawai *et al.*, 1977) by comparing the enzyme activities of intact and broken cells; and 2) the change of antibiotic susceptibilities (Rutz *et al.*, 1992; *Newton et al.*, 1999).

What Are the Components of the Biphasic Binding Between FeEnt and FepA?

Payne *et al.* (1997) observed a biphasic binding between FepA and ferric enterobactin, in which ferric enterobactin binds to FepA in at least two steps, an initial rapid binding stage and a subsequent slower absorption step. Therefore, two binding events are probably involved in the ligand recognition, where ferric enterobactin first contacts the residues responsible for the initial interaction, which brings the ligand close to the second binding site for the formation of a stable complex.

Different approaches may be used to investigate the multi-step interaction between FepA and ferric enterobactin. Due to the complexity of the multicomponent binding and transport system, it is technically difficult to study the thermodynamics and kinetics of ferric enterobactin binding processes in intact cell systems. Therefore, we employed a purified protein system to further study the interaction between FepA and ferric enterobactin.

Biophysical methods have proven to be efficient in studying the ferric enterobactin-FepA interaction. Liu *et al.* (1994) used Electron Spin Resonance (ESR) technique to study the FepA protein environment upon ferric enterobactin binding. A cysteine residue was introduced to the E280 residue by site directed mutagenesis, and two ESR probes, MAL6 and MTSL, were specifically labeled to the introduced cysteine. This research was made possible by the specificity of the labeling reaction, the intact functionality of the mutant FepA protein, and the location of the E280 residue. E280 is within the proposed binding domain (Rutz *et al.*, 1992), and ESR probes attached to E280C showed the probe environment change both *in vitro* (Liu *et al.*, 1994) and *in vivo* (Jiang *et al.*, 1997). Therefore, E280C mutant FepA protein was a good candidate for different biophysical analyses.

We used a fluorescent measurement system to study the ligand-receptor interaction. Fluorescent measurement is a very important tool to study biological systems in that (1) fluorescent measurement can sensitively detect the environment of the fluorophore given the various techniques (Lakowicz, 1983); (2) intrinsic fluorescent residues, including tryptophan, tyrosine, and phenylalanine, are common in all biological systems. Therefore, the intrinsic fluorescent measurement is technically possible without introducing any fluorescent probes; (3) various extrinsic fluorescent probes are available (Haugland, 1996) for the study of different systems.

For the FepA system, an intrinsic fluorescent study would not present much useful information due to the large amount of tryptophan residues in the protein

(Lundrigan & Kadner, 1986). Therefore, it would be necessary to introduce an extrinsic fluorophore to the mutant E280C to perform the fluorescent measurement. In this study, we used several probes with distinctive fluorescent features to study the interaction between ferric enterobactin and its receptor.

Fluorescence

Fluorescent molecules have been used in the study of various systems, from *in vivo* to *in vitro* (for reviews, see Lakowicz, 1983; Haugland, 1996; Hermanson, 1996). This technique has been widely used, due to the convenience of the instrument operation, the development of various methods (Lakowicz, 1983; Haugland, 1996), and the availability of a large amount of fluorescent probes (Haugland, 1996) with different reaction specificity (Hermanson, 1996) for different research purposes in various biological systems (Haugland, 1996). Therefore, it has been found to be a very useful tool, especially in its application in the development of high-throughput screening (HTS) technique where sensitive and quick data analysis is essential (Fernandes, 1998).

Upon light absorption, fluorophores populate the excited energy states, where there are several processes for the excited electrons to return to the ground energy state, including the internal conversion, the emission from singlet states, or the emission from triplet states. The electrons populated at the higher vibrational energy levels of the excited states rapidly relax to the lowest vibrational energy level (the

internal conversion), followed by the emission of photons (fluorescence). Alternatively, phosphorescence may occur through triplet states formed from intersystem crossing.

One way for the excited molecules to return to the ground state without emitting photons is through the quenching processes, which in turn decreases the fluorescence intensity of the fluorophore. Quenching is very common for fluorophores in an aqueous environment. There are two types of quenching: dynamic quenching (also called collisional quenching) and static quenching. Both dynamic quenching and static quenching require the direct contact between the fluorophore and the quencher. In the case of dynamic quenching, the quencher diffuses to the excited fluorophore and quenches it before the fluorophore returns to the ground state by emitting photons; in static quenching, on the other hand, a complex that does not emit photons is formed between the quencher and the fluorophore.

The dynamic quenching can be described by the Stern-Volmer equation:

$$F_0/F - 1 = K_{sv}[Q] \qquad (1\text{-}1)$$

where F_0 and F are the fluorescence intensities in the absence and presence of fluorescent quenchers, respectively; K_{sv} is the Stern-Volmer quenching constant; and [Q] represents the concentration of the quencher. There are various fluorescent quenchers available, and each of them may provide different information regarding

the charge around the fluorophore, the polarity of the environment, the localization of the fluorophore, the features of the fluorophore itself and so on.

The similar equation can be used to represent the static quenching:

$$F_0/F - 1 = K_s [Q] \qquad (1\text{-}2)$$

where F_0, F and [Q] have the same meaning, while K_s represents the association constant between quencher (Q) and the fluorophore.

CPM and Binding Site

The probe 7-diethylamino-3-(4'-maleimidylphenyl)-4-methylcoumarin (CPM) is a derivative of coumarin with a chemically reactive maleimidyl group (Figure 1-2). The most important feature of this fluorophore is that it is not very fluorescent until the maleimidyl group is modified by a thiol group (Berman and Leonard, 1990; Sippel, 1981a; Sippel, 1981b). Therefore, a small amount of available thiol groups can be detected quantitatively by the chemical modification of this probe (Parvari *et al.*, 1983).CPM is very specific to free thiol groups. In FepA, the two native cysteines are disulfide bond linked and are not available for thiol specific chemical modifications (Liu *et al.*, 1994). Therefore, the only target for thiol specific modification in E280C FepA is the introduced cysteine at the 280 site. The availability of the thiol group for chemical modification is, hence, an indication of

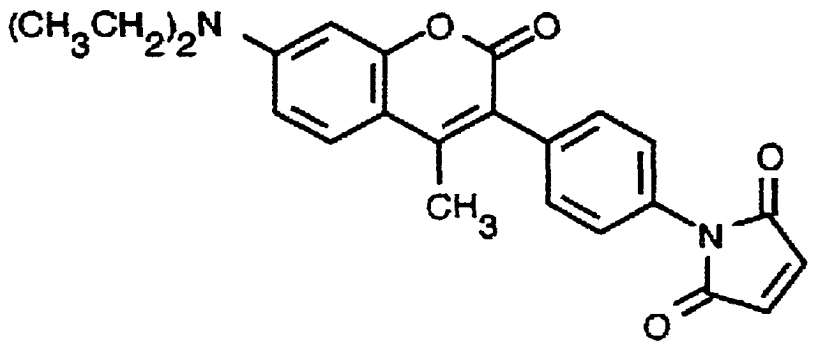

7-diethylamino-3-(4'-maleimidylphenyl)-4-methylcoumarin (CPM)

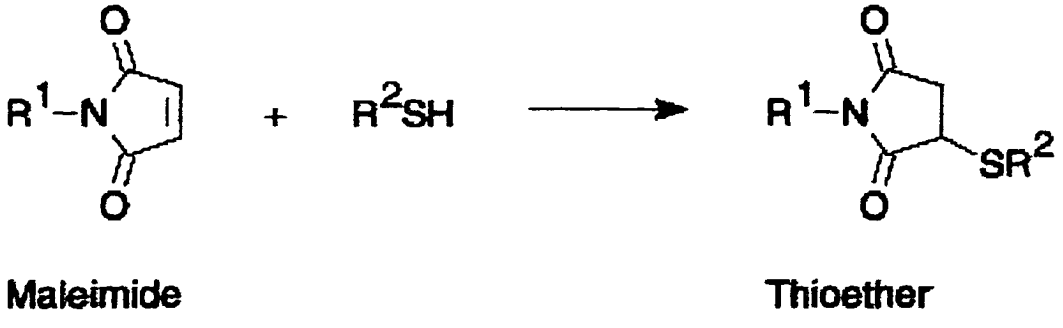

Figure 1-2. CPM structure and its reaction mechanism

whether the E280C site is exposed to the aqueous environment where chemical modification takes place.

The feature of the dramatic increase of the fluorescence intensity was used to investigate the ligand-receptor binding interaction. We looked at genetically introduced cysteines to see if the site chosen is located within the ferric enterobactin binding domain. Such a study was essential for the further investigation of the receptor protein because the fluorescent measurement system depended on the fluorescent parameter changes upon ferric enterobactin absorption.

IAF and binding interaction

5-iodoacetamidofluorescein (5-IAF) is a fluorescein derivative, specifically reactive to thiol group (Figure 1-3), and most importantly, with a strong fluorescence emission. The strong fluorescence emission makes an accurate fluorescent measurement possible without using a substantial amount of proteins. Therefore, 5-IAF was chosen as the main fluorescent probe used in this study.

One of the important aspects of this study was the fluorescent quenching in 5-IAF labeled E280C FepA. Although various processes, including excited state reactions, energy transfer, formation of complex, and collisional quenching, can result in the fluorescence intensity decrease of the fluorophore (Lakowicz, 1983), we were especially interested in the collisional quenching and the formation of complex. The former reveals the environment of the fluorophore in biological systems while the

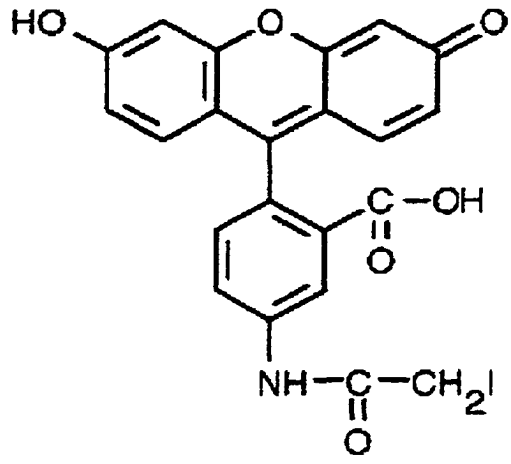

5-iodoacetamidofluorescein (5-IAF)

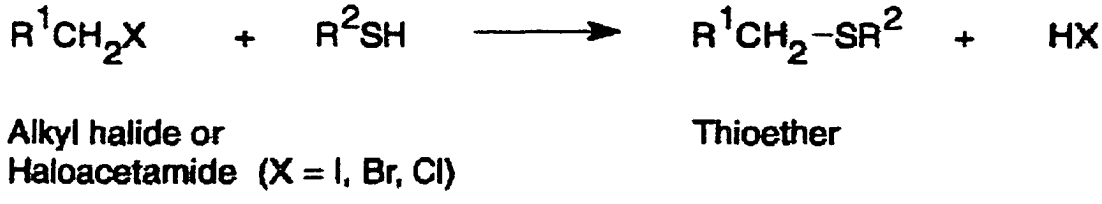

Figure 1-3. 5-IAF and its reaction mechanism

latter represents the interaction between the ligand and the receptor.

IAEDANS and environmental change

5-((((2-iodoacetyl)amino)ethyl) amino)naphthalene-1-sulfonic acid (1,5-IAEDANS) is a fluorescent probe very sensitive to the environment. It is water soluble, and specific to the sulfhydryl groups (Figure 1-4). Therefore, it is a very useful probe to study the protein environmental change under various conditions.

IAEDANS is a good energy donor to IAF. Therefore, IAEDANS and IAF can be used together to study protein conformational changes by measuring the energy transfer between these two probes. Such an energy transfer study depends on the complete and specific labeling of two different sites with different probes.

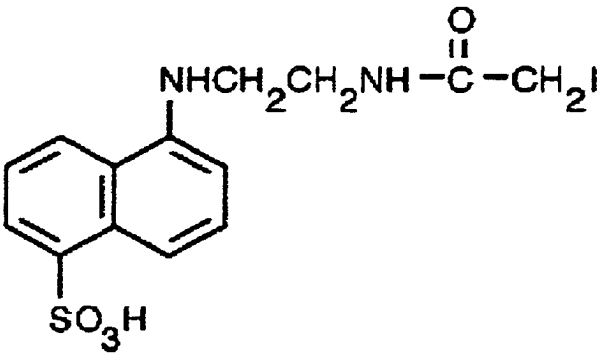

5-((((2-iodoacetyl)amino)ethyl) amino)naphthalene-1-sulfonic acid (1,5-IAEDANS)

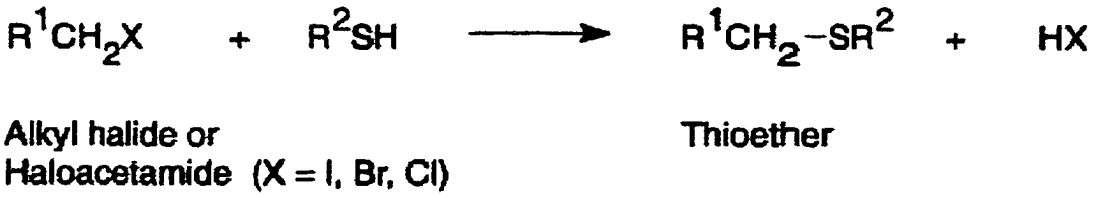

Figure 1-4. IAEDANS and its reaction mechanism

CHAPTER II

EXPERIMENTAL PROCEDURES

Materials, Strains and Plasmids

Strains and plasmids

All bacterial strains used in this study were derived from *Escherichia coli* K-12 as listed in Table 3-2.1. AN102 was used for the purification of enterobactin. JM101 and CJ236 were used for the site-directed mutagenesis. KDF541 and UT5600 were the host strains for phenotype analysis and protein purification, respectively. Plasmid pITS449 carries the wild type *fepA* allele, under the control of its native promoter, while the plasmids carrying the mutant alleles were designated as XnY, where X and

Y represent the one-letter abbreviations for the wild-type residue and the substituted amino acid at position n, respectively.

Table 2.1. Bacterial strains, plasmid and phage

Strain, plasmid or phage	Genotype or genotype	Reference
strains		
AN102		Cox *et al.*, 1970
CJ236	*dut⁻ ung⁻ thi⁻/pCJ105 (Cm^r)*	
JM101	*Δlacpro supE thi* F' *traD36 proAB lacq ZΔM15*	Messing, 1983
KDF541	F⁻ *pro⁻ leu⁻ trp⁻ thi⁻ tonA⁻ lac⁻ entA⁻ recA⁻ rpsL fepA⁻ cir⁻*	Rutz *et al.*, 1992
UT5600	*pro⁻ leu⁻ trp⁻ thi⁻ lac⁻ entA⁻ ompT⁻ tonA⁺*	McIntosh *et al.*, 1979
plasmid		
pITS449	pUC18 *E. coli fepA⁺*	Armstrong *et al., 1990*
phage		
m13mp18		Messing, 1983

Media

Table 2.2 is a list of iron-deficient media (T media and MOPS media) for protein expression and rich media (Luria-Bertani Broth) for bacterial growth. 2 x YT media and Nutrient Broth were used for site-directed mutagenesis and nutrition

assays, respectively.

Table 2.2. media and references

Media	*Reference*
2 x YT media	Messing, 1983
T media	Klebba *et al.*, 1982
MOPS media	Neidhardt *et al.*, 1974
Luria-Bertani Broth	Miller, 1972

Ferric enterobactin

Enterobactin was purified from the supernatant of AN102 cultures grown to late exponential phase (Wayne *et al.*, 1976). For the preparation of ferric enterobactin, 1 mg of enterobactin was dissolved in 0.5 ml of methanol, mixed with 0.5 ml of 4 mM $FeSO_4$ in dilute HCl, incubated at room temperature for one to two hours, and concentrated NaH_2PO_4, pH 6.9 was added to make the final buffer concentration 10mM. The mixture was loaded onto a Sephadex LH20 column equilibrated with 10 mM NaH_2PO_4, pH 6.9 and eluted with the same buffer. The concentration of ferric enterobactin was determined by measuring the absorbance at 495nm (ε_{mM} = 5.6; Pollack *et al.*, 1970) using a DU Beckman 640 spectrophotometer. The ratio of absorbance at 395nm and 495nm was used to determine the purity of ferric enterobactin. The ferric enterobactin thus prepared was stored on ice, and used within two days. After two days, it would be repurified by running through the Sephadex LH20 column. For the preparation of ^{59}ferric enterobactin, 0.05 mCi of $^{59}FeCl_3$ was

mixed with $FeSO_4$ before being added to the reaction.

Colicins B, D and Colicin B-Sepharose resin

ColB and ColD were purified from *E. coli* strains DM1187/pCLB1 (obtained from M. A. McIntosh) and CA23, respectively (Payne *et al.*, 1997) by selective precipitations and chromatography (Timmis, 1972; Pugsley and Reeves, 1977b), using their specific killing activities and SDS-PAGE as measures of purity. Colicin B-sepharose resin preparation procedures were adapted from Mishell & Shiigi (1980) (Payne *et al.*, 1997).

Site-Directed Mutagenesis

Sequence comparisons

Five FepA amino acid sequences from *Escherichia coli* (Lundrigan *et al.*, 1986), *Salmonella typhimurium* (Tumumuru *et al.*, 1990), *Pseudomonas aeruginosa* (Dean *et al.*, 1993), *Salmonella enterica* (Baumler *et al.* 1998), and *Bordetella pertussis* (Beall *et al.*, 1995) were compared by a PILEUP program (Genetics Computer Group, Madison, WI). The conserved residues were then used in the subsequent site-directed mutagenesis.

Site-directed mutagenesis

Using PstI and SacI sites, fepA structural gene from pITS449, was subcloned into the multiple cloning site of M13 mp19. Site-directed mutagenesis was performed on the M13 mp19 structural gene by Kunkel's method (Messing, 1983; Kunkel, 1985). The primers used in the *in vitro* mutagenesis reactions are listed in Table 2.2. The mutant fepA gene was then cloned back into the pITS449 fepA structural gene using the same cloning sites. The whole structural gene was sequenced to rule out any random mutagenesis. The plasmids thus constructed were finally transformed into KDF541 for mutant analysis and into UT5600 for protein purification.

Preparation of uracylated template for mutagenesis

A single M13mp19 plague carrying fepA allele was obtained from a LB plate of JM101 transformed with the phage DNA. The plague was then resuspended in 1ml 2 x YT media, incubated at 60°C for 5min to kill JM101 host cells, vortexed to release the phage, and centrifuged to get the supernatant containing the phage for uracylation. 25µl of the above supernatant was then added to 50ml 2 x YT media containing 5ml CJ236 midlog phase culture supplemented with 0.25µl/ml uridine, and allowed to grow for 5 to 6 hours. The cell culture was then centrifuged, and the supernatant was used for another round of uracylation. After the repeat of the uracylation step, the phage containing supernatant was then analyzed for the extent of uracylation by comparing the infection between *ung*$^+$ *dut*$^+$ host JM101 and *ung*$^-$ *dut*$^-$ host CJ236.

The uridine containing single stranded phage DNA template was then purified by precipitating the phage using 3% polyethylene glycol (PEG 8000, Amersham) followed by phenol/chloroform extraction.

Phosphorylation of mutagenesis primers

200 pmoles of primers (GIBCO) were added to a 30μl phosphorylation reaction containing 500μM ATP and 5 units of T4 polynucleotide kinase (USB) in kinasing buffer. After incubating for 45 min at 37°C, the reaction was incubated at 65°C for 10 minute to denature the enzyme.

In vitro mutagenesis reaction

Mutagenesis reaction was performed using Muta-Gene® In Vitro Mutagenesis Kits, Version 2 (BioRad). For the primer hybridization, 200ng of uracylated template was annealed with 6 pmoles of phosphorylated primer in 10μl annealing buffer by incubating at 70°C for 2 minute and letting cool down to 30°C over a period of 30 minutes. The elongation and ligation were then performed by adding 1μl of 10 x synthesis buffer, 1μl of T4 DNA ligase (3-5 units), and 1μl of T7 DNA polymerase (1unit) on ice. The reaction was incubated on ice for 5 minutes, then at 25°C for 5 minutes, followed by 37°C inoculation for 45 minutes. 90 μl stop solution was then added to the reaction.

Table 2.3. Primers for site-directed mutagenesis in the structural gene of FepA

Mutant	*Primer*
Y260A	CGC CAG GGT AAC CTG GCA GCA GGC GAC ACC CAG
Y272A	ACC AAC TCC GAT TCC GCA ACA CGC TCG AAA TAT
Y285A	GAA ACC AAC CGT CTA GCA CGC CAG AAC TAC GCG
Y289A	CTG TAT CGC CAG AAC GCC GCG CTG ACC TGG AAC
W297A	TGG AAC GGT GGC GCG GAT AAC GGC GTG
Y309A	AAC TGG GTG CAG GCT GAA CAC ACC CGT
R316A	ACC CGT AAC TCG GCT ATT CCG GAA GGT C
F329A	GGT ACC GAA GGG AAA GCA AAC GAA AAA GCG ACA
E280C	GC TCG AAA TAT GGC GAT TGT ACC AAC CGT CTG TAT CG
C486A	AGT AAA GGT CAG GGT GCC TAT GCC AGC GCG GGC
C493A	TAT GCC AGC GCG GGC GCC TAT CTG CAA GGT AAC

Mutant selection

The mutagenesis reaction was transformed into *dut*$^+$ *ung*$^+$ strain JM101, and proper dilution was plated out on a LB plate together with well grown JM101 culture. After an incubation of a 8 hours at 37°C, 3 to 6 single plagues were picked, and allowed to multiply at 37°C for 6 hours with vigorous shaking in 5 ml LB media containing 100 µl JM101 culture. The cell culture was then precipitated, and the pellet was used to purify RF M13 phage DNA using CONCERT™ Rapid Plasmid Miniprep System (GIBCOBRL).

RF DNA's were sequenced using Thermo Sequenase fluorescent labeled primer cycle sequencing kit (Amersham) on an ALFexpree™ DNA sequencer (Pharmacia). The DNA sequence was then compared with the wild type DNA sequence (Lundrigan

and Kadner, 1986) using BESTFIT algorithm (Genetics Computer Group, Madison, WI). The M13 DNA containing the mutant allele was then used for the construction of the mutant pITS449 plasmid.

Transformation of the mutant DNA into the expression vector

The pITS449 vector was obtained by digesting pITS449 plasmid with PstI and SacI (or SstI) digestion enzymes (GIBCOBRL), and purified using a 5% acrylamide gel. The mutant insert was generated by digesting RF M13 DNA with the same set of digestion enzymes, and purified using GENECLEAN® III kit (BIO 101). The concentrations of the insert and the vector band were then estimated by running a 1% agarose gel.

The ligation experiment was set up as following: 100ng of pITS449 vector band was added to 200ng of fepA mutant band containing 1 unit of T4 DNA ligase (GIBCOBRL) in 15 μl of ligase buffer, and incubated at 16°C for 6 to 12 hours. 1 μl of the above ligation solution was then electroporated into KDF541 competent cells using an electroporation apparatus (BioRad). The electroporation mixture was then incubated at 37°C for 45 minutes, and plated out on a plate containing 100μg/ml ampicillin.

Three isolated colonies from the above plate were then grown up in LB media containing 100μg/ml ampicillin at 37°C for 12-16 hours with vigorous shaking. The plasmids were purified using CONCERT™ Rapid Plasmid Miniprep System, and

sequenced as described in *Mutant Selection.*

FepA Mutant Phenotypic Analysis

FepA mutant expression

KDF541 strains harboring pITS449 or its mutant derivatives were grown in LB broth with 100μg/ml ampicillin and 100μg/ml streptomycin at 37°C for 16 hours before being inoculated to MOPS media with ampicillin (10μg/ml). After being grown for another five and half hours at 37°C with vigorous aeration, an aliquot of 5 x 10^7 subcultured bacterial cells was harvested, heat denatured in the presence of β-mercaptoethanol and loaded on a 10% SDS-PAGE gel. After SDS-PAGE electrophoresis, the gel was transferred to a nitrocellulose paper, and then the nitrocellulose paper was subjected to I-125 protein A immunoblot analysis (Newton *et al.*, 1997) using FepA mAb41 or mAb45 (Murphy *et al.*, 1990). Briefly, the blot was first coated with 1% gelatin in Tris buffered saline (TBS), and treated then with the anti-FepA monoclonal antibody (1:300 dilution with coating buffer). After an extensive wash with 0.5% Tween-20 in TBS, the blot was incubated with I-125 protein A in coating buffer. The blot was then washed, dried, exposed to film overnight, and developed.

Colicin killing

To examine the colicin sensitivity of each mutant FepA, a series of 2-fold dilution of Colicins B and D were made in LB broth in a 96 well microplate. Using a clone master, 5μl of diluted ColB or ColD was then transferred from the master plate to LB plates plated with bacteria KDF541 cultures harboring different fepA plasmid or its mutant derivatives containing 100μg/ml streptomycin and 10μg/ml ampicillin. After incubation at 37°C for over 6 hours, colicin sensitivity was determined by the maximum colicin dilution which resulted in killing.

Siderophore nutrition assay

Ferric enterobactin uptakes were examined by siderophore nutrition assay. Bacterial strains KDF541 harboring pITS449 or its mutant derivatives were inoculated from frozen stock into LB media containing 100μl/ml ampicillin. After being grown to mid-log phase ($O.D._{600nm}$ 0.5-0.9), 100μl of bacterial cultures were plated into the assay plate with 3ml Nutrition top agar plus 300nmoles apoferrichrome A (final concentration 0.1mM; Wayne *et al.*, 1976), 300μg streptomycin and 30μg ampicillin. After the plate was solidified, a 1/4" diameter paper disc (Becton Dickinson Microbiology Systems, MD) was placed in the middle of each well and 10μl of 50μM ferric enterobactin was added to the center of the disc. The assay plate was then incubated at 37°C for at least 6 hours. For some mutants, the plates were incubated for up to 24 hours for maximum development.

Siderophore binding affinities and their screening

The following strategy was used to investigate siderophore binding: a Fe-siderophore screening carried out by comparing the binding at two different concentrations and a detailed binding study to those mutants revealing defective binding in the screening. ^{59}Fe-enterobactin binding experiments were performed by a modification of prior methods (Rutz *et al.*, 1991; Ecker *et al.*, 1986; Newton *et al.*, 1997; Newton *et al.*, 1999). Bacteria KDF541 harboring wild type fepA or mutant fepA genes on pUC19 (pITS449 or its mutant derivatives) were grown in Luria-Bertani broth with streptomycin (100μg/ml) and ampicillin (100μg/ml) for 16 hours, subcultured into MOPS minimal media with streptomycin (100μg/ml) and ampicillin (10μg/ml), and grown for 5.5-6.0 hours at 37°C with vigorous aeration (typically, $O.D._{600nm}$ 0.5-0.7). The binding assay was performed as described (Newton *et al.*, 1999) with some modifications to optimize the binding of each specific mutant. Above culture was incubated on ice for 60 minutes before the binding assay. Different amount of cells were used in the assay for wild type FepA and mutants with lower affinity. For wild type FepA, 2 x 10^8 cells were diluted into 10 ml of chilled MOPS media. 1ml of the above solution containing 2 x 10^7 cells was then pipetted into a series of 50-ml pre-cooled assay tubes on ice. Appropriate amounts of freshly prepared, purified, ice-cold ^{59}Fe-siderophore (the specific activity was about 200-500 CPM/pmole) in 24-ml MOPS media were poured into the assay tubes containing 2 x 10^7 cells. After 5 minutes of incubation on ice, the assay solution in each tube was

filtered through a 25mm nitrocellulose filter (Schleicher & Schuell, NH), and the filters were counted in a Cobra counter (Packard) after a 10-ml 0.9% LiCl wash. Cell density for each culture was determined by visible spectroscopy at 600nm, and FepA protein expression was examined by Western immunoblot. For mutants with lower binding affinities, when K_d of the mutant was at least 10 times lower than that of the wild type protein, 10 times more cells were used in the assay, and the ^{59}FeEnt used was diluted with non-radioactive FeEnt to reduce the specific activity to about 20 CPM/pmole. For mutants with K_d > 100nM, 5 x 10^8 cells were used and the specific activity of ^{59}FeEnt was further diluted to about 10 CPM/pmole. To optimize the assay, 5-ml of assay volume was employed when FeEnt concentrations were above 40nM, which avoided the unnecessary use of extra amount of FeEnt, and most importantly, decreased the KDF541 background, thus allowing more reproducible results. Each assay was corrected with the negative control KDF541 before determining the ratio of the binding at two different concentrations in the screening assay or before GraFit4 (Erathicus) was used to determine the binding affinities of the defective mutants.

Siderophore uptake capabilities and their screening

For transport experiments, bacteria were grown and quantitated in the same way, and the uptake of ^{59}Fe-enterobactin was measured (Newton *et al.*, 1999) at 37°C. To avoid the substrate depletion problem encountered in the previous assays (Rutz *et al.*, 1991; Ecker *et al.*, 1986; Newton *et al.*, 1997; Thulasiraman *et al.*, 1998), besides

the same precautions as in the binding assay were taken concerning the assay volume, the specific activities of ^{59}FeEnt and the amount of cells used in the assay, further modifications were made with regard to the uptake time in the assay. For 25-ml assays, series of ^{59}FeEnt at different concentrations in 37°C MOPS media was poured into the assay tubes, while for 5-ml assays, the appropriate amount of ^{59}FeEnt was directly added to the assay tube and vortexed right away to well mix the solution. The assay solutions were then incubated at 37°C for different times, quenched with 100-fold excess cold FeEnt, and filtered through a 25mm nitrocellulose filter. After LiCl wash, the filters were counted. The assay times were 5 seconds and 20 seconds for wild type FepA, 30 seconds and 60 seconds for mutants with K_m between 1 and 100nM, and 1 minute and 2 minutes for mutants with K_m above 100nM, respectively. GraFit4 was used to determine the kinetic parameters.

Data Analysis

For binding assays, the following bound versus total equation was used:

$$\text{Bound} = \frac{b - \sqrt{b^2 - 4 * \text{total} * \text{capacity}}}{2} \qquad (2\text{-}1)$$

where $b = K_d + \text{total} + \text{capacity}$; total is the amount of substrate added to the assay,

and K_d and capacity are the two parameters determined by the least squared fitting using GraFit4.

For the uptake of ferric enterobactin, the Michaelis-Menten equation was used in the fitting:

$$v = \frac{V_{max}[S]}{K_m + [S]} \qquad (2\text{-}2)$$

where [S] is the substrate concentration, and K_m and V_{max} are the parameters determined by the least squared fitting using GraFit4.

Polyclonal Antibodies Against Fluorescent Probes

Preparation of fluorescent probes

The fluorescent probes were stored in a desiccator at -20°C freezer. To prepare the fluorescent probe solutions, 1mg of CPM was dissolved into 200µl methanol in dark before diluting into the reaction buffer. For 5-IAF, 200µl of DMSO was used instead. IAEDANS was dissolved directly into H_2O. The concentrations of the probes were further verified using the extinguish coefficients at 387nm ($\varepsilon = 30{,}000\ M^{-1}\ cm^{-1}$; Zot *et al.*, 1990), 492nm ($\varepsilon = 73{,}000\ M^{-1}\ cm^{-1}$; Tyson *et al.*, 1989) and 337nm ($\varepsilon = 6{,}100\ M^{-1}\ cm^{-1}$; Hudson and Weber, 1973) for CPM, 5-IAF, and IAEDANS,

respectively. The above prepared probe solutions were kept in dark and used within 30 minutes.

Preparation of antigens for immunization

To prepare the antigens for immunization, 1mg of bovine serum albumin (BSA) was dissolved in 1ml 50mM NaH_2PO_4 pH7.4 buffer. 10-fold molar excess of the above prepared fluorescent probe was then added in dark. The reaction was carried out in dark at room temperature for 5 hours with shaking before it was loaded onto a Sephadex-50 column to separate the unreacted probes from BSA. After eluting the column with 50mM pH7.4 sodium phosphate buffer, the fractions were assayed for fluorescent probe distribution using absorbance at 280nm where proteins strongly absorb. The probe-conjugated BSA fractions were then pooled together, dialyzed against 50mM pH7.4 sodium phosphate, and checked for fluorescent labeling as per the procedures discussed in later sections. As controls, 1mg of ovalbumin was labeled following the same procedures, and fluorescent probe conjugated BSA and ovalbumin concentrations were determined.

Generation of polyclonal antibodies

New England white rabbits were immunized once a week with 100 μg of the fluorescent probe conjugated BSA emulsified with complete Freund's Adjuvant (CFA; Sigma Immuno Chemicals) for the first two weeks, and emulsified with

incomplete Freund's Adjuvant (IFA; Sigma Immuno Chemicals) the following two weeks. One week after the fourth immunization, the rabbits were bled. To get more antisera after first bleeding, rabbits were immunized with 10 μg of the probe conjugated BSA in Aluminium Hydroxide Gel Adjuvant (Superfos Biosector a/s, Denmark) one week before the bleeding.

Polyclonal antibody analysis

Western blot was used to determine the specificity of the antibodies to the fluorescent probes, and ELISA was performed to determine the titer of the antisera.

Preparation of Fluorescent FepA Mutant Proteins

Purification of FepA wild type and mutant proteins

Wild type and mutant FepA proteins were purified from UT5600 (harboring the corresponding plasmid) T media cultures grown to the stationary phase. Outer membrane proteins were extracted using differential Triton X-100 extractions (Hollifield and Neilands, 1978; Fiss *et al.*, 1982). Briefly, cell membranes were extracted with the inner membrane extraction buffer (100mM Tris, pH8.0, 2% Triton X-100, 10mM $MgCl_2$, and 10mM benzamidine) twice before the outer membrane proteins were extracted two times with 10mM Tris, pH8.0, 2% Triton X-100, 5mM EDTA and 10mM benzamidine buffer. FepA protein was purified from other outer

membrane proteins by running through a colicin B affinity column (Payne *et al.*, 1997).

Protein concentration determinations

For protein samples not containing any detergent, Lowry's method (1951) was used to determine the protein concentration. Otherwise, protein concentrations were determined using Micro BCA method (Pierce) or the modified Lowry's method (Dulley *et al.*, 1975) in the presence of 2% sodium dodecyl sulfate (SDS).

Labeling FepA proteins with IAEDANS and 5-IAF

E280C (final concentration 0.15 mg/ml) in TTE buffer (50mM Tris, pH7.2, 2% Triton X-100, 5mM EDTA) was incubated with 10μM IAEDANS or 5-IAF at room temperature in the dark with shaking for 45 minutes, ethanol precipitated twice, and resuspended in 1mM n-dodecyl β-D-maltoside (DM; SIGMA), 50mM MOPS pH7.0, 60mM NaCl buffer. The reaction then was transferred to dialysis tubing (MWCO 12,000-14,000), and dialyzed against the above buffer at 4°C with three changes of buffer for 48 hours to remove unreacted probes. The concentration of the labeled proteins was determined before the labeled protein was aliquoted and stored at -80°C. The same fluorescent labeling procedures were performed on wild type protein FepA as a control. Y272A/F329A/E280C and Y260A/R316A/E280C mutants were labeled in the same way.

Fluorescent labeling specificity

Fluorescent labeling specificity was determined by Western blot. Briefly, 4 μg of labeled E280C protein was heat treated for 5 minutes before it was loaded on a 10% SDS-PAGE gel. After electrophoresis, the protein was transferred to a nitrocellulose paper which was then subjected to the polyclonal antibody against the fluorescent probe conjugated BSA generated as described above and I-125 protein A. The blot was then exposed to a film. Wild type FepA treated with fluorescent probes was loaded on the same SDS-PAGE as a control.

Fluorescent labeling specificity was also determined by the fluorescent measurement of the labeled E280C protein by comparing the fluorescence intensities of the fluorescent probe treated wild type and E280C proteins. The procedures for fluorescent measurement will be discussed later.

Fluorescent Measurements

CPM time-course labeling of purified proteins

For the time-course labeling reaction of FepA proteins in the presence of ferric enterobactin, wild type FepA and E280C in 50 mM MOPS, pH6.9, 60 mM NaCl and 1 mM DM buffer (final FepA concentration 200nM) were first incubated with ferric enterobactin in 50 mM NaH_2PO_4, pH 6.9 (final FeEnt concentration 10 μM) at room temperature for 10 minutes. 5-fold excess of CPM in methanol (less than 0.5% of the

final reaction volume) was added, and the fluorescence intensity of the reaction was recorded versus time on an SLM 8000C fluorimeter upgraded to 8100 functionality (SLM-Aminco, Urbana, IL), equipped with a 450-watt xenon light source and a cooled photomultiplier tube housing and operated in photon-counting mode. The excitation and emission wavelengths were set at 385 and 471 nm, respectively, with both slits set at 4 nm.

When ferric enterobactin was used, a small amount of 10 mM NaH_2PO_4, pH 6.9 buffer was introduced into the reaction, but it had no influence on the spectra (data not shown). For time-course labeling experiments in the absence of ferric enterobactin, an equal amount of 10 mM NaH_2PO_4, pH 6.9 buffer was added in place of ferric enterobactin, and the rest of the experimental procedures were kept the same. In some experiments, the proteins were partially denatured with 6M urea in TTE, pH7.2 prior to labeling (Liu *et al.*, 1994), followed by reaction with 5-fold excess of CPM under denaturing conditions.

Emission scan and labeling specificity

The excitation and emission scans were made at a final protein concentration of 500 nM of labeled protein in TTE, pH7.2 buffer under the same fluorescent measurement conditions as described above. The maximum excitation wavelength was determined to be 336nm and 491nm for IAEDANS and IAF labeled proteins, respectively. Labeling specificity was assured by the fluorescence intensity difference

between same amount of E280C and wild type FepA treated with fluorescent probes in the same way. Further analysis was performed by emission scan using the excitation wavelengths above determined. When ferric enterobactin was added, the mixtures were incubated at room temperature for 10 minutes before the first emission scan was made, and was re-scanned after another 10 minutes to assure reproducible spectra.

Fluorescence quenching by ferric enterobactin and determination of K_d

50nM FepA-IAF in 50 mM MOPS, pH6.9, 60 mM NaCl, and 1 mM DM buffer was titrated with 2μM ferric enterobactin, and the fluorescence intensity was measured with the excitation and emission wavelengths set at 490nm and 520nm, respectively. The fluorescence intensity of E280C was corrected first with that of the wild type FepA, and then with the dilution factor. The concentration of the protein was also corrected in the data fit program. The titration data were fit using GraFit4 to obtain K_d.

Epitope proximity

To study epitope proximity, 50nM IAF labeled E280C in 1mM Tris-buffered DM detergent solution was incubated at 25°C till stable fluorescent signals were obtained. The mixture was then incubated with 10μl of monoclonal antibodies against different epitopes of FepA (Murphy *et al.*, 1990) for 10 minutes before fluorescent

measurement was taken. Ferric enterobactin was added to a final concentration of 1μM, and following a 30-minute incubation at 25°C, the fluorescence intensity was measured again.

Antibody competition

E280C protein labeled with 5-IAF was added to 1mM Tris-buffered DM detergent solution to an E280C final concentration of 2.5nM. fluorescent time course measurement was performed using at 25°C with the excitation and emission wavelengths set at 490nm and 520nm, respectively. FeEnt was added to a final concentration of 47nM when E280C-IAF reached a stable signal. The time course for FeEnt quenching was then recorded. After the quenching reached the maximum, 10μl of different antibodies against FepA were added instantly to record the release of FeEnt in the presence of antibodies.

FeEnt binding time course

E280C labeled with IAF was diluted into 1mM DM, 50mM MOPS pH7.0, 60mM NaCl buffer to a final concentration of 2.5nM, and incubated at 25°C for an hour to ensure the stabilization of E280C-IAF. The time course was then started on the SLM8100 fluorimeter at an excitation and an emission wavelength of 490nm and 520nm, respectively, with the slits all set at 4nm, and an integration time of 1 second. After about 5 minutes of pre-run, ferric enterobactin in 50mM MOPS pH7.0, 60mM

NaCl was added to a final concentration of 1μM. Following the same procedures, IAF treated FepA was used as a control. Also, another control was run on E280C-IAF by adding the plain buffer in place of ferric enterobactin.

CHAPTER III

RESULTS

The Aromatic Component

Experimental strategies:

Aromatic residues are very good candidate residues for the direct interaction between FepA and its ligand ferric enterobactin, due to the aromatic characteristics of both ferric enterobactin and its receptor. This study was aimed at finding the importance of each aromatic residue in the central region of FepA by performing alanine scanning mutagenesis on the conserved aromatic residues. A previous study (Newton *et al.*, 1997) indicated that the interaction between FepA and its ligand was multi-component. Also, it was shown that single mutations to introduce "neutral" amino acids (i.e., alanine) in the central region would not always be destructive

enough to show a significant decrease, if any, in FepA functionality. Therefore, the conserved aromatic residues were mutated to alanine singly and in combinations in order to disrupt the multi-component interaction system to render meaningful characterization of the mutants.

Candidates of the aromatic component:

To choose the important aromatic residues in the central region of FepA, the *E. coli* FepA amino acid sequence (Lundrigan & Kadner, 1986) was compared to three other known FepA sequences from *Salmonella typhimurium* (Tumumuru *et al.*, 1990), *Pseudomonas aeruginosa* (Dean & Poole, 1993) and *Bordetella pertussis* (Beall & Sanden, 1995) using a PILEUP algorithm (Genetics Computer Group, Madison, WI). Seven of the ten aromatic residues in the region of interest, Y260, Y272, Y285, Y289, W297, Y309, and F329, were found conserved among the five FepA sequences. Figure 3-1 shows the amino acid alignment of the five sequences and the location of each aromatic residue in the secondary structure of *E. coli* FepA. The incomplete crystal structure of FepA (Buchanan *et al.*, 1999) shows that among the seven aromatic residues, aromatic residues Y285, Y289 and Y309 are buried in the trans-membrane β-sheet with the residues facing the barrel. Y260 is located right at the hinge of the transmembrane β-sheets and the surface loops. W297 is one of the loop residues at the periplasmic side of the protein joining two β-transmembrane strands. Y272 and F329 are the two surface residues, with the position of F329 not determined

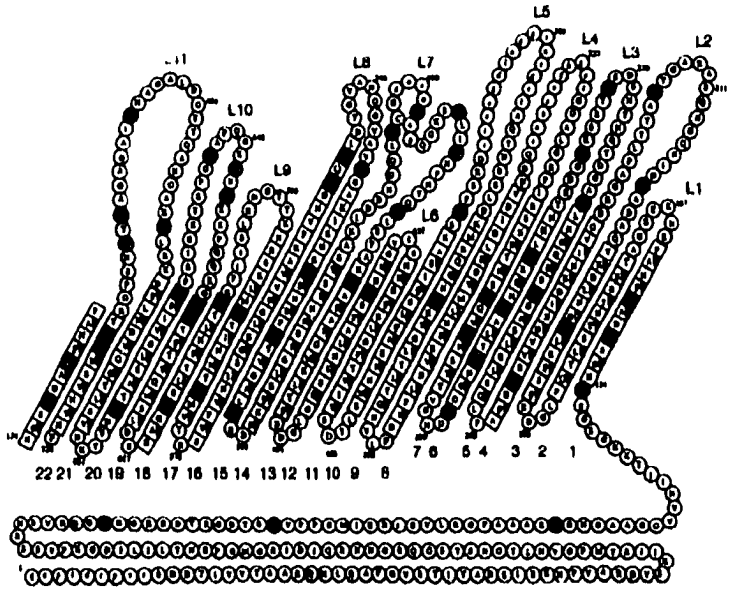


```
EFepA 255 RQGNLYAGDTQNTNSDSYTRSKY..GDETNRLYRQNYALTWNGGWDNGVTTSNWVQYEHTRNSRIPEGLAGGTEGKFNEKATQ
SFepA 255 RQGNLYAGDTQNTNTNQLVKDNY..GKETNRLYRQNYSLTWNGGWNNGVTTSNWVQYEHTRNSRMPEGLPGGTEGIFDPKASQ
PFepA 257 RQGNIYTGDTQNTNSNNYVKQML..GHETNRMYRETYSVTHRGEWDFGSSLA.YLQYEKTRNSRINEGLAGGTEGIFDPNNA.
BFepA 259 RQGNLFAGDTMNNANSDFSDSLY''GKETNAMYRENYALTHRGVYDWGTSRAS.VGYDYTRNARQREGLAGGPEG...APTAG
SIroN 247 RQGNIYAGDTQNSNSNAVTKSLAQSGRETNRLYRQNYGLTHNGIWGWGQSRLG.FYYEKTDNTRMNEGLSGGGEGR..ITNDQ
```

Figure 3-1. FepA Secondary Structure and Central Region Alignment

in the crystal structure.

Site-directed mutagenesis:

Seven single amino-acid substitutions were generated using site-directed mutagenesis. Aromatic residues were mutated to alanine to test the participation of each aromatic residue in the interaction between FepA and its ligands. Twenty-one possible double combinations were also generated using the single substitutions as templates for site-directed mutagenesis. All the above mutants, when transformed into the KDF541 strain, did not affect the siderophore-dependent cell growth. The mutants were expressed at the same level as the wild type protein without OmpT (Baneyx and Georgiou, 1990) digestion, when mAb41 was used to check the expression of the mutants (figure 3-2).

Surprisingly, when mAb45 was used in immunoblotting, no bands were observed for all the mutants containing F329A (data not shown). Since the SDS-PAGE was run on heat denatured proteins, it is certain that in my immunoblots, denatured amino acid sequences were recognized by the monoclonal antibodies. This indicated that F329 residue was important for mAb45 epitope recognition. In the immunoblot analysis, when the alkaline-phosphatase conjugated secondary antibody was used instead of ^{125}I-protein A, faint bands were observed for all the mutants with F329A when extensive development was allowed. This result further suggested that F329 is a critical residue for mAb45 in the epitope recognition.

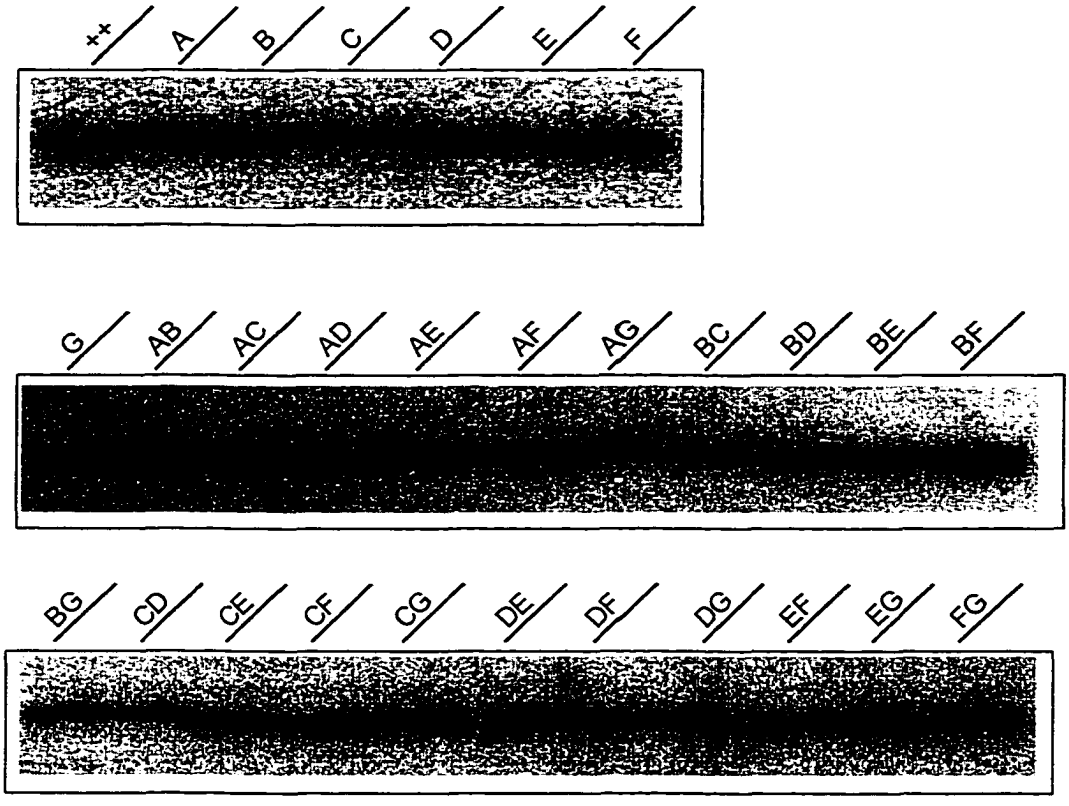

Figure 3-2. Expression of FepA aromatic mutants. 5 x 10^7 cells grown in MOPS media were harvested, lysed and subjected to Western immunoblot with mAb41 and ^{125}I-protein A. The nitro cellulose paper was then subjected to autoradiography. Y260A, Y272A, Y285A, Y289A, W297A, Y309A, and F329A were abbreviated as A, B, C, D, E, F, and G, respectively.

Optimization of siderophore binding and transport assays:

Previously, wild type FepA was reported to have a K_d and K_m of 22nM and 155nM, respectively (Newton *et al.*, 1997). It was found by Newton *et al.* (1999) and this study that previous studies were performed under substrate depletion conditions. In other words, in both binding and transport assays, the amount of substrate was not enough to keep the binding in equilibrium, let alone to keep the uptake rate constant.

To optimize assay conditions, the binding and transport experiments were designed in such a way (by increasing the assay volume, decreasing the number of cells, and decreasing the period of time for the uptake experiment) that at the lowest FeEnt concentration, the ratio of the amount of FeEnt added to the amount of cells used was at least 1pmole/10^7 cells. For wild type receptor and Y272A, the transport assay was performed from 5 seconds to 20 seconds; for any mutants with K_m larger than 200nM, from 1 minute to 2 minutes; and for all the other mutants, from 30 seconds to 60 seconds. Under such assay conditions, the ligand-receptor binding interaction was measured without any substrate depletion possibility, since for the binding assay it is only necessary for a significant amount of the substrate to remain unbound, to reach binding equilibrium. For the uptake experiment, the observed maximum substrate depletion was around 5% at the lowest FeEnt concentrations.

Aromatic residues important in siderophore binding:

The FeEnt binding screening experiment (Figure 3-3) was used to scan the

binding affinities of all the aromatic residue replacement mutants, including all single mutants and double combinations, to find the mutants with the activity at the wild type level. In the first screening experiment, the binding capability of the mutants at 0.2nM FeEnt concentration compared with the saturation concentration for wild type protein (70nM) was used. The experiment showed that all the mutants, except Y260A and F329A, retain binding affinities at the wild type level. Among the mutants with decreased affinities, Y260A did not have any binding at 0.2nM, while F329A had slightly lower affinity. Though Y272A mutant did not show any affinity change by itself, a significant affinity decrease was observed when it was combined with F329A. Therefore, Y260, Y272, and F329 might be important residues to consider for further studies.

Since Y260A itself showed reduced binding affinity in the initial screening experiment, the Y260A series was further studied by comparisons with wild type at 20nM (Figure 3-4). The result showed that Y260A did not have any further affinity decrease when combined with Y285A, Y289A, W297A, or Y309A, while significant affinity decrease was observed for Y260A/Y272A and Y260A/F329A. From the above screening result, it was revealed that the possible residues involved in the binding were Y260, Y272 and F329. Therefore, it was necessary to further study the binding affinities in more detail for mutants Y260A, Y272A, F329A, and their double combinations. All the other mutants, in any kind of double combinations, did not show any significant, distinguishable decrease in binding affinities. Therefore,

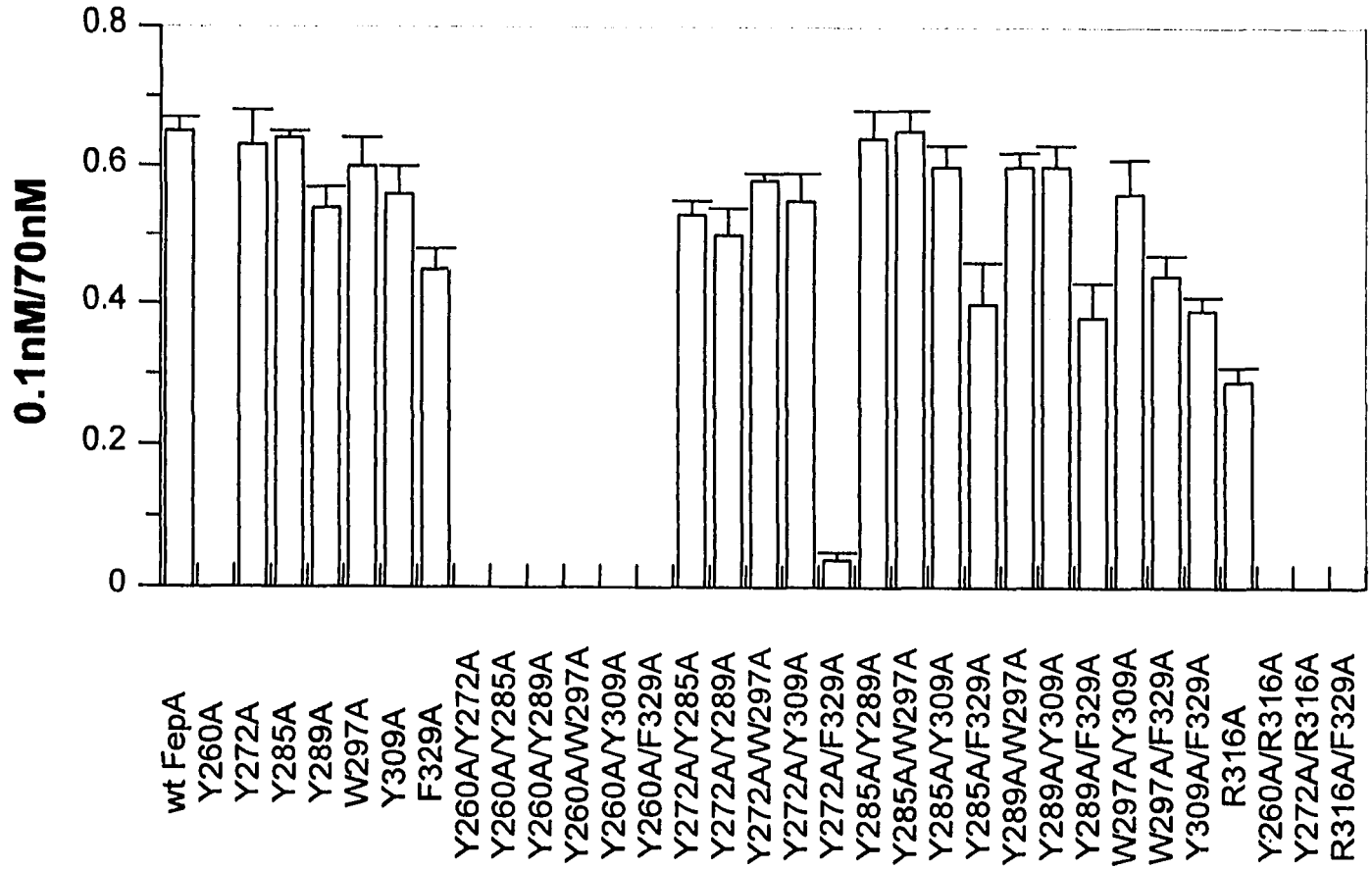

Figure 3-3. Siderophore binding screening at wild type Kd FeEnt concentration. Ferric enterobactin binding assays were performed at two concentrations (0.1nM and 70nM) for wild type FepA and the aromatic substitution mutants. The binding affinities were compared using the ratio at these two concentrations. The error bars represent the standard deviations from three experiments.

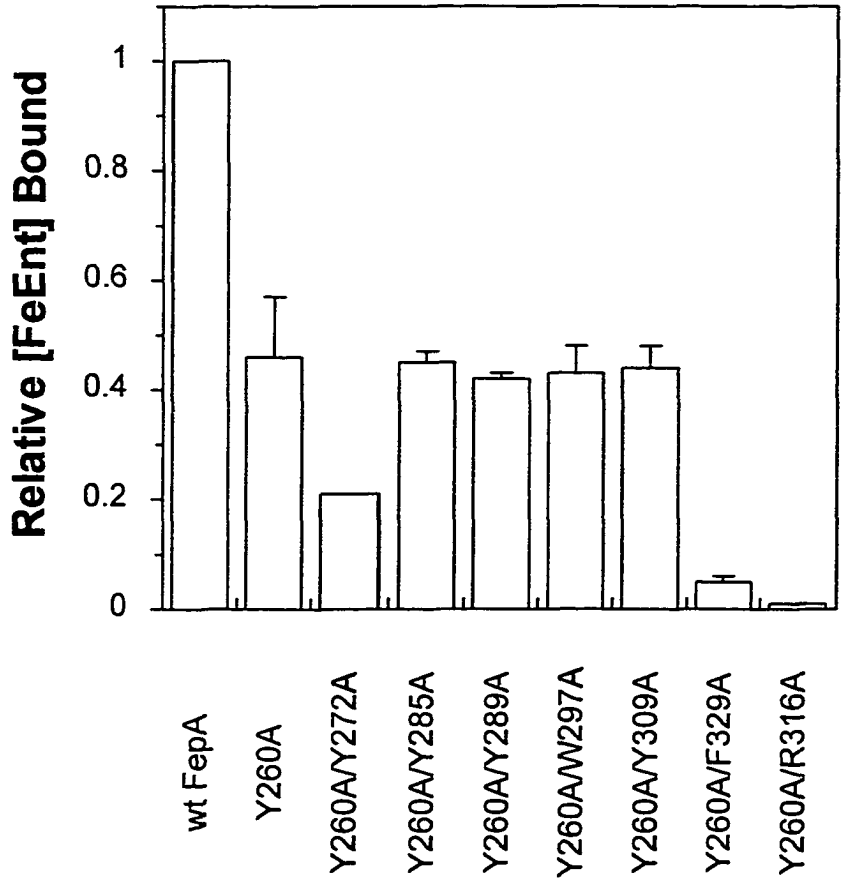

Figure 3-4. Siderophore binding abilities of Y260A series compared with wt FepA at 20nM substrate concentration. Ferric enterobactin binding assays were performed at 20nM on 2 x 10^7 cells. The total binding of each mutant was then compared with that of the wt protein. The standard deviations from three experiments were shown.

no further binding analysis was needed for them.

Effect of aromatic residue replacement on siderophore binding:

A detailed FeEnt binding experiment was conducted to study to what extent each mutant changed the binding affinity. As shown above, three single mutants, Y260A, Y272A, and F329A, and three double mutants derived from them, Y260A/Y272A, Y260A/F329A, and Y272A/F329A, were compared with the wild type protein in the binding affinity (Figure 3-5, Figure 3-6 & Table 3-1). All the measurements were made at 0°C, using KDF541 as a negative control.

Among the single substitutions (Figure 3-5), Y272A showed the same affinity as the wild type receptor. F329A showed only a slightly weaker affinity. Y260A, however, significantly decreased the binding affinity for FeEnt, with a K_d of 9.7nM, compared with that of the wild type receptor 0.086nM.

Y272A only showed reduced affinities when combined with either Y260A or F329A (Figure 3-6). From all mutants, both single and in combinations, it was revealed that Y272A had the weakest effect on binding. However, Y272A changed the receptor function significantly when combined with F329A. This combination resulted in a 90-fold decrease in the binding affinity compared with only a 2-fold decrease by F329A itself. With the previous method for FeEnt binding assays, the effects of Y272A, in any of the combinations, were not experimentally detectable, illustrating the efficacy of our new binding techniques. The aromatic residues

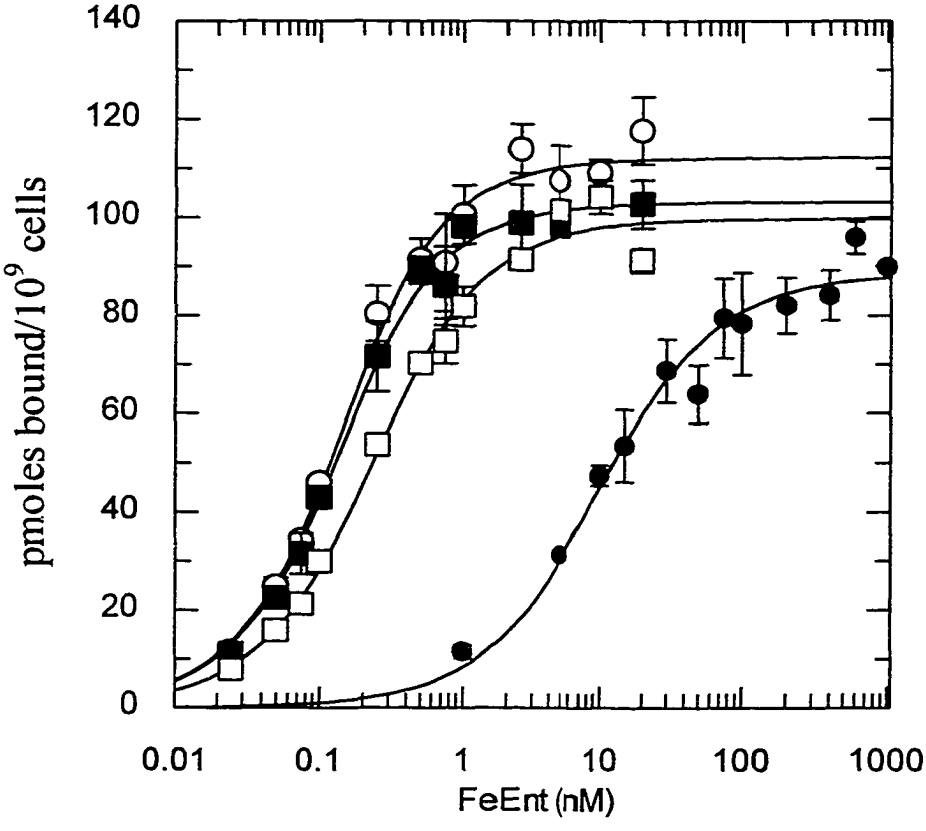

Figure 3-5. Concentration dependence of ferric enterobactin binding by single aromatic replacement mutants. Data points are the mean values of three experiments. ○, ++ (K_d, 0.085nM); ●, Y260A (K_d, 9.7nM); ■, Y272A (K_d, 0.085nM); and □, F329A (K_d, 0.18nM).

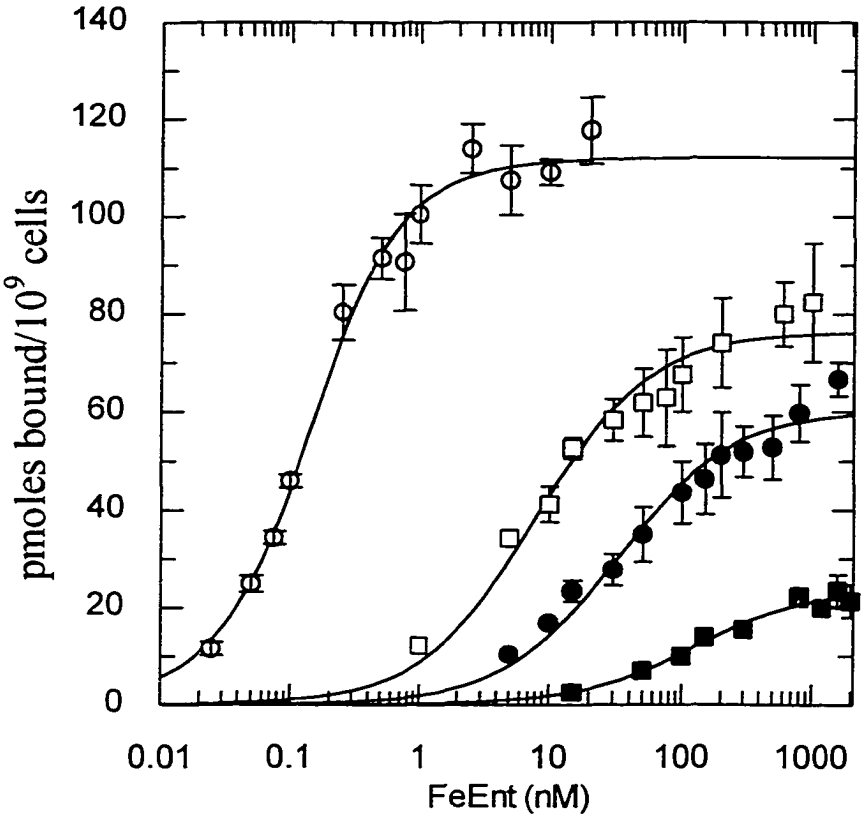

Figure 3-6. Concentration dependence of ferric enterobactin binding by double aromatic substitution mutants. Data points are the mean values of three experiments. O, ++ (K_d, 0.085nM); ●, Y260A/Y272A (K_d, 33nM); ■, Y260A/F329A (K_d, 126nM); and □, Y272A/F329A (K_d, 7.8nM).

Table 3-1. Phenotypic properties of FepA aromatic substitution mutants

FepA mutant	Ferric enterobactin					Colicin B	Colicin D
	Binding* and transport ‡						
	K_d	Cap.	K_m	V_{max}	Nutrition	Killing≠, ++	Killing≠, ++
++	0.086	112	0.27	181	19	100	100
Y260A	9.7	88	33	148	23	50	100
Y272A	0.085	103	0.33	150	19	100	100
F329A	0.18	100	5.5	135	19	50	100
Y260A/Y272A	33	60	128	126	25	50	100
Y260A/F329A	126	24	367	161	25	50	100
Y272A/F329A	7.8	76	23	128	23	50	100

* K_d (nM) and Capacity (pmoles bound/10^9 cells) were determined from the concentration-dependence of ferric enterobactin binding; the mean values from three sets of experiments were plotted with GraFit 4.0 (Erithacus), using the "Bound versus Total" equation. The mean standard errors (SE) for K_d and Capacity were 14% and 3%, respectively.

‡ K_m (nM) and V_{max} (pmoles transported/min per 10^9 cells) of uptake were determined from ferric enterobactin transport assays. The mean values of three independent assays were plotted with GraFit 4.0, using "Enzyme Kinetics" equation. The mean SE's for K_m and V_{max} were 19% and 5%, respectively. Nutritional test results shown were the diameters of the growth halo in millimeters around ferric enterobactin discs.

≠ Colicin killing was determined based on the mutant sensitivities to colicins compared with the wild-type FepA.

involved adequately explain that the interaction between ferric enterobactin and its receptor is multi-component. It involves positively charged residues (Newton *et al.*, 1997), aromatic residues (this study), and, possibly, other components not yet revealed. More importantly, among the single aromatic component, the interaction is multi-dimentional. The stereospecificity of the interaction most likely determined that each aromatic residue would contribute differently to the binding affinity, due to the specific orientation of the ligand when it interacts with the receptor. That is, there is not as much π-π interaction between Y272 and the ligand as there is between Y260 and the ligand.

Effect of aromatic residue replacement on siderophore transport:

To further test the effect of aromatic residue replacement on the ferric siderophore transport, a screening test was performed on the mutants which did not show any decreased binding affinity. The mutants showing decreased binding affinities were not included in the transport screening assay because they were expected to have decreased transport abilities. Therefore, it would be necessary to perform detailed transport assays on those mutants. The screening assays (Figure 3-7) indicated that there were no transport abilities for Y260A and F329A single mutants at the ligand concentration of wild type K_d, while single mutant Y272A retained its wild type transport capability. All the other mutants, as expected, did not show any significant decrease in transport ability. To test if Y260A and F329A would show

further decrease in their transport abilities when combined with Y285A, Y289A, W297A or Y309A, Y260A, and F329A series of mutants were assayed using different concentrations (Figure 3-8 and Figure 3-9). No further decreases were observed for any of the combinations tested. Therefore, I concluded that Y285, Y289, W297 and Y309 were not important in the interaction between FeEnt and its receptor.

The important roles played by Y260, Y272 and F329 were again revealed in the concentration dependence of the siderophore transport. While Y272A did not show much change in transport capability (Figure 3-10), neither FepA Y260A nor FepA F329A showed any significant transport at FeEnt concentration below the wild type K_m (Figure 3-7 and Figure 3-10). It was noteworthy that the latter mutant demonstrated a difference between binding affinity and transport capability. While F329A only had a slightly lower binding affinity (Figure 3-5, Table 3-1; K_d 2-fold of wild type receptor), its transport capability was further decreased (Figure 3-10, Table 3-1; K_m 20-fold of wild type receptor). On the other hand, for both Y260A and Y272A, the changes in the binding affinity was reflected in capable decreases of the transport (Table 3-1). For mutants containing any two of the three important residues, further deficiencies in transport were observed, in the order of Y272, F329A and Y260A, with Y260A/F329A least effective in transport (Figure 11, Table 3-1).

The uptake ability of the mutants was further studied by siderophore nutrition assays. Except Y260A series and the Y272A/F329A combination, all the other mutants showed wild type uptake ability with a halo 19mm in diameter. Y260A, by

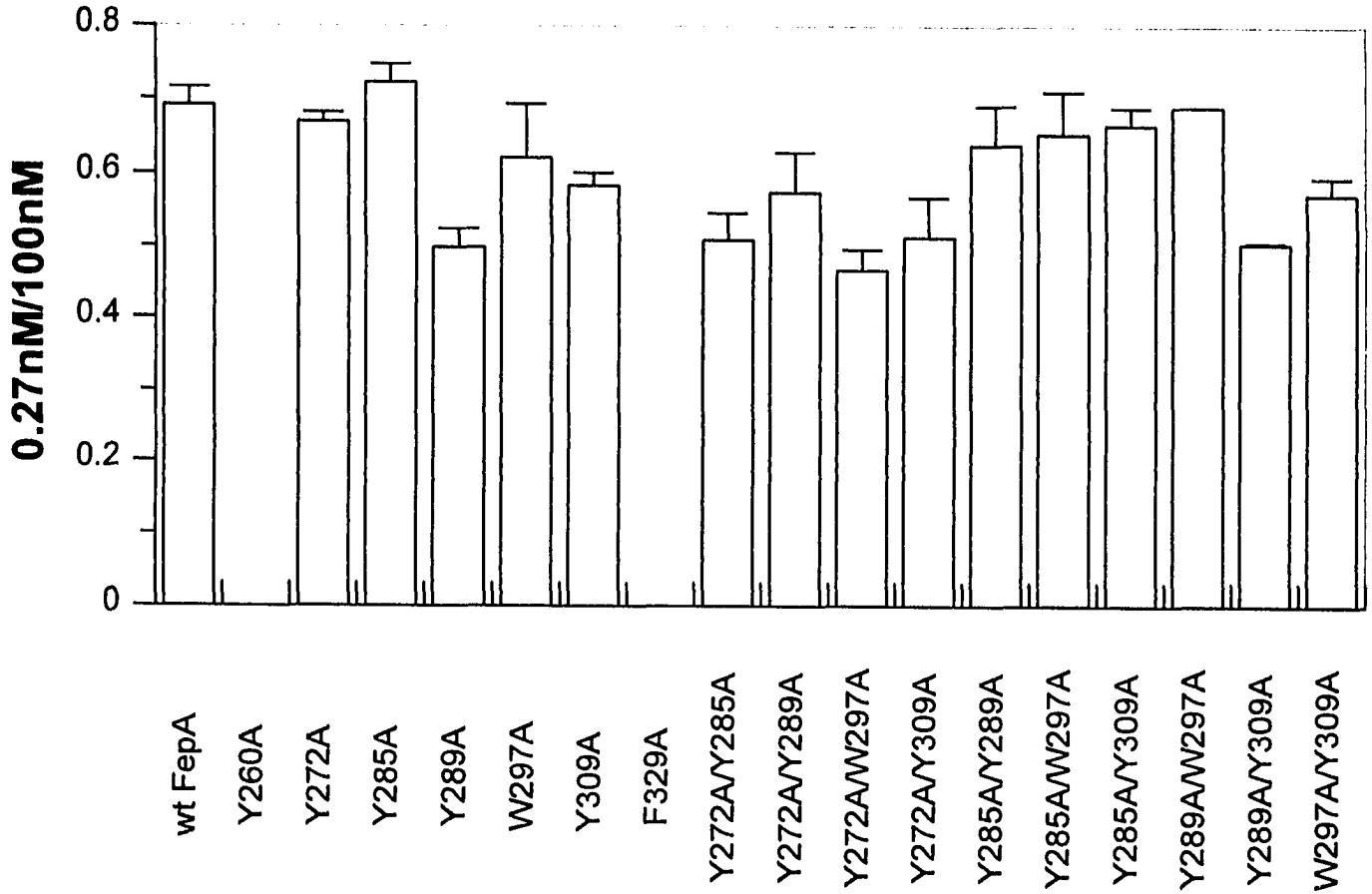

Figure 3-7. Siderophore uptake screening at wild type K_d FeEnt concentration. Ferric enterobactin transport assays were performed at two concentrations (0.27nM and 100nM) for wild type FepA and the aromatic substitution mutants. The transport capabilities were compared using the ratio at these two concentrations. The error bars represent the standard deviations from three experiments.

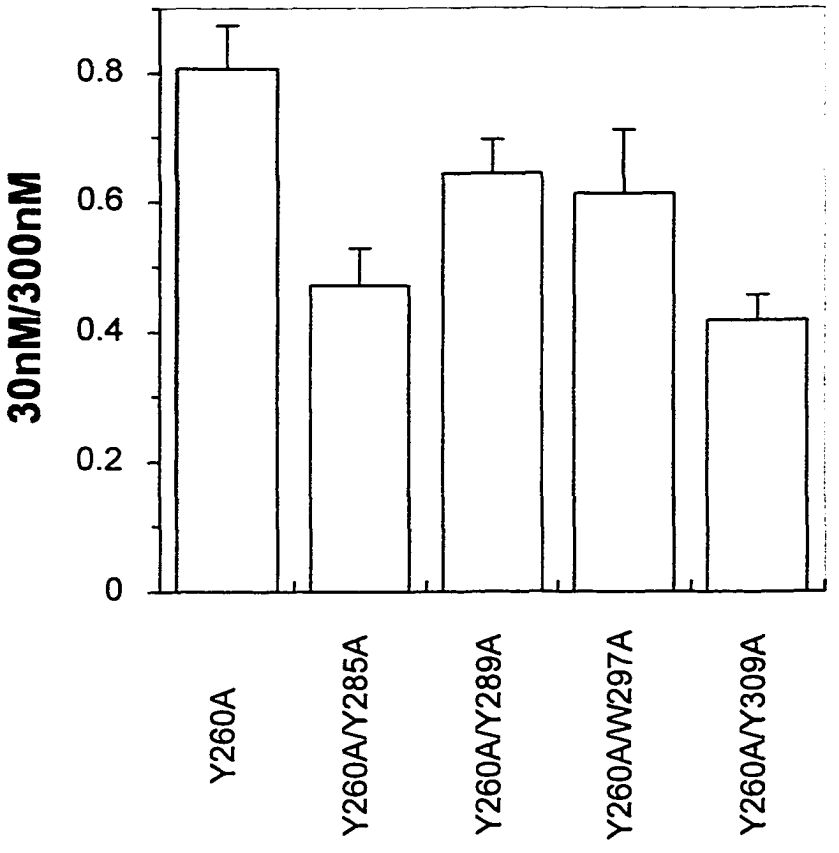

Figure 3-8. Siderophore uptake screening for Y260A mutant series. Ferric enterobactin transport assays were performed at two concentrations (30nM and 300nM) for the aromatic substitution mutants containing Y260A. The transport capabilities were compared with Y260A mutant using the ratio at these two concentrations. The error bars represent the standard deviations from three experiments.

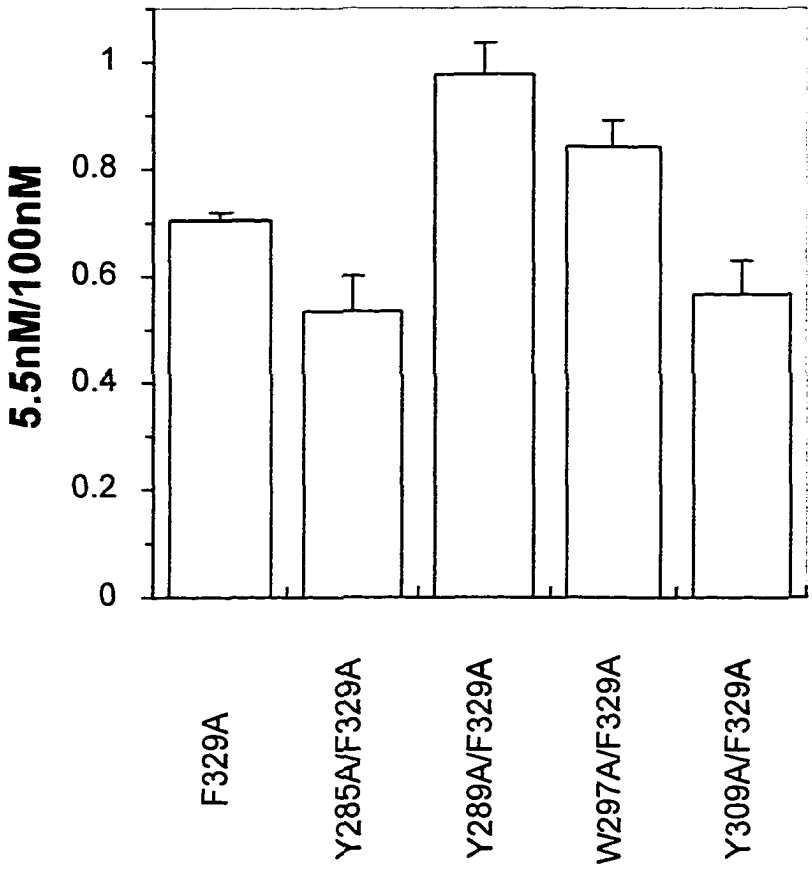

Figure 3-9. Siderophore uptake screening for F329A mutant series. Ferric enterobactin transport assays were performed at two concentrations (5.5nM and 100nM) for the aromatic substitution mutants containing F329A. The transport capabilities were compared with F329A mutant using the ratio at these two concentrations. The error bars represent the standard deviations from three experiments.

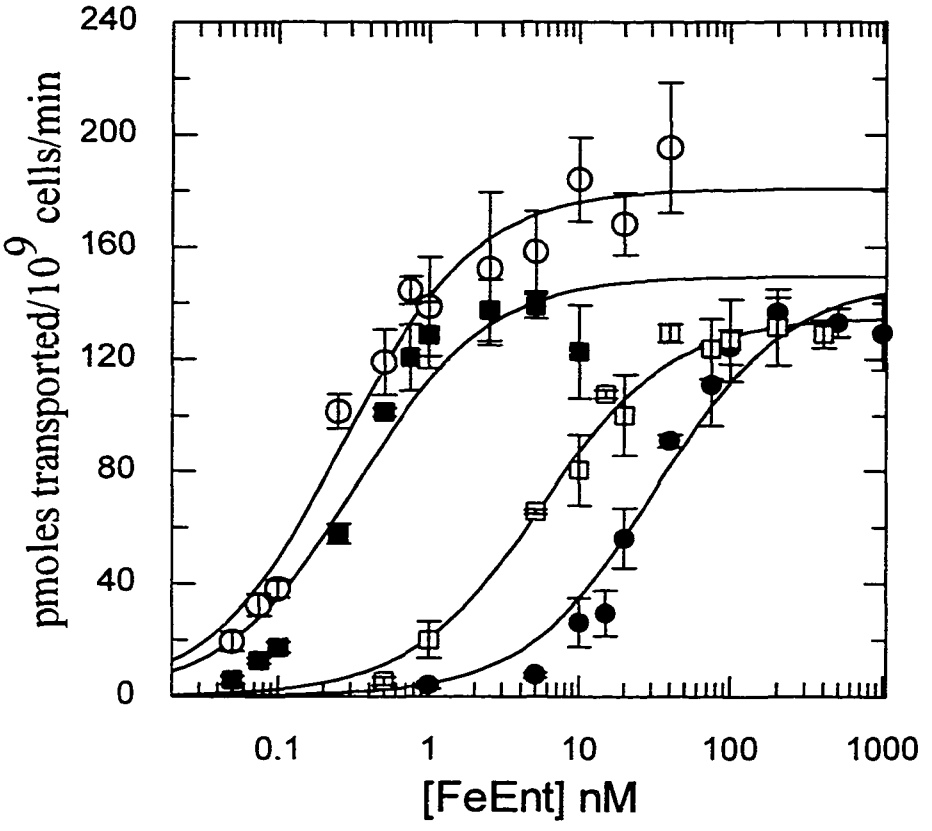

Figure 3-10. Concentration dependence of ferric enterobactin uptake by single aromatic replacement mutants. Data points are the mean values of three experiments. O, ++ (K_m, 0.27nM); ●, Y260A (K_m, 33nM); □, Y272A (K_m, 0.33nM); and ■, F329A (K_m, 5.5nM).

itself or combined with any of the other four nonessential residue substitutions, had the same uptake pattern, i.e., slow absorption, and a faint halo relatively large in size (23mm, Table 3-1). Y272A and F329A, by themselves, did not reveal any alteration of growth on siderophore. However, when they were combined, a halo (23mm, Table 3-1) similar to that of Y260A was observed. Y260A, when combined with Y272A or F329A, had an even fainter halo 25mm in diameter (Table 3-1). All the nutrition assay results agreed very well with those of the siderophore binding and transport experiments. In conclusion, Y260, Y272, and F329 play an important role in siderophore absorption: their mutation to alanine was detrimental enough that the growth of cells was affected when ferric enterobactin was the only source for iron, as in the case of the above nutrition assay.

Effect of aromatic residue replacement on colicin sensitivities:

None of the aromatic replacement mutants, whether alone or in combinations, showed any effect on colicin sensitivity: the mutations introduced into the receptor did not change the functionality of FepA as the receptor for colicins B and D. Y260, Y272 and F329, though important for siderophore binding and transport, do not appear essential in the function of FepA as a receptor for colicins. Previous research on positively charged residues (Newton *et al.*, 1997) indicated that arginines 286 and 316 were important for colicin susceptibility, although in the case of ColB the mutations did not directly change the colicin binding reaction.

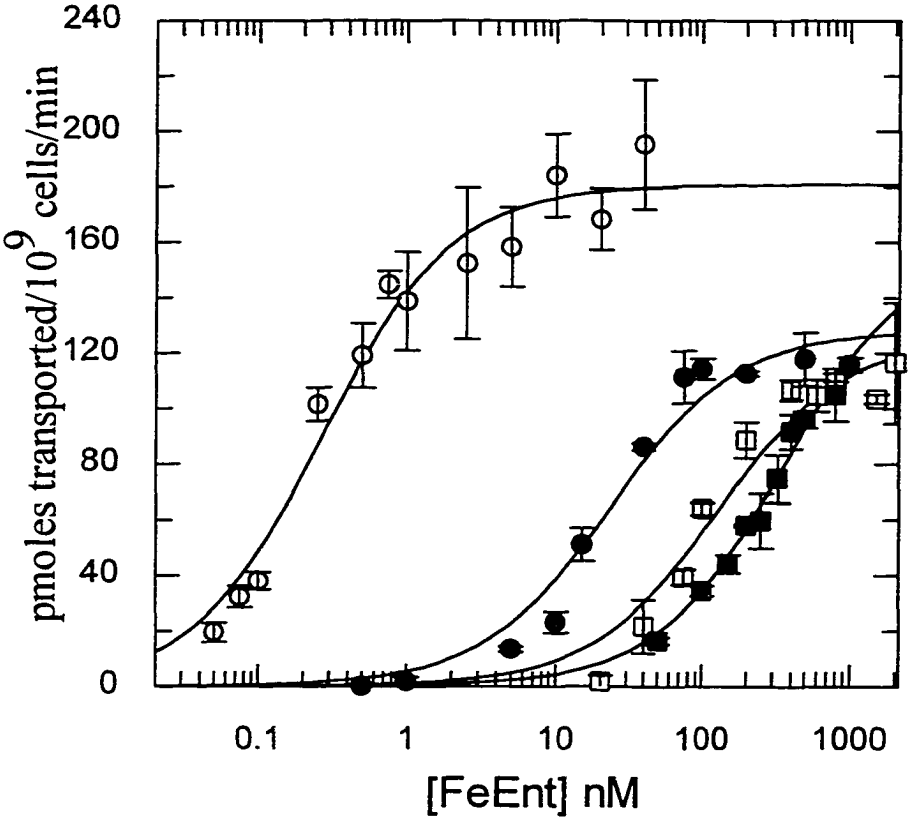

Figure 3-11. Concentration dependence of ferric enterobactin uptake by double aromatic substitution mutants. Data points are the mean values of three experiments. O, ++ (K_m, 0.27nM); □, Y260A/Y272A (K_m, 128nM); ■, Y260A/F329A (K_m, 367nM); and ●, Y272A/F329A (K_m, 23nM).

The Aromatic and Positively Charged Components

Experimental strategies:

Studies on the aromatic component showed that three aromatic residues, Y260, Y272, and F329, are the residues involved in the interaction between ferric enterobactin and its receptor. These residues, when mutated to alanine in combinations, showed significant decreases in the functionality as the receptor for ferric enterobactin. An important question, then, arises: is it possible that the double mutation disrupted a specific interaction between the aromatic siderophore and the aromatic residues of FepA, or did the mutations change the global or local protein conformation, which then led to the decrease in the ligand-receptor interaction? The colicin data argue against the latter alternative. Further experiments were designed to test whether the single aromatic substitutions did disrupt the multi-component interaction between ferric enterobactin and its receptor. This goal was accomplished by combining aromatic residue substitutions with arginine substitutions, that comprise another component of the ligand binding event.

Candidates of the positively charged component:

Previous studies on the positively charged component of FepA (Newton *et al.*, 1997) indicated that four arginine residues are conserved in the central region of FepA in which two of them, R286 and R316, are essential in the interaction between ferric

enterobactin and its receptor. Between the two, R316A was more significant to FeEnt binding and transport, and also decreased sensitivities to both colicin B and colicin D. Therefore, R316A was chosen to combine with all the important aromatic residue substitutions, to further study siderophore recognition by the multi-component receptor protein. Ultimately, the analysis of the R316A combinations also strengthened the conclusion that the above three aromatic residues are important for siderophore recognition, but not that of colicins.

Site directed mutagenesis:

R316A mutant was generated previously (Newton *et al.*, 1997). For the double combinations, Y260A, Y272A and F329A mutants were used as the templates for generating the combination with R316A. The mutants thus generated were then transformed into the KDF541 strain. R316A combinations did not have any effect on the growth of the bacterial strain, and the mutant proteins, when grown under iron deficient conditions, were expressed at the same level as the wild type protein (Figure 3-12).

The alteration of siderophore binding due to aromatic/charge replacement:

Since previous research (Newton *et al.*, 1997) was performed under substrate depletion conditions, it was impossible to see the small changes in binding affinity

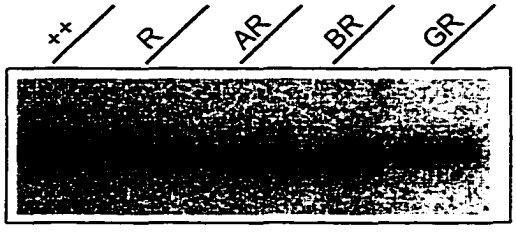

Figure 3-12. Expression of FepA aromatic/charge mutants. 5 x 10^7 cells grown in MOPS media were harvested, lysed and subjected to Western immunoblot with mAb41 and ^{125}I-protein A. The nitro cellulose paper was then subjected to autoradiography. Y260A, Y272A, F329A, and R316A were abbreviated as A, B, G, and R, respectively.

when the residue was replaced (K_d for R316A was reported to be 27nM compared with 22nM for wt FepA). In this study, a 5-fold decrease in the binding affinity was observed (K_d 0.4nM compared with 0.086nM for the wild type protein, Table 3-2). When combined with R316A, Y272A, F329A, and Y260A showed the same relative effects on receptor affinity (Figure 3-13, Table 3-2). Among the three aromatic residues, Y260 was the most important in siderophore recognition, followed by F329, with Y272 being the least important. This result agreed with the evidence gathered in the aromatic residue combination mutants. The binding affinity of R316A, compared with the binding affinities for all the single aromatic residue substitution mutants, was stronger than Y260A, but weaker than both Y272A and F329A (Table 3-1 and Table 3-2). The above conclusions were also confirmed when the binding affinities of all the possible double combinations were carefully reviewed (Table 3-1 and Table 3-2). Therefore, the alteration of the binding interaction between ferric enterobactin and its receptor appears not from an altered conformation when two aromatic substitutions were introduced at the same time. Instead, it is likely that the removal of two contact points between ferric enterobactin and FepA generated a weaker receptor. The affinities of all the mutant receptors, compared with specific channels such as LamB, were still quite high, which makes sense because in biological systems, the iron availability is very low. Therefore, the receptor has to avidly absorb the very low amount of free iron or to compete with other species for iron to meet cell growth requirements.

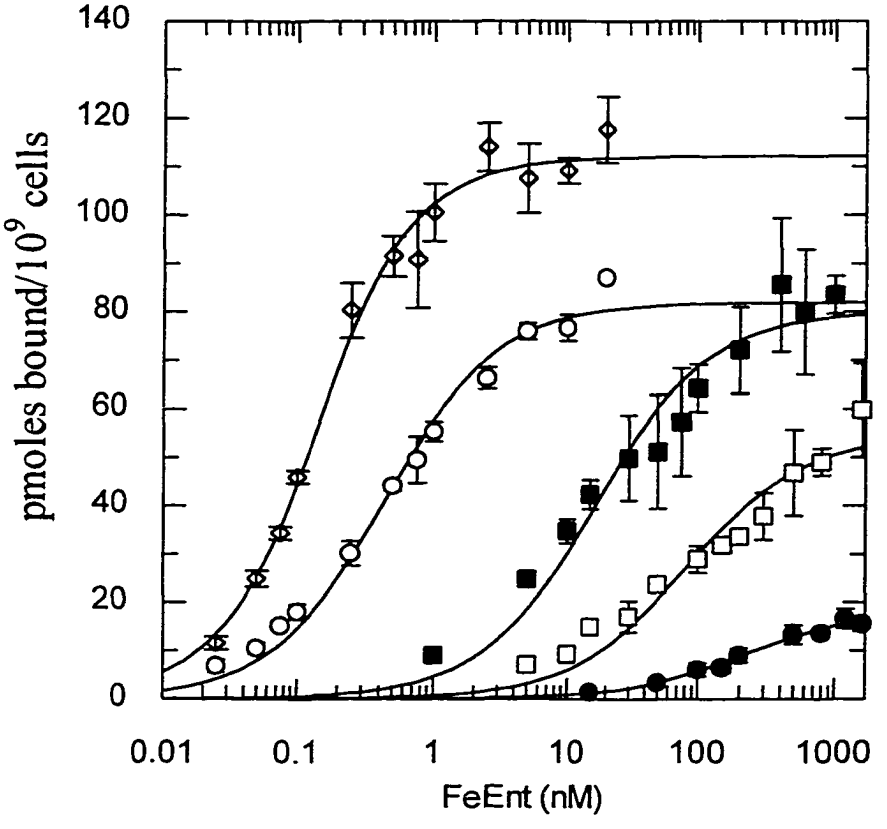

Figure 3-13. Concentration dependence of ferric enterobactin binding by aromatic/charge substitution mutants. Data points are the mean values of three experiments. ◇, +- (K_d, 0.085nM); ○, R316A (K_d, 0.40nM); ●, Y260A/R316A (K_d, 222nM); ■, Y272A/R316A (K_d, 17nM); and □, R316A/F329A (K_d, 83nM).

Table 3-2. Phenotypic properties of FepA aromatic/charge substitution mutants 3-

FepA mutant	Ferric enterobactin					Colicin B	Colicin D
	Binding* and transport‡						
	K_d	Cap.	K_m	V_{max}	Nutrition	Killing≠, ++	Killing≠, ++
++	0.086	112	0.27	181	19	100	100
R316A	0.40	82	16	117	22	2.5	8
Y260A/R316A	222	18	793	93	23	2.5	8
Y272A/R316A	17	80	133	129	24	2.5	8
F329A/R316A	83	55	486	105	24	2.5	8

* K_d (nM) and Capacity (pmoles bound/10^9 cells) were determined from the concentration-dependence of ferric enterobactin binding; the mean values from three sets of experiments were plotted with GraFit 4.0 (Erithacus), using the "Bound versus Total" equation. The mean standard errors (SE) for K_d and Capacity were 14% and 3%, respectively.

‡ K_m (nM) and V_{max} (pmoles transported/min per 10^9 cells) of uptake were determined from ferric enterobactin transport assays. The mean values of three independent assays were plotted with GraFit 4.0, using "Enzyme Kinetics" equation. The mean SE's for K_m and V_{max} were 19% and 5%, respectively. Nutritional test results shown were the diameters of the growth halo in millimeters around ferric enterobactin discs.

≠Colicin killing was determined based on the mutant sensitivities to colicins compared with the wild-type FepA.

The effect of aromatic/charge replacement on siderophore uptake:

The replacement of R316 with alanine generated a mutant receptor with a slightly slower uptake rate (K_m 16nM, about 60-fold less avid; Figure 3-14; Table 3-2), which was not previously observed due to the substrate depletion (Newton *et al.*, 1997). This change was also observed in the nutrition assay, where a slightly larger halo (22mm compared with the normal 19mm; Table 3-2) was obtained. The difference between binding and uptake for mutant R316A was about the same as F329A. In the case of F329A, the change for K_d and K_m is 2-fold and 20-fold, respectively, while for R316A, the change is 5-fold and 60-fold. These differences were reflected in the binding and uptake of the double combination mutants. The binding affinities of all the double mutants in Table 3-1 and Table 3-2 can be summarized in the following order: Y272A/F329A > Y272A/R316A > Y272A/Y260A > R316A/F329A > Y260A/F329A > Y260A/R316A, which agreed with the binding affinities for the single mutants: Y272A > F329A > R316A > Y260A. In other words, the combinational decreases were an additive function of the individual, mutationally induced decreases. However, the above order was not retained in siderophore uptake. While the single mutants still kept the above order, the double mutants turned out to have a different behavior (Figure 3-15; Table 3-1; Table 3-2): Y272A/F329A > Y260A/Y272A > Y272A/R316A > Y260A/F329A > R316A/F329A > Y260A/R316A. While the difference between Y260A/Y272A and Y272A/R316A is within the experimental error, the differences between binding and

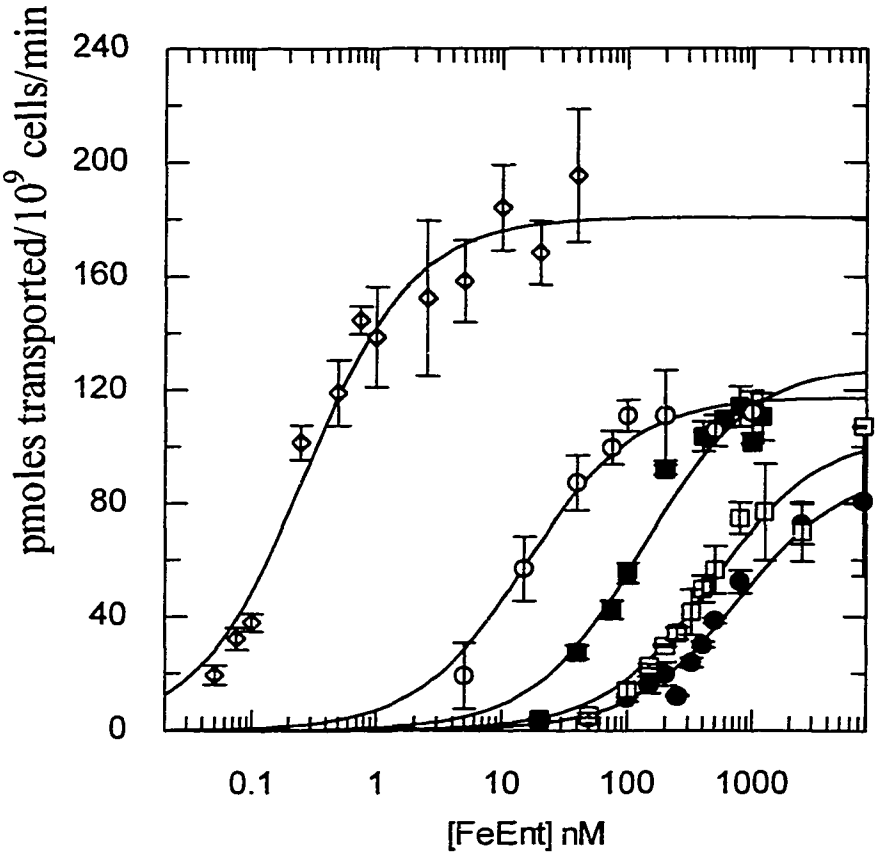

Figure 3-14. Concentration dependence of ferric enterobactin uptake by aromatic/charge substitution mutants. Data points are the mean values of three experiments. ◇, ++ (K_m, 0.27nM); ○, R316A (K_m, 16nM); ●, Y260A/R316A (K_m, 793nM); ■, Y272A/R316A (K_m, 133nM); and □, R316A/F329A (K_m, 486nM).

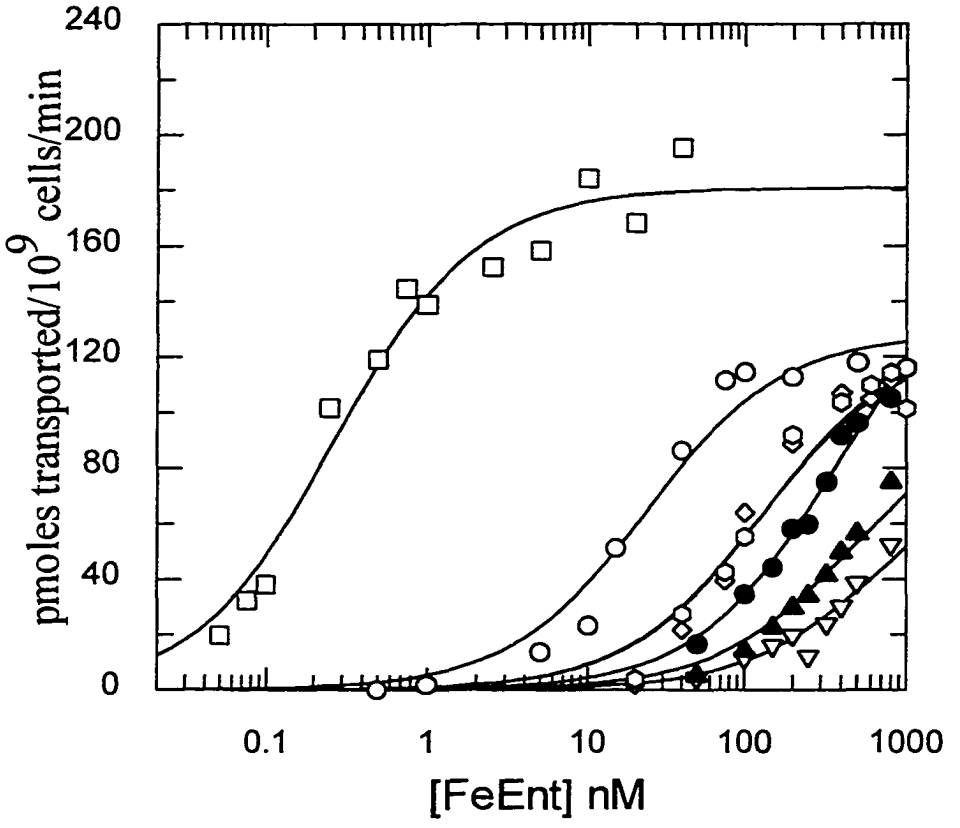

Figure 3-15. Concentration dependence of ferric enterobactin uptake by aromatic and aromatic/charge substitution mutants. Data points are the mean values of three experiments. □, ++ (K_m, 0.27nM); ▽, Y260A/R316A (K_m, 793nM); ○, Y272A/R316A (K_m, 133nM); ▲, R316A/F329A (K_m, 486nM); ◇, Y260A/Y272A (K_m, 128nM); ●, Y260A/F329A (K_m, 367nM); and ○, Y272A/F329A (K_m, 23nM).

transport for Y260A/F329A and R316A/F329A are apparent. Since both R316A and F329A had larger fold decrease in their uptake, when they were combined, the decrease was more significant than the Y260A/F329A combination.

Effect of aromatic/charge replacement on colicin sensitivities:

R316A mutation slightly changed the colicin sensitivities (Newton *et al.*, 1997). For colicin B, the reduction in killing was not due to the impaired binding affinity (Newton *et al.*, 1997). Reduced binding only occurred when R316A was combined with R286A. In this work, the colicin sensitivities were further extended to aromatic substitution mutants when they were combined with R316A. For all R316A mutants, there was a 40-fold and a 10-fold decrease in the sensitivities to colicin B and colicin D, respectively. Such a decrease, without any doubt, is due to the replacement of R316 residue. The added aromatic substitution did not change the colicin sensitivity at all, which further supported the conclusion made earlier that Y260, Y272, and F329 are only essential for FepA as the receptor for ferric enterobactin. These residues are not directly involved in the interaction between FepA and colicins.

The Structural Information Conveyed in the Disulfide Bond

In the wild type FepA protein, there are two native cysteines, cys486 and cys493, linked together by a disulfide bond (Liu *et al.*, 1994). Previous studies on another outer membrane protein LamB, the outer membrane receptor protein in the maltose transport system, revealed that the intrasubunit disulfide bond formed between cys22 and cys38 does not affect the transport function of the outer membrane protein. Instead, it reduces the heat stability of the LamB trimer (Luckey *et al.*, 1991). Neither the disulfide bond in FepA (Liu *et al.*, 1994) nor the one in LamB (Ling and Luckey, 1994) is exposed to the surface in the native protein. Unfortunately, the disulfide bond was not located in the crystal structure of FepA. Therefore, it is interesting to know whether the disulfide bond formed in FepA is important for the function of FepA by site-directed mutagenesis.

Experimental strategies:

The disulfide bond was removed by replacing one of the cysteines with alanine. To analyze further if the functional change was due to the introduction of alanine instead of the deleted disulfide bond, the other cysteine, and further, both cysteines, were mutated to alanine to investigate whether further activity loss might occur.

Site-directed mutagenesis:

Site-directed mutagenesis for C486A and C493A was performed on the wild type structural gene using the mutagenesis primers for each individual mutant. The double mutant was constructed from the structural gene of C486A using the C493A primer. All the mutants, as shown in the Western blot (Figure 3-16), expressed the FepA protein at the wild type level when transformed into the KDF541 strain. The removal of the disulfide bond did not have any effect on the bacterial growth in iron deficient media.

Effect of disulfide bond removal on siderophore binding:

The binding experiment was performed as described, using the assay conditions for the group of mutants with lowest binding affinities. Preliminary binding assays showed that the cysteine substitution mutants had much lower V_{max} and the affinity was weaker than Y260A/R316A, the most ineffective aromatic/charge mutant studied.

Effect of disulfide bond removal on siderophore transport:

Siderophore nutrition assay was used to investigate the ability of the mutant receptor to utilize ferric enterobactin as the iron source to support growth. The removal of either of the two cysteines resulted in the decrease of the uptake ability and the alteration of the growth pattern. The mutant halo was much fainter and larger

than the wild type FepA, as observed in the aromatic mutants. Compared to the aromatic mutants, the removal of the disulfide bond produced an uptake pattern similar to the worst aromatic mutant. Not much difference was observed between C486A, C493A, and C486A/C493A (Table 3-3), indicating that the alteration in the uptake ability was due to the removal of the disulfide bond alone instead of the structural change introduced by alanines. However, the siderophore nutrition assay result is not conclusive, and kinetic parameters have to be determined to reach the final conclusion.

Effect of disulfide bond removal on colicin sensitivities:

The cysteine mutants were tested for colicin sensitivities (Table 3-3). All the three cysteine mutants showed very low colicin sensitivities, indicating that cysteine residues are important for colicins to function. The three different cysteine mutants did show some differences in the killing ability, where C493A showed the least colicin susceptibility. Surprisingly, the double mutant C486A/C493A had a slightly higher sensitivity than the single mutant C493A, indicating that there might be some additional conformational difference when each individual residue was replaced by alanine.

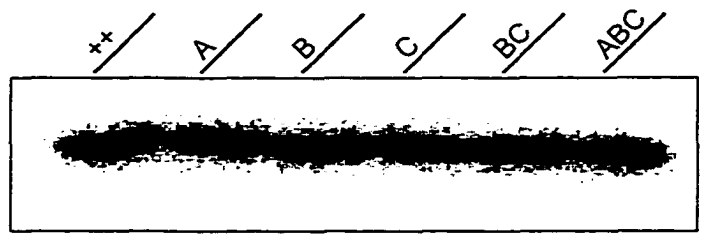

Figure 3-16. Expression of FepA cysteine mutants. 5 x 10^7 cells grown in MOPS media were harvested, lysed and subjected to Western immunoblot with mAb41 and ^{125}I-protein A. The nitro cellulose paper was then subjected to autoradiography. E280C, C486A, and C493A were abbreviated as A, B, and C, respectively.

Table 3-3. Phenotypic properties of FepA cysteine substitution mutants

Mutant	Nutrition	Colicin B	Colicin D
	(mm)	Killing, ++	Killing, ++
++	19	100	100
C486A	25	10	2
C493A	24	0.2	0.05
C486A/C493A	25	1	0.5

Biphasic Binding Between FepA and Ferric Enterobactin

We previously showed that FepA binds its ligands in two phases: an initial rapid phase followed by a much slower second phase (Payne *et al.*, 1997). Therefore, it is very likely that two groups of binding components are involved in the FepA function: while the first group participates in the initial absorption, the second group locks the ligands into the right position. This is reasonable for the function of FepA as a receptor for ferric enterobactin. When FepA absorbs iron siderophore from the aqueous environment where the concentration of the ligand remains low, it has to have an extremely strong "extraction power" to concentrate the iron siderophore on the cell surface. We examined the possible roles of the aromatic residues Y260, Y272, and F329 and the positively charged residue R316 in the ferric enterobactin binding domain.

Experimental strategies:

The crystal structure of FepA was used to determine the location of each essential residue in the barrel structure. The potential mutant candidates were further mutagenized to introduce a free cysteine in the ligand binding domain for the purpose of chemical modification with sulfhydryl specific "reporter" molecules. A fluorescent probe, 5-IAF, was then conjugated to the free cysteine in the purified protein. The fluorescent "reporter" attached protein was used in the binding assays.

What does the crystal structure tell us?

The crystal structure was not solved when we first started to investigate the roles played by the aromatic residues in the proposed ferric enterobactin binding domain. Fortunately, the partially solved crystal structure came out (Buchanan *et al.*, 1999) by the time we were getting close to locating the important residues in ferric enterobactin binding and transport. The two aromatic residues, Y260 and Y272, and the positively charged residue R316 are located at two different positions in the FepA crystal structure (Figure 3-17): Y272 is exposed to the cell surface while Y260 and R316 are further down in the top part of the transmembrane region. F329, though not solved in the crystal structure, is part of the surface-exposed loop, and most likely, located at the cell surface very close to residue Y272. Therefore, we proposed that Y272 and F329 might be involved in the initial binding while Y260 and R316 participate in the subsequent absorption of the ligand.

What do the previous data tell us?

Previous studies indicated that ferric enterobactin binding to FepA is a multi-component system: aromatic residues (this study) and positively charged residues (Newton *et al.*, 1997) are critical for the function of FepA. A ring of aromatic residues were believed to be involved in the initial extraction of FepA (Buchanan *et al.*, 1999) and FhuA (Ferguson *et al.*, 1998; Locher *et al.*, 1998); and FepA can tolerate deletions of various surface loops with the sacrifice of FepA functionality to different

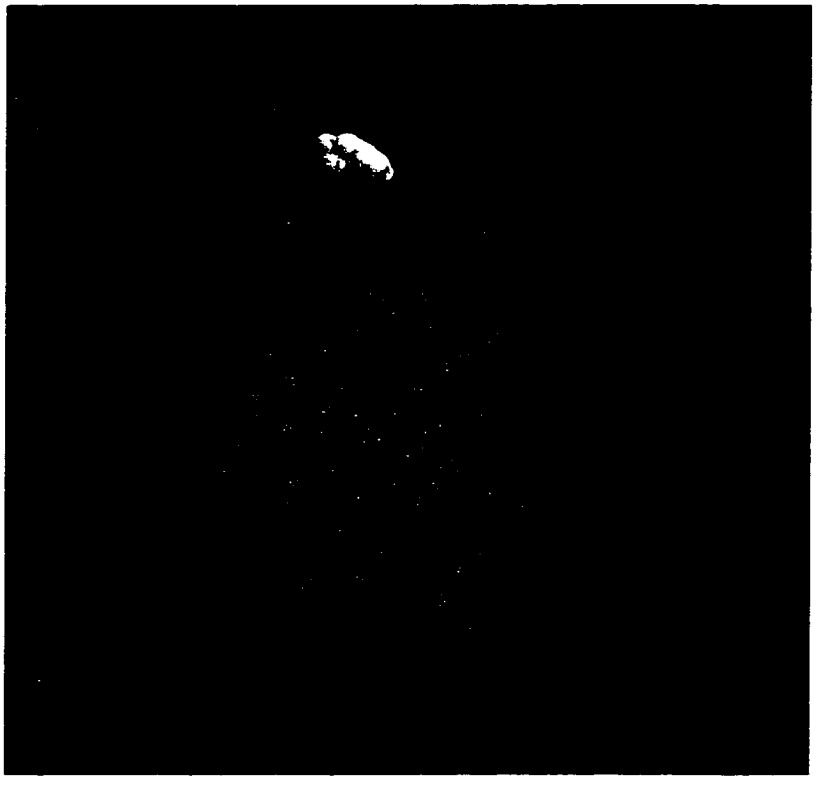

Figure 3-17. The crystal structure of FepA showing the locations of Y260, Y272 and R316. Y260, Y272 and R316 are presented in red, white and green, respectively.

extents (Newton *et al.*, 1999).

The multi-component feature of the ferric enterobactin receptor determines that any single or double substitution of the aromatic or positively charged residues would not completely destroy the functionality of the receptor. From the aromatic and aromatic/charge substitution results I noticed that one of the double combinations, Y272A/F329A, had an activity stronger than Y260A single mutant, which indicated that the proposed initial binding step involves more aromatic residues, and the alteration to any single one of them would not introduce much change to the receptor function. The latter was observed in the single mutation results, where the single alanine substitutions at positions 260 and 316 introduced much stronger deterioration to the receptor than those at positions 272 and 329.

Why was E280C introduced?

Due to the chemical features of ferric enterobactin, it was proposed that the negatively charged residues are not involved in ferric enterobactin-FepA interactions (Liu *et al.*, 1994). All the negatively charged residues in the central binding domain have been mutated to alanine singly and in double combinations (Qi and Klebba, unpublished data). None of the mutations were observed to introduce any change to the function of FepA.

The glutamic acid at residue 280 was negatively charged under physiological conditions. The cysteine mutant of E280 residue was first introduced by Liu *et al.*

(1994), and proven not to have any structural effect on the function of FepA (Liu *et al.*, 1994; *Jiang et al.*, 1997). Conformational changes to the E280C site were observed upon ligand binding both *in vitro* (Liu *et al.*, 1994) and *in vivo* (Jiang *et al.*, 1997).

Generation of polyclonal antibodies:

The fluorescent probes used in this study are too small to be used as antigens directly to immunize rabbits to generate polyclonal antibodies. Therefore, CPM, 5-IAF, and IAEDANS were first conjugated to BSA. The free probe was then removed by running a Sephadex G-50 gel filtration column (Figure 3-18), and probe conjugated BSA was used to immunize the rabbit.

Polyclonal antibodies were analyzed, using Western blot and ELISA. The former was aimed to find the specificity of the antibody and the latter to determine the titer of the antisera. The Western blot showed that the antisera demonstrated a strong immuno-specificity to the probe of our interest with a low affinity to BSA (Figure 3-19). ELISA assay indicated that a 1:500 dilution of the antisera would be appropriate for each of the antisera to be used in immuno assays (Figure 3-20).

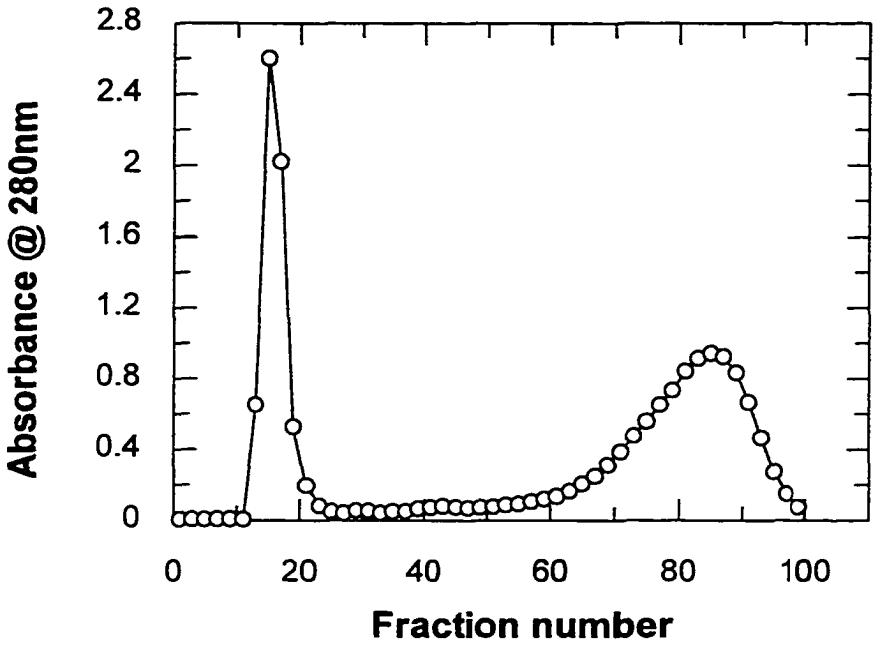

Figure 3-18. Sephadex G-50 column separation of free fluorescent probes from the BSA conjugation. CPM was labeled to BSA and loaded unto a Sephadex G-50 column of size 30mm × 200mm equilibrated in 50mM Tris-HCl pH7.5, 100mM NaCl. The UV absorption of the column fractions was measured at 280nm. Fractions 13-22 were pooled together as BSA-CPM conjugate, subjected to dialysis and used for immunizing rabbits to generate polyclonal antibodies. The same procedures were followed for 5-IAF and IAEDANS, and very similar column profiles were obtained.

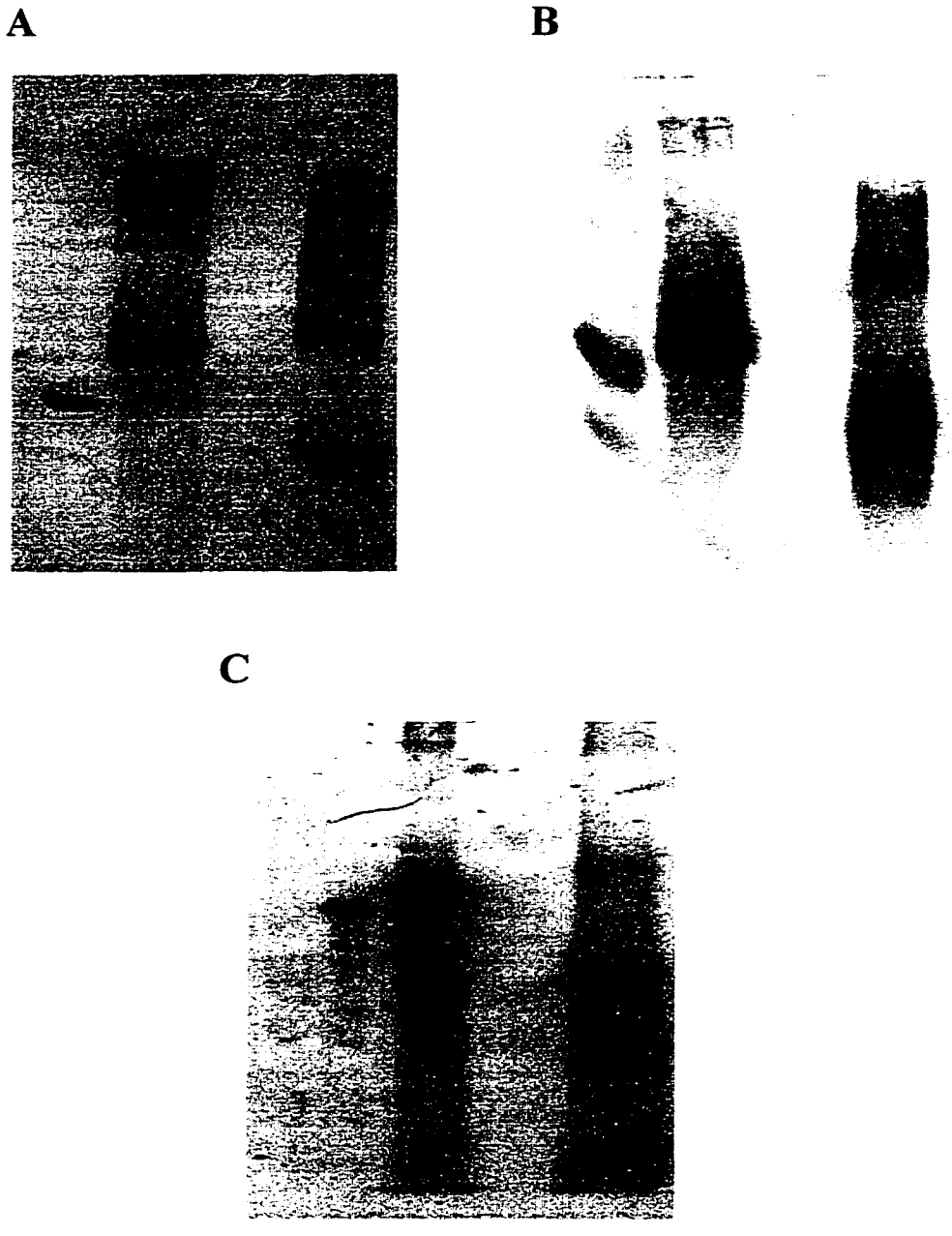

Figure 3-19. Western blot analysis for polyclonal antisera against fluorescent probes. 4 μg of protein was loaded on a 10% SDS-PAGE, and subjected to immunoblotting against anti-BSA-CPM (**A**), anti-BSA-IAF (**B**) and anti-BSA-IAEDANS (**C**). The samples in each blot were: BSA, probe-BSA, ovalbumin and probe-ovalbumin (from left to right).

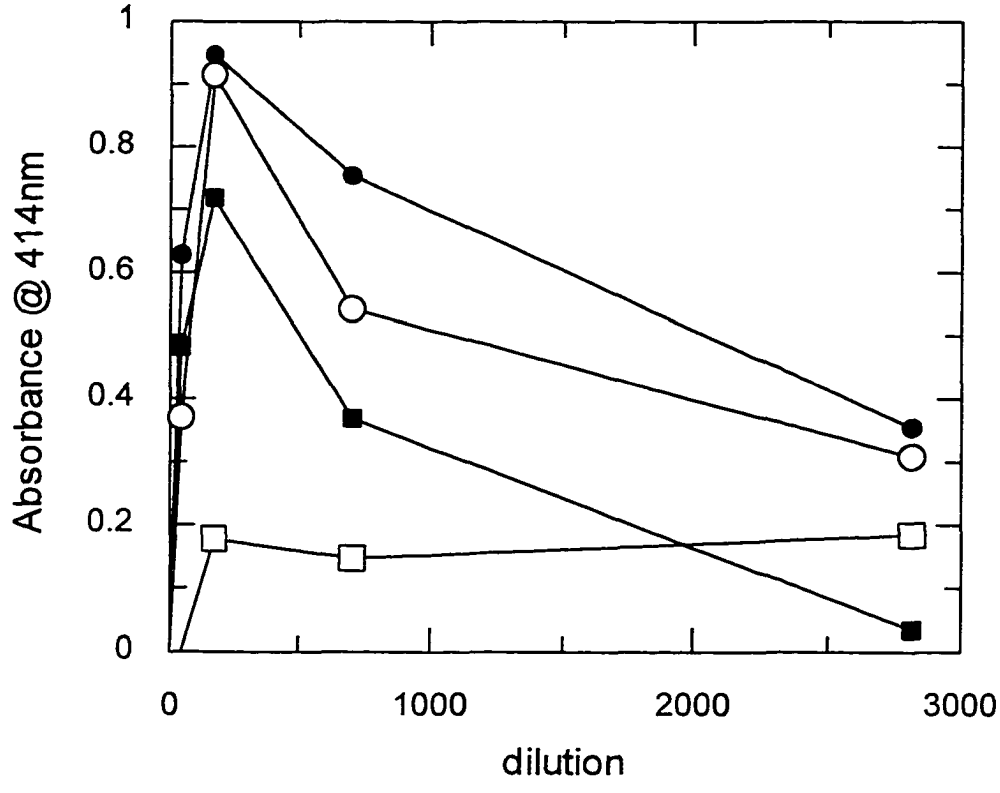

Figure 3-20. ELISA analysis for polyclonal antiserum against BSA-CPM. ELISA assay was performed against BSA (O), BSA-CPM (●), ovalbumin (□), and ovalbumin-CPM (■). Polyclonal antisera against BSA-IAF and BSA-IAEDANS showed similar titers.

E280C can be specifically labeled by fluorescent probes:

Fluorescent probes CPM, 5-IAF, and IAEDANS were used to label E280C FepA mutant proteins in this study. These probes were used for different applications or potential applications as we previously discussed. Their specificity to thiol groups and fluorescence features made them applicable to different aspects of our research. In this study, different methods were used to examine the labeling specificity of each of the fluorescent probes used.

It is relatively easy to check the labeling specificity of CPM to thiol group since CPM has a much stronger fluorescence intensity once being conjugated. In this study, E280C protein was labeled with CPM under denatured conditions at pH7.4, using the wild type FepA as a control (Figure 3-21). The labeling was very specific to the introduced cysteine in E280C protein without significant background labeling even when all the residues were denatured to be subjected to the chemical modification.

The labeling specificity of 5-IAF (Figure 3-22) was examined by Western blot and fluorescent emission scanning measurement. 5-IAF was proven to be very specific for thiol groups. The non-specific labeling for 5-IAF was extremely low. IAEDANS labeling specificity was investigated in a series of conjugation reactions at different pH's (Figure 3-23), which showed that the labeling was quite specific even at pH9.0.

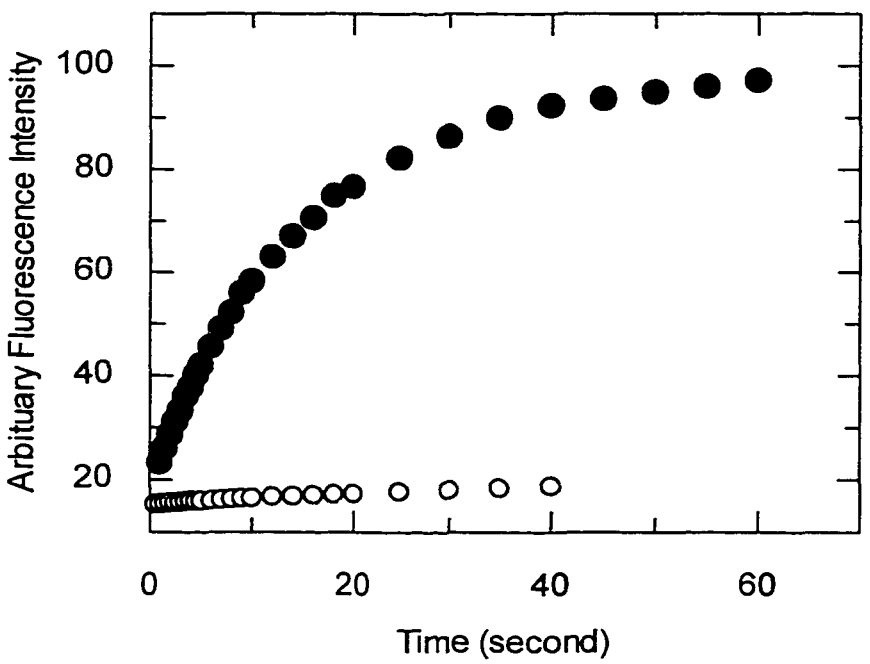

Figure 3-21. Labeling specificity of CPM to the E280C cysteine under denatured conditions. Fluorescent labeling time course was performed at 25°C on a SLM 8100 fluorimeter at excitation and emission wavelengths set at 490nm and 520nm, respectively. E280C (•, final concentration 50nM) in the reaction buffer (TTE, pH7.2) was denatured with 6M urea before CPM (final concentration 10μM) was added. Wild type FepA (O) was used as a control.

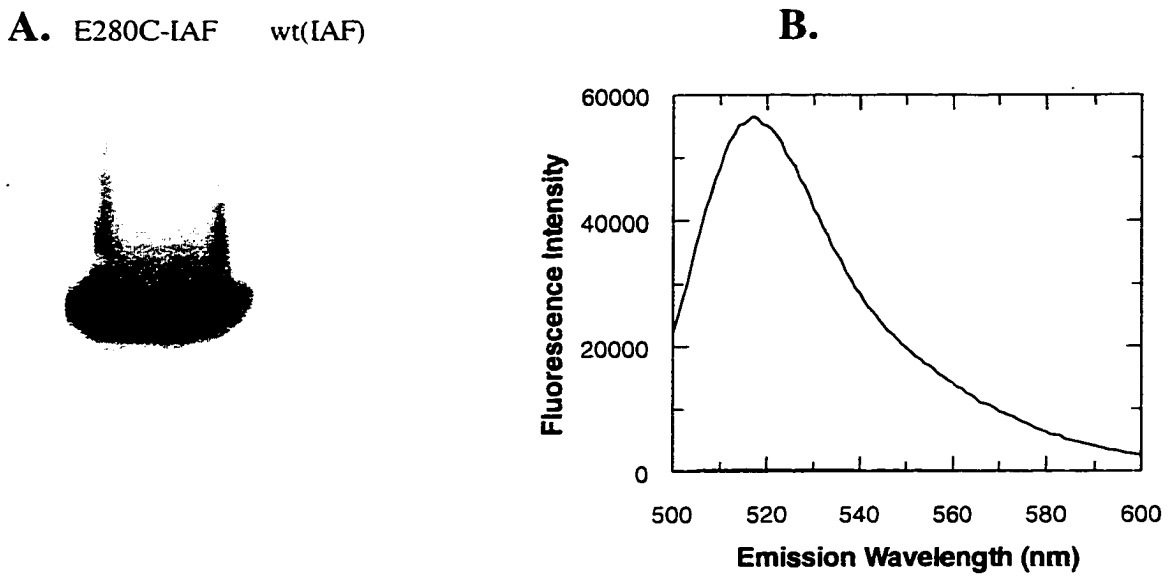

Figure 3-22. Labeling specificity of 5-IAF to thiol group in E280C FepA. E280C FepA (0.15mg/ml) in reaction buffer (TTE, pH7.2) was incubated with 10μM 5-IAF for 45min in dark at room temperature, precipitated by 2 volumes of ethanol and resuspended in 5ml fluorescent measurement buffer (1mM DM, 50mM MOPS pH7.0, 60mM NaCl). The precipitation step was repeated, and the labeled protein was resuspended into the fluorescent measurement buffer to make the final concentration 0.1mg/ml. The labeled protein was then dialyzed against the fluorescent measurement buffer. Wt FepA was used as a negative labeling control following the same labeling procedures. **A.** 10μg of protein was loaded onto a 10% SDS-PAGE gel, subjected to electrophoresis and immunoblotting using polyclonal antibody against BSA-IAF. **B.** The fluorescent emission scans of 5-IAF labeled E280C (blue line) and wt FepA (red line) were measured on a SLM 8100 fluorimeter with excitation wavelength set at 490nm.

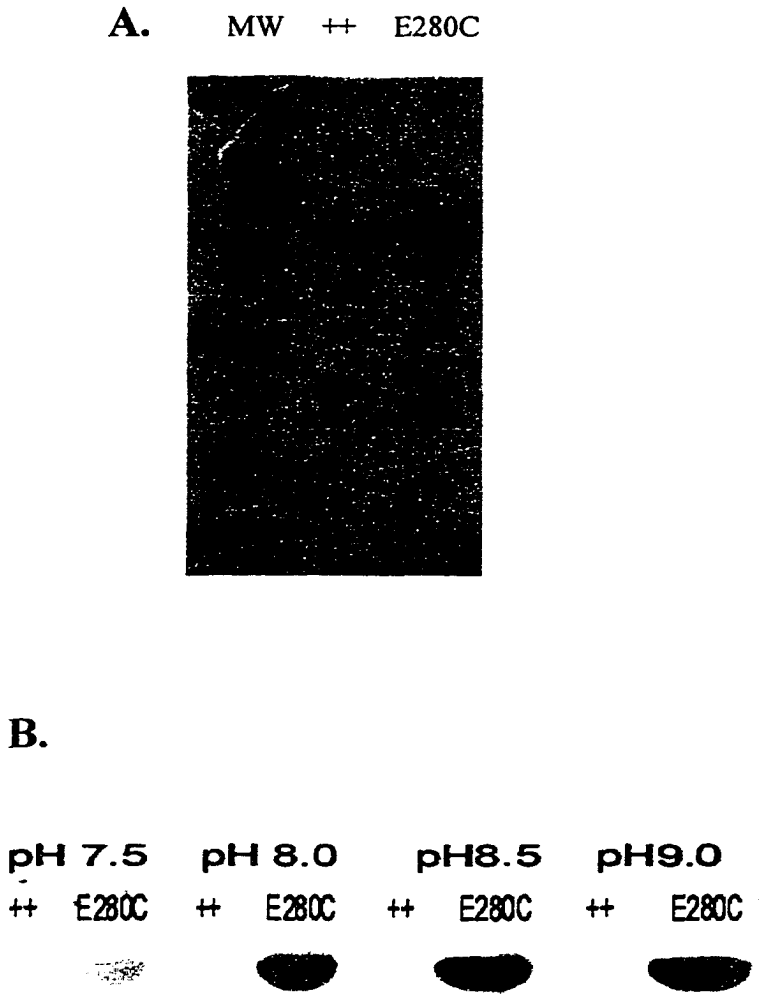

Figure 3-23. Labeling specificity of IAEDANS to thiol group in E280C FepA. E280C FepA (0.15mg/ml) in reaction buffer (TTE) was incubated with 10μM IAEDANS at different pH for 30 min in dark at room temperature. The reactions were stopped by adding SDS-PAGE loading buffer with β-mercaptoethanol, and subjected to electrophoresis and immunoblotting against BSA-IAEDANS polyclonal antibody. **A,** staining gel showing the amount of protein used in the labeling reaction; **B,** Western immunoblot showing the labeling reaction at pH7.5, 8.0, 8.5, and 9.0, respectively.

Ferric enterobactin binding changes the environmental accessibility of E280C site:

The increase of fluorescence intensity of CPM upon conjugation was used to investigate the labeling time course of E280C FepA. The cysteine residue in E280C was readily to be labeled by CPM, but upon the treatment of ferric enterobactin, the labeling of the cysteine was completely blocked (Figure 3-24). FepA undergoes conformational change upon FeEnt binding, which may then have reduced the accessibility of cysteine 280 site.

E280C-IAF can be quenched dynamically and statically:

If E280C is located within the ferric enterobactin binding domain, then, ferric enterobactin could possibly be used as a quencher to 5-IAF, due to the aromaticity of ferric enterobactin. The quenching, if existing, could be of both static and dynamic quenching. But if both of them exist in the same system, it would be difficult to differentiate the dynamic quenching from static binding when studying the interaction between FepA and ferric enterobactin.

Dynamic quenching from NaI on E280C-IAF was studied at two temperatures, 4°C and 25°C (Figure 3-25). The quenching from NaI is a typical dynamic quenching due to the collision between NaI and 5-IAF probe, where the quenching increases at the higher temperature. The quenching due to the collision between NaI and 5-IAF occurs at the millimolar concentration level of the quencher. Such a quencher

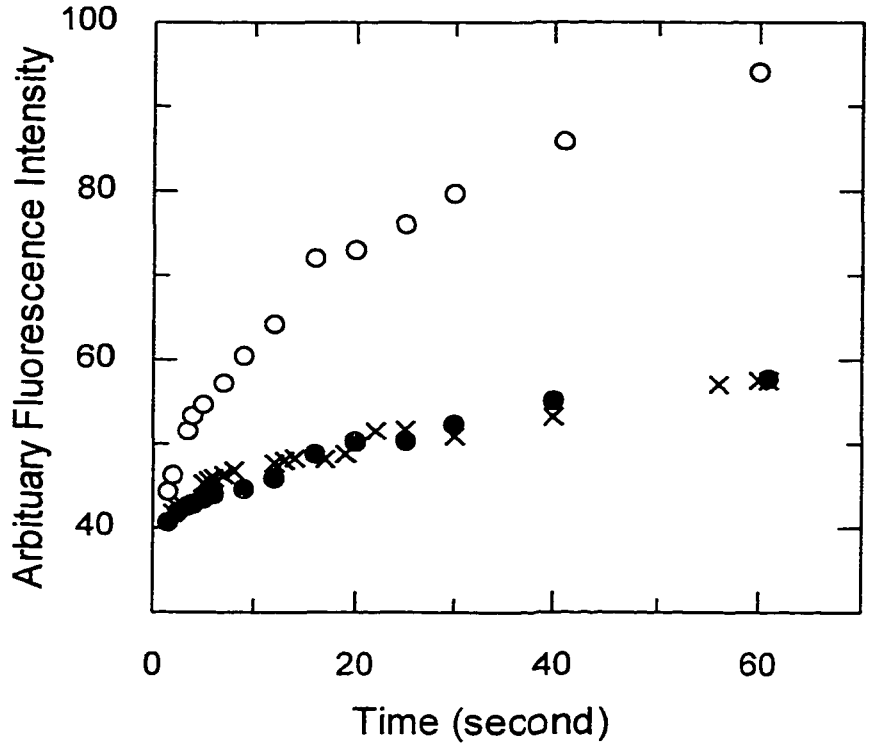

Figure 3-24. The inhibition of E280C FepA labeling by CPM upon ferric enterobactin treatment. 500nM E280C in TTE pH7.2 was labeled with 10μM CPM in the presence (O)and absence (●) of ferric enterobactin with wt FepA in the absence of ferric enterobactin (×) as a control.

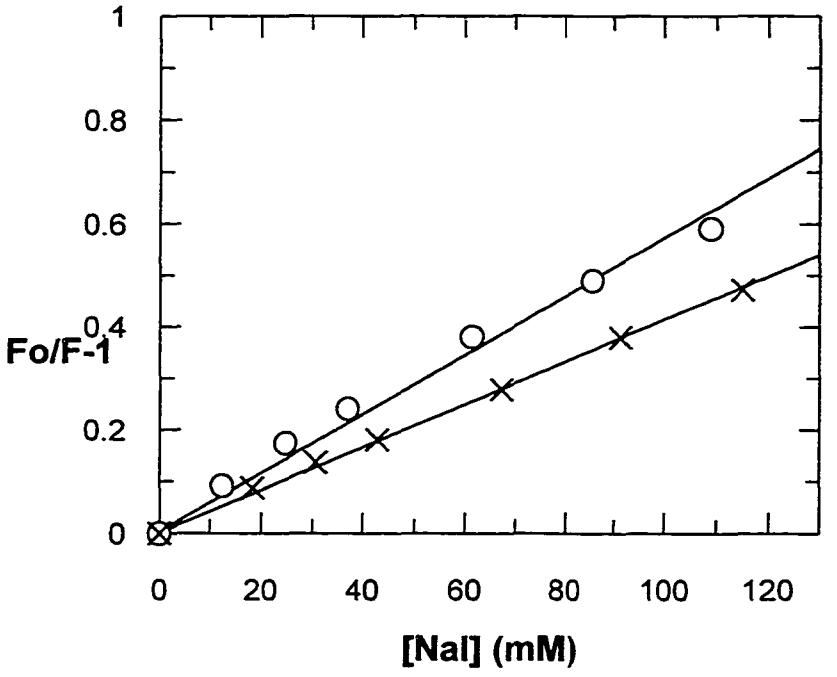

Figure 3-25. E280C-IAF was quenched by NaI. The fluorescence of E280C-IAF was measured on a SLM 8100 fluorimeter with the excitation and emission wavelengths set at 490nm and 520nm, respectively. NaI quenching studies were performed at 4°C (o) and 25°C(×), respectively. The Stern-Volmer equation was used to fit the quenching data, and the Stern-Volmer constant K_{sv} was determined to be 5.7 × 10^{-3} mM^{-1} and 4.1 × 10^{-3} mM^{-1} at 4°C and 25°C, respectively.

concentration requirement could make it possible for us to study the static quenching between FepA and ferric enterobactin because of the avidity of ferric enterobactin to FepA.

The static quenching between E280C-IAF and ferric enterobactin was revealed in Figure 3-26, where a 40% decrease in the fluorescence intensity was observed in the presence of 1μM ferric enterobactin. Such a decrease in fluorescence intensity could be due to either the local conformational change of E280C-IAF, which exposed the probe to the hydrophilic buffer environment and resulted in the quenching, or the formation of the complex between E280C-IAF and ferric enterobactin, which caused the probe to return from the excited state to the ground state without emitting photons. E280C-IAF was titrated with ferric enterobactin to study the binding affinity of ferric enterobactin to FepA *in vitro* (Figure 3-26). The K_d thus obtained was well in agreement with that previously obtained *in vitro* even though it is about 100-fold weaker in binding affinity than in the *in vivo* system (Newton *et al.*, 1999; this study).

Antibodies can block the binding of ferric enterobactin to E280C:

To further study the ferric enterobactin binding site, different antibodies were used to examine their effect on ferric enterobactin binding. E280C-IAF was incubated with monoclonal antibodies against various surface loops of FepA (Murphy *et al.*, 1990) followed by quenching with 1μM ferric enterobactin (Figure 3-27). The addition of monoclonal antibodies only slightly increased the fluorescence intensity

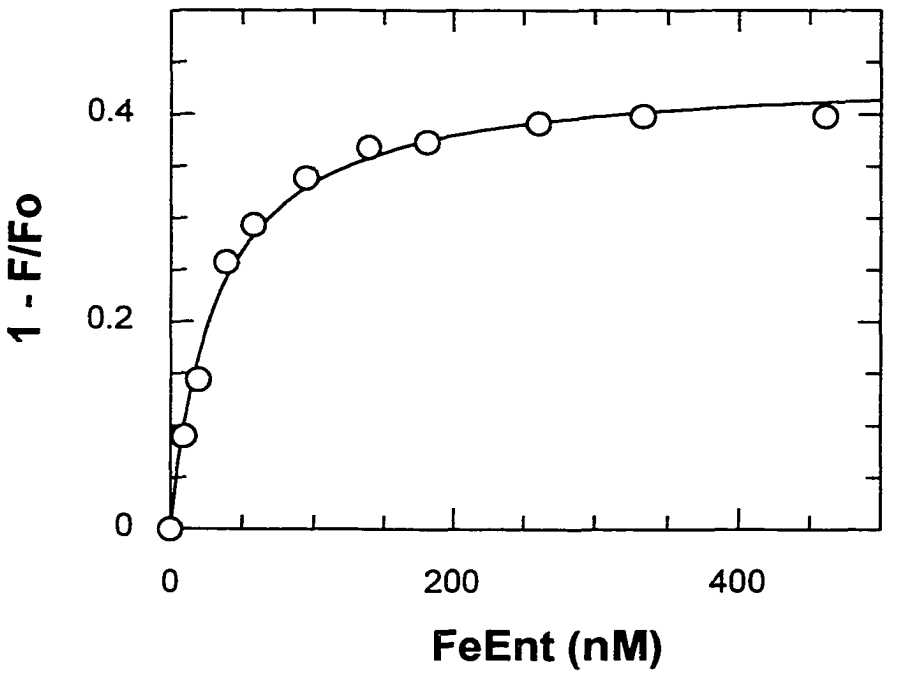

Figure 3-26. Titration of E280C-IAF with ferric enterobactin. E280C-IAF (50nM) was titrated with ferric enterobactin at 25°C, and fluorescence intensity was measured at each addition of ferric enterobactin. The quenching data were analyzed by GraFit4 using the bound versus total equation, and K_d was determined to be 15nM. The same result was obtained when 2.5nM protein was used in the quenching assay.

(3-5% increase). Of the seven monoclonal antibodies used, four of them, mAb29 (recognizing epitope 2-24), mAb2 (epitope 100-178), mAb16 (epitope 258-290) and mAb23 (epitope 382-400) did not have any effect on ferric enterobactin quenching with a 40% decrease in fluorescence intensity observed. Partial protection from mAb33 (epitope 204-227) was observed (only a 15% decrease in fluorescence intensity). On the other hand, mAb1 (epitope 27-37) and mAb45 (epitope 290-339) adequately protected E280C-IAF from ferric enterobactin quenching.

The partial protection from mAb33 might be due to either the proximity of the region recognized by mAb33 to the binding domain or the existence of weak binding components in that region. The existence of other binding components was revealed in the loop deletion mutagenesis of FepA (Newton *et al.*, 1999). The deletion of loop2 (residues 199-226) was the most detrimental surface loop deletion mutant other than the deletions involving disulfide bond (ΔL7) and the partial deletion of the β-strand (ΔL8).

mAb45 is located within the ferric enterobactin binding domain. First, phe329 is a very important residue for mAb45 recognition. Once phe329 was substituted with alanine, no antibody recognition by mAb45 was observed when the immunoblot was performed, using ^{125}I-protein A as the secondary antibody, while only weak recognition was obtained when enzymatic development method was used in the immunoblotting. Furthermore, F329 is one of the critical aromatic residues for ferric enterobactin binding and transport. Therefore, F329 is an important residue for both

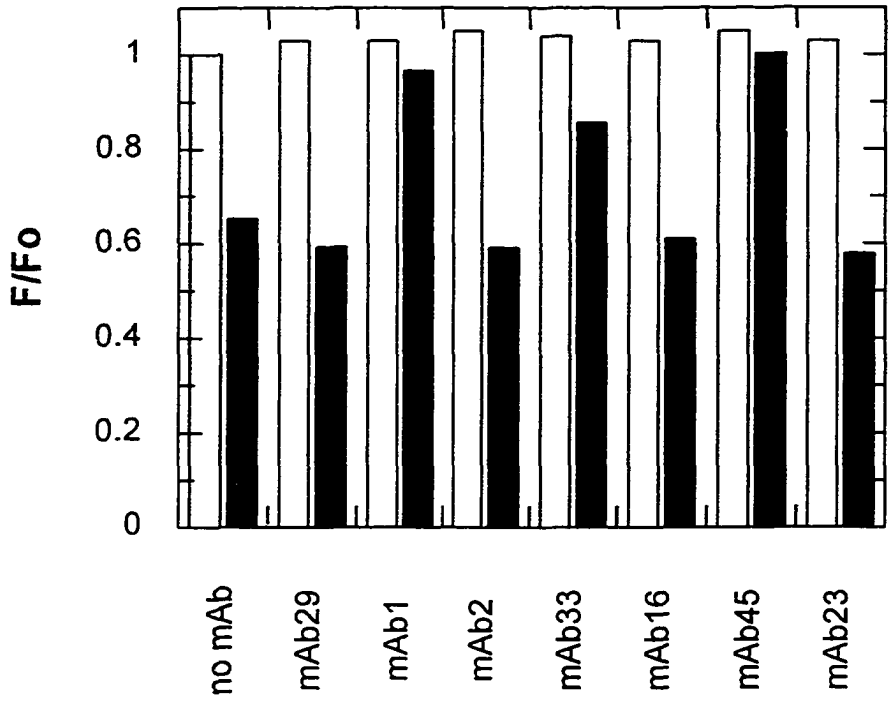

Figure 3-27. Effect of monoclonal antibodies against FepA on ferric enterobactin binding. 50nM E280C-IAF in TTE pH7.2 was incubated with 10μl monoclonal antibody for 10 min, and ferric enterobactin was then added to a final concentration of 10μM. White and blue bars represent the fluorescence intensity change after the addition of the monoclonal antibody and 10μM ferric enterobactin, respectively.

mAb45 recognition and ferric enterobactin absorption. The recognition by monoclonal antibodies is too strong for ferric enterobactin to compete with.

mAb1 inhibition of ferric enterobactin, however, might have another very different inhibition mechanism. Our initial explanation for the inhibition was that the epitope recognized by mAb1 probably was located very close to the ferric enterobactin binding domain. The recently solved crystal structure, however, showed that the N-terminal forms a plug structure which folds back into the barrel. A possible explanation for the mAb1 inhibition is that the binding of mAb1 to the epitope changes the conformation of the ferric enterobactin binding domain.

Antibody can compete off the bound ferric enterobactin:

Monoclonal antibodies against FepA, mAb1 and mAb45, were used to study the inhibition mechanisms by examining the competition of monoclonal antibodies against ferric enterobactin (Figure 3-28). Although both monoclonal antibodies can compete with ferric enterobactin, the result showed very different competing mechanisms. mAb45 competed with ferric enterobactin relatively quickly to reach a saturation, while mAb1, on the other hand, released ferric enterobactin gradually to return to the unquenched state. Therefore, mAb45 competes with ferric enterobactin because they share the same recognition site; mAb1, however, recognizes FepA in a completely different region, and the absorption of mAb1 to FepA changes the conformation of FepA such that ferric enterobactin is released from FepA. How ferric

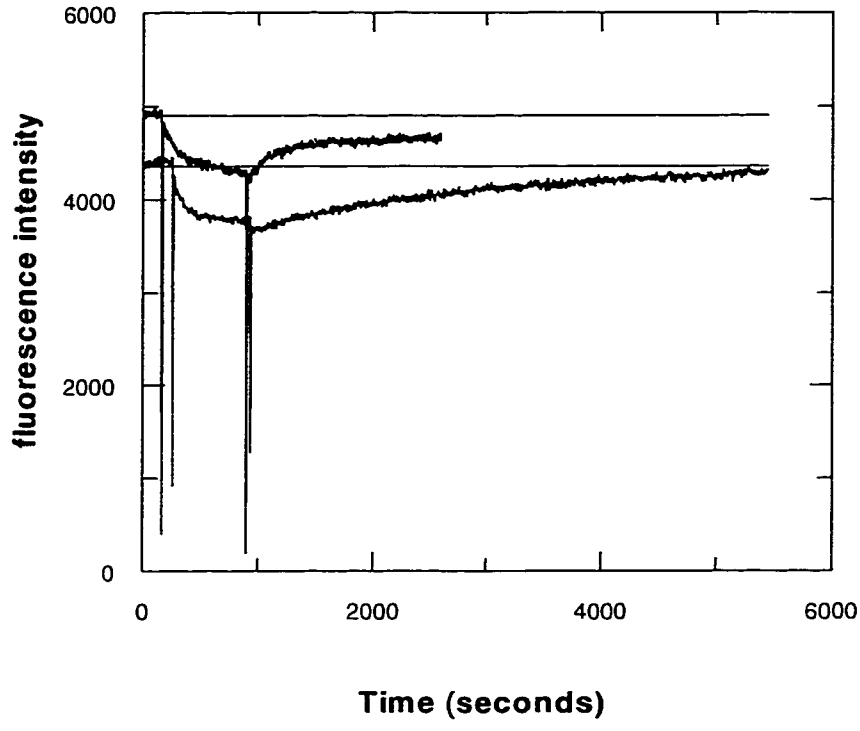

Figure 3-28. Competition of monoclonal antibodies against ferric enterobactin. 2.5nM E280C in 1mM DM, 50mM MOPS pH7.0, 60mM NaCl was incubated at 25°C for at least 30 min to stabilize the fluorescence signal before time course measurement started. Ferric enterobactin was then added to a final concentration of 47nM. After ferric enterobactin quenching leveled off, mAb1 (red curve) or mAb45 (black curve) was added to the cuvette. Ferric enterobactin and mAb were added at the points where fluorescence intensity dropped suddenly due to the opening of the sample chamber. For mAb45, no further increase of fluorescence intensity was observed when measured again 30 min after the stop point of the time course.

enterobactin is released, whether to the environment or through the opened channel, remains to be further investigated.

Biphasic binding between FepA and ferric enterobactin:

The above experiments showed that the interaction between ferric enterobactin and FepA can be monitored by the fluorescent "reporter", from either its conformational change or the formation of a non-fluorescent complex. Such a system is very sensitive, due to the availability of the highly fluorescent probes like 5-IAF. We used this measurement system to study how the fluorescent probes "respond" when ferric enterobactin binds to FepA under two extreme conditions: in the absence of either the two important surface residues (Y272A/F329A) or the two critical residues in the barrel (Y260A/R316A).

Our experiment showed that the measurement of K_d using the fluorescent measurement system was not practical for either Y272A/F329A or Y260A/R316A because of the very slow binding kinetics of the mutants. This reflects the possible structural change when the membrane protein FepA was purified and solublized in detergent. In E280C-IAF measurement system, the binding was much slower than in live cells, and K_d was distinguishably larger than that measurement in live cells also.

The binding time courses were studied for Y260A/R316A/E280C-IAF and Y272A/F329A/E280C-IAF, using the above established fluorescent measurement system (Figure 3-29). Even though Y272A/F329A has a much stronger binding

affinity than Y260A/R316A, we found that Y260A/R316A/E280C-IAF retains the fast first binding phase, while Y272A/F329A/E280C-IAF has a weaker first binding phase and the biphasic binding pattern. This strongly suggests that the residues Y272 and F329 are involved in the initial binding while Y260 and R316 participate in the latter phase following the initial absorption.

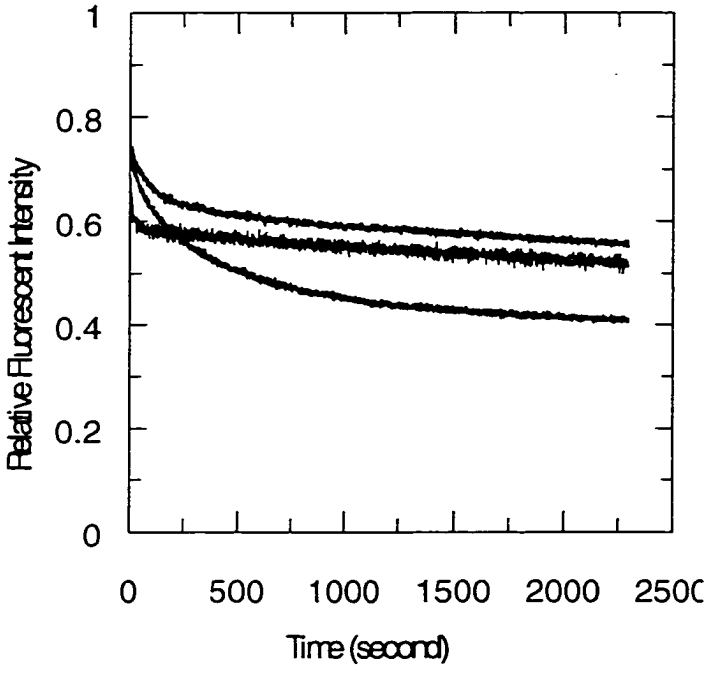

Figure 3-29. Time course of ferric enterobactin binding to mutant FepA. E280C-IAF (black curve), Y272A/F329A/E280C-IAF (blue curve) and Y260A/R316A/E280C-IAF (red curve) were diluted to 1mM DM detergent in 50mM MOPS pH7.0, 60mM NaCl buffer, to a final concentration of 2.5nM, equilibrated at 25°C for 1 hr before fluorescent time course measurement was performed with excitation and emission wavelengths set at 490nm and 520nm, respectively. Ferric enterobactin in 50mM MOPS pH7.0, 60mM NaCl was added to a final concentration of 10μM at the beginning of the time course measurement.

CHAPTER IV

DISCUSSION

The ferric enterobactin binding and transport domain was first identified by the generation of a general diffusion channel by deleting the central region, previously the proposed PL5 loop (Rutz *et al.*, 1992) which was L3 and L4 loops and the transmembrane sheets between them in the crystal structure (Buchanan *et al.*, 1999). The similar structural feature was also found in FhuA (Killmann *et al.*, 1993). The identification of essential interactions involving both charged residues and aromatic residues, therefore, was focused on this central region. Although the crystal structures and the deletion mutagenesis studies (Newton *et al.*, 1999) indicated that the central region might not be the only region involved in ferric enterobactin recognition, the result from this research and the previous charged residue study (Newton *et al.*, 1997) showed that the five residues identified in this region, Y260, Y272, R286, R316, and

F329, have significant contributions to the interactions between FepA and ferric enterobactin.

At the very beginning of the study of the aromatic residues in the central region of FepA, it was proposed that the three tryptophan residues, W293, W297, and W306, might be important, due to the location of the three residues in the original proposed model, the aromaticity, and other structural features of ferric enterobactin. The alanine replacement mutants generated for the three residues, including all single, double and triple combinations, did not show any effect on the functionality of FepA as the receptor for all the three ligands (data not shown). Current advances on the FepA study have made it clear that these three residues are either part of the transmembrane domain (residues W293 and W306) or located at the periplasmic side of the protein (W297). The above study, however, proved that the alanine replacement study could possibly be performed without the defective effect on the protein function.

We have studied in detail the seven conserved aromatic residues singly and in double combinations. Among the other three aromatic residues not conserved in the FepA sequences from different bacterial strains, Y277, W293 and W306, in the central region of our research interest, two of them, W293 and W306, as mentioned earlier, are located at the periplasmic side of the plug domain, while Y277 did not show any change in the substitution studies performed (data not shown), although systematic analysis on Y277 has not been carried out.

The location of the residues involved in ferric enterobactin interaction suggests that the multicomponent system is organized to obtain the optimal "extraction" power and transport rate. The three aromatic residues and one positively charged residue studied are organized into two tiers. While Y272 and F329 reside at the surface well exposed to the environment, Y260 and R316 are down at the bottom of the surface loops. In this study, we found that the single mutation to either Y272 or F329 did not change much to the receptor functionality, and even the double combination retains the protein activity quite well. That is, the removal of a single component at the surface loop did not have much effect, indicating that more surface loop residues are involved in the initial interaction. This finding is in agreement with the role of the residues involved in the interaction: ferric enterobactin receptor FepA has to "extract" ferric siderophore from the environment where siderophore concentration may be very low. Ferric enterobactin transport, however, is different with regard to the local "scarcity" of the ligand. Once ferric enterobactin is initially attracted, the second group of binding components probably are in charge of the formation of the ferric enterobactin-FepA complex compatible for uptake. Therefore, for the second group of interaction components, an efficient transport mechanism involving fewer residues are probably more practical. This was revealed in the fact that both Y260A and R316A single mutants changed the receptor activity to a much larger extent than the other mutants.

The role that the aromatic residues play in the interaction between FepA and its

ligands is also justified by the avidity of FepA for ferric enterobactin. The three aromatic residues studied here "selectively" interact with ferric enterobactin among the three ligands. This "selectivity" most likely contributes to the extremely strong binding affinity between FepA and ferric enterobactin, which is over 1000-fold stronger than those between FepA and the colicin ligands (K_d 145nM and 169nM for colicin B and colicin D, respectively; Newton *et al.*, 1997).

The difference in the transport system design between the specific channels and the TonB-dependent transporters lies in the difference between the ligand availability. The absorption of maltose and maltodextrins is a LamB facilitated diffusion process, where the receptor is restricted by one inwardly folded loop L3 (Schirmer *et al.*, 1995). At the constriction of the channel, the sugar ligand is tightly surrounded by protein side chains and forms an extensive hydrogen-bonding network with ionizable amino-acid residues (Dutzler et al., 1996). The extended binding site within the channel - the "greasy slide" structure (Dutzler et al., 1996; Wang et al., 1997) - guides the sugar into and through the channel constriction via hydrophobic interactions between the ligands and the greasy slide. Calculations showed that the measured V_{max} of 20 nmol per min per 10^9 cells is close to the maximum diffusion rate of maltose, demonstrating that the facilitated diffusion of maltose through LamB and the following uptake by the ABC transporter are very well matched at the maltose concentration level (Boos and Shuman, 1998). For the FepA active outer membrane transport system, the experiment showed that the binding K_d matches very well with

the transport K_m, both around 0.2nM. However, even with a much higher binding affinity, the uptake rate is much smaller (over 100-fold less) than that of the LamB system. This probably can not be accounted for by the presence of fewer receptor protein in FepA since both LamB and FepA are supposed to have similar number of copies per cell, around 10,000 (Boos and Shuman, 1998) and 80,000 (Newton et al., 1997) copies for LamB and FepA, respectively. Apparently, the uptake in the active transport system is much slower than the diffusion controlled facilitated uptake of LamB system.

Loop deletion mutagenesis and site-directed mutagenesis results showed that different cell surface loops have different responses to the loop "environmental" change. The least receptor functionality change was observed in the deletion mutants involving surface loops L3 and L4, even though the four essential aromatic and positively charged residues in this study reside in this region. FepA, however, can not tolerate the deletion of either loop L7 or loop L8, indicating that this region probably carries conformational information of the global structure of the receptor protein. This assumption is confirmed in the cysteine mutagenesis studies where the removal of the cysteine disulfide bond by changing one cysteine to alanine dramatically decreased the binding affinity and uptake capability of FepA as a receptor for either ferric enterobactin or colicins B and D.

The native cysteines in LamB were found not to be important for the LamB function, where the receptor acts as a specific channel to facilitate the absorption of

ligands too large for general porins. But meanwhile, LamB retains the diffusion channel function. The very different function performed by FepA in the active transport system probably would explain why the native cysteines are not essential in LamB, while being critical for FepA function. The "lock and key" relationship between FepA and its ligands has to be maintained for the ligand to be absorbed by the receptor followed by the opening of the gate.

One argument about the result we obtained from the double replacement mutant analysis with regard to the aromatic residues was that the double replacement might have introduced a local conformational change of FepA due to the removal of the aromatic-aromatic interaction within the receptor itself. Such a concern, to certain extent, was reasonable because when we first gathered the aromatic replacement results, all the single mutations did not show any effect on ferric enterobactin binding and transport due to the substrate depletion that occurred in previous binding and transport methods used. Even with the new method where the substrate depletion was taken care of, no effect was observed for Y272A mutant, and the change from F329A mutation was not significant compared with the double replacements. On the other hand, aromatic-aromatic interactions can play a crucial role in the local and global conformations of the protein. If we could combine two different interaction components, such as the charged residue replacement and the aromatic replacement together, we would be looking at the removal of two independent components, and the removal of two of them would not change the conformation on the condition that

each individual replacement did not introduce the conformational change. In the current research, we combined each individual aromatic residue replacement with R316A, one of the positively charged residue substitutions that were found to be essential in the interaction between FepA and ferric enterobactin. These combination studies showed that any of the double combinations among residues Y260, Y272, R316, and F329 resulted in a significant decrease in receptor functionality, and the defective binding and transport came from the removal of the direct interaction components.

Previously it was shown that charge interactions are essential in the FepA-ferric enterobactin interaction (Newton *et al.*, 1997), while the current research indicated that the interactions involving aromatic components are critical. It seems that these are the two major interactions that are involved in FepA-ligand interaction since the alteration due to the removal of any two of the essential residues is significant with regard to the number of residues might be involved. One question, then, that needs to be addressed here is whether or not the positively charged residues are involved in the charge-charge interaction by forming salt bridges or they act through the cation-π interaction. The salt bridge formation, in many cases, is not favored, due to the "desolvation penalty" (Sun *et al.*, 1991) which may not be paid by the formation of the salt bridge alone. On the other hand, arginine residue is a good candidate for the cation-π interaction which has been found to be of importance in many biological systems. Therefore, R316 may act as a cation to interact with the aromatic rings of

ferric enterobactin. However, the present mutagenesis study was not sufficient to identify these two interactions.

The previous study with a enterobactin analog TRENCAM (Thulasiraman *et al.*, 1998) showed that the introduction of a positive charge in the analog center decreased the binding capacity to about one third of that of ferric enterobactin. Even though no significant change in the k_d was observed, we now know that the change could be relatively large if the substrate depletion had not occurred. The authors assumed that the introduced charge might introduce a repulsion if the second ligand intends to occupy the same binding domain as in the case of a trimeric outer membrane structure. This result, however, might be caused by the repulsion interaction between the positive charge on TRANCAM and the one on R316, which in turn reduced the cation-π interaction. If this is true, the binding interaction between R316A and ferric TRANCAM should be very close to that of ferric enterobactin.

Other experimental designs might be helpful for the further understanding of the interaction between arginine residues and ferric enterobactin. Amino acid R316 can be modified to two different positively charged residues, such as lysine, which is a good candidate for the cation-π interaction, and histidine, which is a poor one (Gallivan and Dougherty, 1999). These mutagenesis studies might be a key to exploring the possible cation-π interaction. Also, the interaction can possibly be investigated in an *in vitro* purified protein system by studying the ligand-receptor interaction using positively charged salt conditions to form ion pairs with the negative

charges in ferric enterobactin. Although such experimental conditions might introduce other effects into the FepA-ligand interaction, it should be able to tell the difference between the receptor with R316 removed and the wild type one. Unfortunately, the fluorescent method can not be used in such an experimental design due to the sensitivity of the fluorescent probes to salt concentrations.

The results we obtained for biphasic studies were far from being conclusive. Part of the difficulties might be due to the experimental design of the fluorescent measurement. While E280C-IAF provides a unique technique to study the interaction between FepA and its ligands, where residue 280 is located in the membrane might be a very important issue in the study of ligand-protein interaction by fluorescent measurement. Although the protein measurement uses a simple system which involves only the ligand and its receptor, the physical interaction between the probe and ferric enterobactin is far more complicated than it appears to be. The fluorescence intensity change during the binding processes mainly comes from two sources: the conformational change of the residue where the probe resides and the formation of a non-fluorescent complex. For quenching to occur in the formation of the complex, the probe has to be in physical contact with the quencher (Lakowicz, 1983), that is, besides the formation of the complex, the probe needs to be in a certain conformation for the interaction.

FepA crystal structure (Buchanan *et al.*, 1999) showed that E280 residue is located very close to Y260 and R316, and the residue points to the outside of the

barrel to face the aqueous environment (Figure 4-1), suggesting that E280 probably does not interact directly with ferric enterobactin upon ligand binding. Meanwhile, ESR studies (Liu *et al.*, 1994) showed that ferric enterobactin absorption on the surface of FepA caused the ESR probe attached to E280C cysteine slightly more immobilized, indicating that the L3 loop changes its conformation upon ferric enterobactin binding to stimulate the ESR probe away from the aqueous milieu. This is further evidenced by the inhibition of fluorescent probe labeling of E280C cysteine upon ferric enterobactin binding.

The fluorescent measurement system is complicated by the presence of additional sources of fluorescence intensity change. If the conformational change stimulated the attached probe away from the aqueous environment to be less exposed to the quenching agent in the aqueous solution, the fluorescence intensity would increase upon ferric enterobactin binding as we see in the case of ColB absorption (Payne *et al.*, 1997). However, the fluorescence intensity decreases in the presence of ferric enterobactin, indicating another quenching interaction, i.e., the formation of the non-fluorescent complex. How the fluorescent probe directly interacts with the ferric enterobactin still remains to be investigated. One possibility is that the conformation of E280C changed when the cysteine was introduced and further the bulky fluorescent probe was attached, although such a conformational change did not change the protein functionality (Liu *et al.*, 1994; Jiang *et al.*, 1997; Payne *et al.*, 1997). Alternatively, the initial binding of ferric enterobactin triggered the conformational

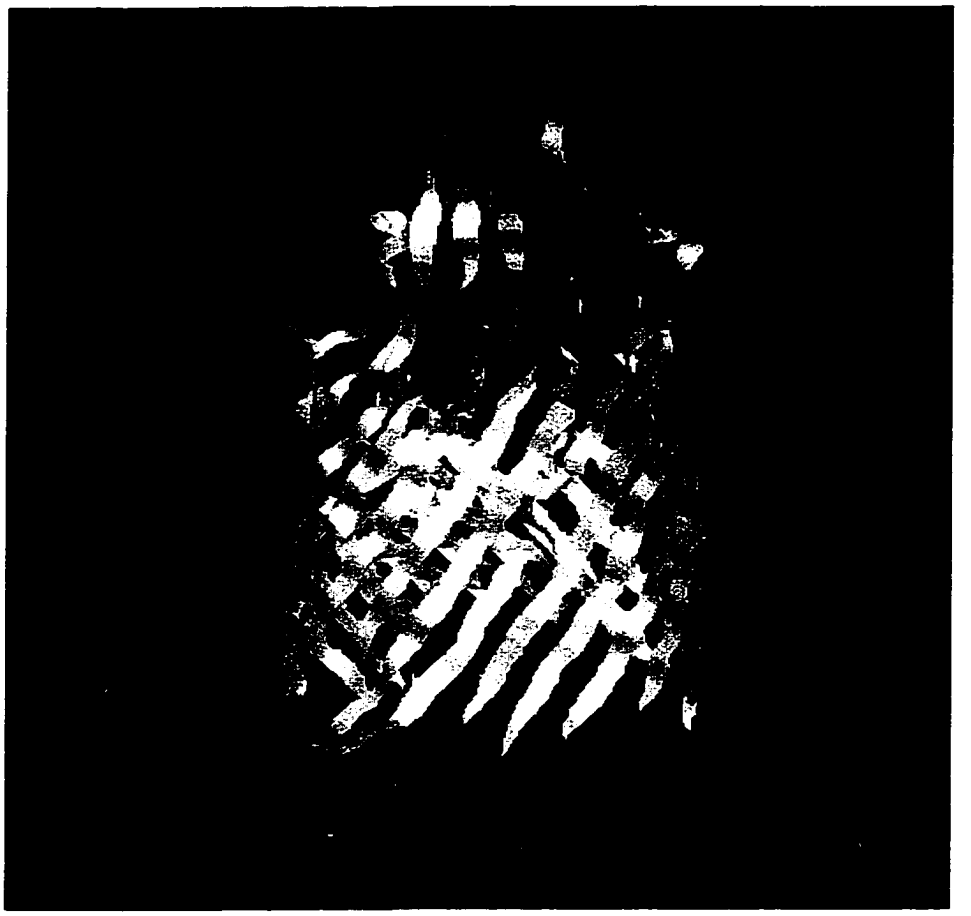

Figure 4-1. The Location of E280 Residue in the Crystal Structure. E280 (red) and Y260, Y272, and R316 (green) are displayed in sticks.

change of 280 site to a position where the direct contact between FepA and ferric enterobactin became possible.

Further research using the fluorescent measurement system might be very helpful to provide more conclusive results. By far, we know that Y260, Y272, R316, and F329 are residues involved in a direct physical interaction with the ligand. Therefore, if the fluorescent probes are introduced at any of these residues, the fluorescent measurement system would be much more simple in the sense of data explanation than in the case of E280C being labeled. Such a study might include the generation of the following mutants: Y260C/R316A, Y260A/R316C, Y272C/F329A, and Y272A/F329C. Fluorescent probes then can be introduced to the site where cysteine is introduced in each mutant. The only problem which occurs in this design is the lack of the experimental control. However, from the current study it was shown that the single mutant Y272A did not have any effect on the receptor function and R316A only introduced a very small change in the ligand binding affinity. Therefore, it is possible to study Y272C/F329A and Y260A/R316C mutants using Y272C and R316C as controls, respectively.

Our results indicated that aromatic residues play different roles among the three different FepA ligands. While Y260, Y272,and F329 are crucial in ferric enterobactin absorption, none of them are important in colicin killing. On the other hand, the arginine residues R286 and R316 were demonstrated to be essential in all three ligands, though different mechanisms were established for R286 and R316 in their

colicin B and colicin D sensitivities. This indicated that although colicins and ferric enterobactin share the same domain for ligand functions, the absorption mechanisms are different. Furthermore, our unpublished data showed that the inhibition pattern for fluorescent probe accessibility to E280C was slightly different among ferric enterobactin, ColB, and ColD. While ferric enterobactin and ColB inhibited IAEDANS labeling, residue labeling to E280C by IAEDANS was observed when ColD was present. Since ColD (MW 75Kda; Timmis, 1972) is much larger than ColB (MW 55Kda; Schramm *et al.*, 1987) and ferric enterobactin (MW 716Da; Neilands, 1993), the three ligands probably do not have exactly the same binding domain. Instead, it is more likely that their binding domains overlap with each other.

REFERENCES

Altenbach, C., Cai, K., Khorana, H.G., and Hubbell, W.L. (1999) Structural features and light-dependent changes in the sequence 306-322 extending from helix VII to the palmitoylation sites in rhodopsin: a site-directed spin-labeling study. *Biochemistry* **38**: 7931-7937.

Archibald, F. (1983) *Lactobacillus plantarum*, an organism not requiring iron. *FEMS Microbiol. Lett.* **19**: 29-

Armstrong, S.K., Francis, C.L., and McIntosh, M.A. (1990) Molecular analysis of the *Escherichia coli* ferric enterobactin receptor FepA. *J. Biol. Chem.* **265**: 14536-14543.

Avdeef, A., Sofen, S.R., Bregante, T.L, and Raymond, K.N. (1978) Coordination chemistry of microbial iron compounds. IX. Stability constants for catechol models of enterobactin. *J. Am. Chem. Soc.* **100**, 5362-5370.

Baneyx, F., and Georgiou, G. (1990) *In vivo* degredation of secreted fusion proteins by the *Escherichia coli* outer membrane protease OmpT. *J. Bacteiol.* **172**: 491-494.

Bauer, K., Struyve, M., Bosch, D., Benz, R., and Tommassen, J. (1989) One single lysine residue is responsible for the special interaction between polyphosphate and the outer membrane porin PhoE of Escherichia coli. *J. Biol. Chem.* **264**: 16393-16398.

Baumler, A.J., Norris, T.L., Lasco, T., Voigt, W., Reissbrodt, R., Rabsch, W., and Heffron, F. (1998) IroN, a novel outer membrane siderophore receptor

characteristic of *Salmonella enterica. J. Bacteriol.* **180**: 1446-1453.

Beall, B. and Sanden, G.N. (1995) A Bordetella pertussis fepA homologue required for utilization of exogenous ferric enterobactin. *Microbiology* 141: 3193-3205.

Befort, K., Tabbara, L., Kling, D., Maigret, B., and Kieffer, B.L. (1996) Role of aromatic transmembrane residues of the delta-opioid receptor in ligand recognition. *J. Biol. Chem.* 271: 10161-10168.

Bell, P.E., Nau, C.D., Brown, J.T., Konisky, J., and Kadner, R.J. (1990) Genetic suppression demonstrates interaction of TonB protein with outer membrane transport proteins in *Escherichia coli. J. Bacteriol.* **172**: 3826-3829.

Benson, S.A., Occi, J.L.L., and Sampson, B.A. (1988) Mutations that alter the pore function of the OmpF porin of *Escherichia coli* K12. *J. Mol. Biol.* 203: 961-970.

Bonhivers, M., Ghazi, A., Boulanger, P., and Letellier, L. (1996) FhuA, a transporter of the *Escherichia coli* outer membrane, is converted into a channel upon binding of bacteriophage T5. *EMBO J.* **15**: 1850-1856.

Boos, W. and Shuman, H. (1998) Maltose/maltodextrin system of *Escherichia coli*: transport, metabolism, and regulation. *Microbiol. Mol. Biol. Rev.* **62**: 204-229.

Bos, C., Lorenzen, D., and Braun, V. (1998) Specific *in vivo* labeling of cell surface-exposed protein loops: reactive cysteines in the predicted gating loop mark a ferrichrome binding site and a ligand-induced conformational change of the *Escherichia coli* FhuA protein. *J. Bacteriol.* 180: 605-613.

Bradbeer, C., Woodrow, M.L., and Khalifah, L.I. (1976) Transport of vitamin B12 in *Escherichia coli*: common receptor system for vitamin B12 and bacteriophage BF23 on the outer membrane of the cell envelope. *J. Bacteriol.* **125**: 1032-1039.

Bradbeer, C. (1993) The proton motive force drives the outer membrane transport of cobalamin in *Escherichia coli. J. Bacteriol.* **175**: 3146-3150.

Braun, M., Killmann, H., and Braun, V. (1999) The β-barrel domain of FhuAΔ5-160 is sufficient for TonB-dependent FhuA activities of *Escherichia coli. Mol. Microbiol.* **33**: 1037-1049.

Braun, V. and Killmann, H. (1999) Bacterial solutions to the iron-supply problem. *TIBS* **24**: 104-109.

Braun, V., Killmann, H., and Benz, R. (1994) Energy coupled transport through the outer membrane of *Escherichia coli* small deletions in the gating loop convert the FhuA transport protein into a diffusion channel. *FEBS Lett.* **346**: 59-64.

Brewer, S., Tolley, M., Trayer, I.P., Barr, G.C., Dorman, C.J., Hannavy, K., Higgins, C.F., Evans, J.S., Levine, B.A., and Wormald, M.R. (1990) Structure and function of X-Pro dipeptide repeats in the TonB proteins of *Salmonella typhimurium* and *Escherichia coli. J. Mol. Biol.* **216**: 883-895.

Buchanan, S.K., Smith, B.S., Venkatramani, L., Xia, D., Esser, L., Palnitkar, M., Chakraborty, R., van der Helm, D., and Deisenhofer, J. (1999) Crystal structure of the outer membrane active transporter FepA from *Escherichia coli. Nature Struct. Biol.* **6**: 56-63.

Cadieux, N., and Kadner, R. (1999) Site-directed disulfide bonding reveals an interaction site between energy-coupling protein TonB and BtuB, the outer membrane cobalamin transporter. *Proc. Natl. Acad. Sci. USA* **96**: 10673-10678.

Charbit, A., Boulain, J.C., Ryter, A. and Hofnung, M. (1986) Probing the topology of a bacterial membrane protein by genetic insertion of a foreign epitope. *EMBO J.* **5**: 3029-3037.

Charbit, A., Wang, J., Michel, V., and Hofnung, M. (1998) A cluster of charged and aromatic residue in the C-terminal portion of maltoporin participates in sugar binding and uptake. *Mol. Gen. Genet.* **260:** 185-192.

Constable, E.C. (1999) Coordination Chemistry of Macrocyclic Compounds. Oxford University Press, NY, USA.

Corey, E.J., and Bhattacharyya, S. (1977) Total synthesis of enterobactin via an organotin template. *Tetrahedron Lett.* pp.3919-3922.

Cowan, S.W., Schirmer, T., Rummel, G., Steiert, M., Ghosh, R., Pauptit, R.A., Jansonius, J.N., and Rosenbusch, J.P. (1992) Crystal structures explain functional properties of two *E. coli* porins. *Nature* **358**: 727-733.

Cowan, S.W. (1993) Bacterial porins - lessons from 3 high-resolution structures. *Curr. Opin. Struct. Biol.* **3:** 501-507.

Cox, G.B., Gibson, F., Luke, R.K., Newton, N.A., O'Brien, I.G., and Rosenberg, H. (1970) Mutations affecting iron transport in Escherichia coli. *J. Bacteriol.* **104**: 219-226.

Davies, J.K., and Reeves, P. (1975) Genetics of resistance to colicins in Escherichia coli K-12: cross-resistance among colicins of group B. *J. Bacteriol.* **123**: 96-101.

Dean, C.R. and Poole, K. (1993) Cloning and characterization of the ferric enterobactin receptor gene (pfeA) of Pseudomonas aeruginosa. *J. Bacteriol.*, **175**: 317-324.

Deisenhofer, J., Epp, O., Miki, K., Huber, R., and Michel, H. (1985) Structure of the subunits in the photosynthetic reaction center of *Rhodopseudomonas viridis* at 3 Å resolution. *Nature* **318**: 618-624.

Dickerson, R.E., Drew, H.R., Conner, B.N., Wing, R.M., Fratini, A.V., and Kopka, M.L. (1982) The anatomy of A-, B-, and Z-DNA. *Science* **216**: 475-485.

Doyle, D.A., Cabral, J.M., Pfuetzner, R.A., Kuo, A., Gulbis, J.M., Cohen, S.L., Chait, B.T., and MacKinnon, R. (1998) The structure of the potassium channel: molecular basis for K^+ conductance and selectivity. *Science* **280**: 69-77.

Dougherty, D. A. (1996) Cation-π interactions in chemistry and biology: a new view of benzene, Phe, Tyr, and Trp. *Science* **271**: 163-168.

Dulley, J.R., and Grieve, P.A. (1975) A simple technique for eliminating interference by detergents in the Lowry method of protein determination. *Anal. Biochem.* **64**: 136-141.

Dutzler, R., Wang, Y.F., Rizkallah, P., Rosenbusch, J.P., and Schirmer, T. (1996) Crystal structures of various maltooligosaccharides bound to maltoporin reveal a specific sugar translocation pathway. *Structure* **4**: 127-134.

Earhart, C.F. (1996) Uptake and metabolism of iron and molybdenum. In *Escherichia coli and Salmonella Cellular and Moleculr Biology,* second edition. Edited by Neidhardt, F.C., ASM Press, Washington D.C.

Ecker, D.J., Matzanke, B.F. and Raymond, K.N. (1986) Recognition and transport of ferric enterobactin in *Escherichia coli. J. Bacteriol.* **167**: 666-673.

Ferenci, T., and Stretton, S. (1989) Cysteine-22 and cysteine-38 are not essential for the functions of maltoporin (LamB protein). *FEMS Microbiol. Lett.* **52**: 335-339.

Ferguson, A.D., Hofmann, E., Coulton, J.W., Diederichs, K., and Welte, W. (1998) Siderophore-mediated iron transport: crystal structure of FhuA with bound lipopolysaccharide. *Science* **282**: 2215-2220.

Fernandes, P.B. (1998) Technological advances in high-throughput screening. *Curr. Opin. Chem. Biol.* **2**: 597-603.

Fiss, E.H., Stanley-Samuelson, P. and Neilands, J.B. (1982) Properties and proteolysis of ferric enterobactin outer membrane receptor in *Escherichia coli* K12. *Biochemistry* **31**: 4517-4522.

Frillingos, S., Sahin-Toth, M., Wu, J., and Kaback, H.R. (1998) Cys-scanning mutagenesis: a novel approach to structure function relationships in polytopic membrane proteins. *FASEB J.* **12**: 1281-1299.

Gallivan, J.P., and Dougherty, D.A. (1999) Cation-π interactions in structural biology. *Proc. Natl. Acad. Sci. USA* **96**: 9459-9464.

Garavito, R.M., Jenkins, J., Jansonius, J.N., Karlsson, R., and Rosenbusch, J.P. (1983) X-ray diffraction analysis of matrix porin, an integral membrane protein from *Escherichia coli* outer membrane. *J. Mol. Biol.* **164**: 313-327.

Gelder, P.V., Saint, N., Phale, P., Eppens, E.F., Prilipov, A., van Boxtel, R., Rosenbusch, J.P., and Tommassen, J. (1997) Voltage sensing in the PhoE and OmpF outer membrnae porins of *Escherichia coli*: role of charged residues. *J. Mol. Biol.* **269:** 468-472.

Gouaux, E. (1998) Roll out the barrel. *Nat. Struct. Biol.* **5**: 931-932.

Griffiths, E. (1991) Iron and bacterial virulence - a brief overview. *Biol. Metals* **4**: 7-13.

Gudmundsdottir, A., Bell, P.E., Lundrigan, M.D., Bradbeer, C., and Kadner, R.J. (1989) Point mutations in a conserved region (TonB box) of *Escherichia coli* outer membrane protein BtuB affect vitamin B12 transport. *J. Bacteriol.* **171**: 6526-6533.

Guerinot, M.L. (1994) Microbial iron transport. *Annu. Rev. Microbiol.* **48**: 743-772.

Gunter, K., and Braun, V. (1990) *In vivo* evidence for FhuA outer membrane receptor interaction with the TonB inner membrane protein of *Escherichia coli. FEBS Lett.* **274**: 85-88.

Guterman, S.K. (1971) Inhibition of colicin B by enterochelin. *Biochem. Biophys. Res. Commun.* **44**: 1149-1155.

Guterman, S.K. (1973) Colicin B: mode of action and inhibition by enterochelin. *J. Bacteriol.* **114**: 1217-1224.

Hannavy, K. and Higgins, C.F. (1991) TonB; a model for signal transduction between membranes. *Biochem. Soc. Trans.* **19**: 530-2.

Hannavy, K., Barr, G.C., Dorman, C.J., Adamson, J., Mazengera, L.R., Gallagher, M.P., Evans, J.S., Levine, B.A., Trayer, I.P., and Higgins, C.F. (1990) TonB protein of *Salmonella typhimurium*. A model for signal transduction between membrnaes. *J. Mol. Biol.* **216**: 897-910.

Haugland, R.P. (1996) Handbook of Fluorescent Probes and Research Chemicals. Molecular Probes, Inc. Eugene, OR.

Heller, K.J., Kadner, R.J., and Gunther, K. (1988) Suppression of the btuB451 mutation by mutations in the tonB gene suggests a direct interaction between TonB and TonB-dependent receptor proteins in the outer membrane of *Escherichia coli*. *Gene* **64**: 147-153.

Henderson, R., and Unwin, P.N. (1975) Three-dimensional model of purple membrane obtained by electron microscopy. *Nature* **257**: 28-32.

Hermanson, G.T. (1996) Bioconjugate techniques published by Academic Press, San Diego, CA.

Hollifield, W.C., Jr., and Neilands, J.B. (1978) Ferric enterobactin transport system in Escherichia coli K-12. Extraction, assay, and specificity of the outer membrane receptor. *Biochemistry* **17**: 1922-1928.

Jiang, X., Payne, M.A., Cao, Z., Foster, S.B., Feix, J.B., Newton, S.M.C. and Klebba, P.E. (1997) Ligand-specific opening of a gated channel in the outer membrane of living bacteria. *Science* **276**: 1261-1264.

Kadner, R.J., and Heller, K.J. (1995) Mutual inhibition of cobalamin and siderophore uptake systems suggests their competition for TonB function. *J. Bacteiol.* **177**: 4829-4835.

Kadner, R.J. (1990) Vitamin B12 transport in *Escherichia coli*: energy coupling between membranes. *Mol. Microbiol.* 4: 2027-2033.

Kasahara, T., and Kasahara, M. (1998) Tryptophan 388 in putative transmembrane segment 10 of the rat glucose transporter Glut1 is essential for glucose transport. *J. Biol. Chem.* **273**: 29113-29117.

Killmann, H., Benz, R. and Braun, V. (1993) Conversion of the FhuA transport protein into a diffusion channel through the outer membrane of *Escherichia coli*. *EMBO J.* 12: 3007-3016.

Killmann, H., Benz, R. and Braun, V. (1996) Properties of the FhuA channel in the *Escherichia coli* outer membrane after deletion of FhuA portions within and outside the predicted gating loop. *J. Bacteiol.* 178: 6913-6920.

Klebba, P.E., and Newton, S.M.C. (1998) Mechanisms of solute transport through outer membrane porins: nurning down the house. *Curr. Opin. Microbiol.* 1: 238-248.

Klebba, P.E., Rutz, J.M., Liu, J. and Murphy, C.K. (1993) Mechanisms of TonB-catalyzed iron transport through the enteric bacterial cell envelope. *J. Bioenerg. and Biomem.* 6: 603-611.

Klebba, P.E., McIntosh, M.A., and Neilands, J.B. (1982) Kinetics of biosynthesis of iron-regulated membrane proteins in *Escherichia coli*. *J. Bacteriol.* 149: 880-888.

Klug, C.S., Su, W., Liu, J., Klebba, P.E., and Feix, J.B. (1995) Denaturant unfolding of the ferric enterobactin receptor and ligand-induced stabilization studied by site-directed spin labeling. *Biochemistry* 34: 14230-14236.

Klug, C.S., Su, W., and Feix, J.B. (1997) Mapping of the residues involved in a proposed β-strand located in the ferric enterobactin receptor FepA using site-directed spin-labeling. *Biochemistry* 36: 13027-13033.

Klug, C.S., Eaton, S.S., Eaton, G.R., and Feix, J.B. (1998) Ligand-induced conformational change in the ferric enterobactin receptor FepA as studied by site-directed spin labeling and time-domain ESR. *Biochemistry* **37**: 9016-9023.

Koebnik, R., and Braun, V. (1993) Insertion derivatives containing segments of up to 16 amino acids identify surface- and periplasm-exposed regions of the FhuA outer membrane receptor of Escherichia coli K-12. *J. Bacteriol.* **175**: 826-839.

Kunkel, T.A. (1985) Rapid and efficient site-specific mutagenesis without phenotypic selection. *Proc. Natl. Acad. Sci. USA.* **82**: 488-492.

Lakowicz, J.R. (1983) *Principles of Fluorescence Spectroscopy.*

Lambert, O., Moeck, G. S., Levy, D., Plancon, L., Letellier, L., and Rigaud, J. L. (1999) An 8-Å projected structure of FhuA, a "ligand-gated" channel of the *Escherichia coli* outer membrane. *J. Struct. Biol.* **126**: 145-155.

Lathrop, J.T., Wei, B.Y., Touchie, G.A., and Kadner, R.J. (1995) Sequences of *Escherichia coli* BtuB protein essential for insertion and function in the outer membrane. *J. Bacteiol.* **177**: 6810-6819.

Lazdunski, C.J. (1995) Colicin import and pore formation: a system for studying protein transport across membranes? *Mol. Microbiol.* **16**: 1059-1066.

Leatherbarrow, R.J. (1998) Grafit Version 4.06, Erathicus Software Ltd., Staines, UK.

Letain, T.E. and Postle, K. (1997) TonB protein appears to transduce energy by shuttling between the cytoplasmic membrane and the outer membrane in *Escherichia coli. Mol. Microbiol.* **24**: 271-83.

Levvit, M. and Perutz, M.F. (1988) Aromatic rings act as hydrogen bond acceptors. *J. Mol. Biol.* **201**: 751-754.

Ling, R., and Luckey, M. (1994) Use of single-cysteine mutants to probe the location of the disulfide bond in LamB protein from *Escherichia coli. Biochem. Biophys. Res. Commun.* **201**: 242-247.

Liu, J., Rutz, J.M., Feix, J.B. and Klebba, P.E. (1993) Permeability properties of a large gated channel within the ferric enterobactin receptor, FepA. *Proc. Natl. Acad. Sci. USA.* **90**: 10653-10657.

Liu, J., Rutz, J.M., Klebba, P.E. and Feix, J.B. (1994) A site-directed spin-labeling study of ligand-induced conformational change in the ferric enterobactin receptor, FepA. *Biochemistry* **33**: 13274-13283.

Locher, K.P., and Rosenbusch, J.P. (1997) Oligomeric states and siderophore binding of the ligand-gated FhuA protein that forms channels across *Escherichia coli* outer membrnaes. *Eur. J. Biochem.* **247**: 770-775.

Locher, K.P., Rees, B., Koebnik, R., Mitschler, A., Moulinier, L., Rosenbusch, J.P., and Moras, D. (1998) Transmembrane signaling across the ligand-gated FhuA receptor: crystal structures of free and ferrichrome-bound states reveal allosteric changes. *Cell* **95**: 771-778.

Lowry, O.H., Rosebrough, N.J., Farr, A.L., and Randall, R.J. (1951) Protein measurement with the Folin phenol reagent. *J. Biol. Chem.* **193**: 265-275.

Luckey, M., Ling, R., Dose, A., and Malloy, B. (1991) Role of a disulfide bond in the thermal stability of the LamB protein trimer in *Escherichia coli* outer membrane. *J. Biol. Chem.* **266**: 1866-1871.

Lundrigan, M.D. and Kadner, R.J. (1986) Nucleotide sequence of the gene for the ferrienterochelin receptor FepA in *Escherichia coli*. Homology among outer membrane receptors that interact with TonB. *J. Biol. Chem.* **261**: 10797-10801.

Mannuzzu, L.M., Moronne, M.M., and Isacoff, E.Y. (1996) Direct physical measurement of conformational rearrangement under potassium channel gating. *Science* **271**: 213-216.

McGaughey, G.B., Gagné, M., and Rappé, A.K. (1998) π-stacking interactions: alive and well in proteins. *J. Biol. Chem.* **273**: 15458-15463.

McIntosh, M.A., Chenault, S.S., and Earhart, C.F. (1979) Genetic and physiological studies on the relationship between colicin B and ferrienterochilin uptake in *Escherichia coli*. *J. Bacteriol.* **137**: 653-657.

Messing, J. (1983) New M13 vectors for cloning. *Methods Enzymol.* **101**: 20-78.

Miller, J.H. (1972) Experiments in molecular genetics. Cold Spring Harbor Laboratory, Cold Spring Harbor, NY.

Mishell, B.B., and Shiigi, S.M. (eds) (1980) Selected Methods in Cellular Immunology, W. H. Freeman, San Francisco.

Mitchell, J.B.O., Nandi, C.L., McDonald, I.K., Thornton, J.M. and Price, S.L. (1994) Amino/aromatic interactions in proteins: is the evidence stacked against hydrogen bonding? *J. Mol. Biol.*, **239**: 315-331.

Moeck, G.S., Coulton, J.W., and Postle, K. (1997) Cell envelop signaling in *Escherichia coli*. Ligand binding to the ferrichrome-iron receptor FhuA promotes interaction with the energy-transducing protein TonB. *J. Biol. Chem.* **272**: 28391-28397.

Murphy, C.K., Kalve, V.I. and Klebba, P.E. (1990) Surface topology of the Escherichia coli K-12 ferric enterobactin receptor. *J. Bacteriol.*, **172**: 2736-2746.

Neidhardt, F.C., Bloch, P.L. and Smith, D.F. (1974) Culture medium for enterobacteria. *J. Bacteriol.*, **119**: 736-747.

Neilands, J.B. (1973) Microbial iron transport compounds (siderochromes), in Inorganic Biochemistry Vol.1 edited by G.L. Eichhorn, Elsevier, New York.

Neilands, J.B. (1981) Microbial iron compounds. *Ann. Rev. Biochem.* **50**: 715-731.

Neilands, J.B., Erickson, T.J., and Rastetter, W.H. (1981) Stereospecificity of the ferric enterobactin receptor of *Escherichia coli* K-12. *J. Biol. Chem.* **256**: 3831-3832.

Neilands, J.B. (1991) A brief history of iron metabolism. *Biol. Metals* **4**: 1-6.

Neilands, J.B. (1995) Siderphores: structure and function of microbial iron transport compounds. *J. Biol. Chem.* **270**: 26723-26726.

Newton, S.M., Allen, J.S., Cao, Z., Qi, Z., Jiang, X., Sprencel, C., Igo, J.D., Foster, S.B., Payne, M.A. and Klebba, P.E. (1997) Double mutagenesis of a positive charge cluster in the ligand-binding site of the ferric enterobactin receptor, FepA. *Proc. Natl. Acad. Sci. U S A* **94**: 4560-4565.

Newton, S.M., Igo, J.D., Scott, D.C., and Klebba, P.E. (1999) Effect of loop deletions on the binding and transport of ferric enterobactin by FepA. *Mol. Microbiol.* **32**: 1153-1165.

Nikaido, H. (1994) Porins and specific diffusion channels in bacterial outer membranes. *J. Biol. Chem.* **269**: 3905-3908.

Nikaido, H. (1992) Porins and specific channels of bacterial outer membranes. *Mol. Microbiol.* **6**: 435-442.

Nikaido, H. and Saier, M.H.J. (1992) Transport proteins in bacteria: common schemes in their design. *Science* **258**: 936-942.

O'Brien, I.G., and Gibson, F. (1970) *Biochim. Biophys. Acta* **215**: 393

Oh, K.J., Zhan, H., Cui, C., Altenbach, C., Hubbell, W.L., and Collier, R.J. (1999) Conformation of the diphtheria toxin T domain in membranes: a site-directed spin-labeling study of the TH8 helix and TL5 loop. *Biochemistry* **38**: 10336-10343.

Pautsch, A. and Schulz, G.E. (1998) Structure of outer membrane protein A transmembrane domain. *Nat. Struct. Biol.* **5**: 1013-1017.

Parvari, R., Pecht, I., and Soreq, H. A. (1983) Microfluorometric assay for cholinesterases, suitable for multiple kinetic determinations of picomoles of released thiocholine. *Anal. Biochem.* **133**: 450-456.

Payne, M.A., Igo, J.D., Cao, Z., Foster, S.B., Newton, S.M., and Klebba, P.E. (1997) Biphasic binding kinetics between FepA and its ligands. *J. Biol. Chem.* **272**: 21950-21955.

Pebay-Peyroula, E., Rummel, G., Rosenbursch, J.P., and Landau, E.M. (1997) X-ray structure of bacteriorhodopsin at 2.5 angstroms from microcrystals grown in lipidic cubic phases. *Science* **277**: 1676-1681.

Pollack, J.R., and Neilands, J.B. (1970) *Biochem. Biophys. Res. Commun.* **38**: 989.

Postle, K. (1999) Active transport by customized β-barrels. *Nature Struc. Biol.* **6:** 3-6.

Pugsley, A.P. and Reeves, P. (1976) Characterization of group B colicin-resistant mutants of *Escherichia coli* K-12: colicin resistance and the role of enterochelin. *J. Bacteriol.* **127**: 218-228.

Pugsley, A.P. and Reeves, P. (1977a) Uptake of ferrienterochelin by *Escherichia coli*: energy dependent stage of uptake. *J. Bacteriol.* **130**: 26-36.

Pugsley, A.P., and Reeves, P. (1977b) Comparison of colicins B-K260 and D-CA23: purification and characterization of the colicins and examination of colicin immunity in the producing strains. *Antimicrob. Agents Chemother.* **11**: 345-353.

Randall-Hazelbauer, L., and Schwartz, M. (1973) Isolation of bacteriophage lamda receptor from *Escherichia coli. J. Bacteriol.* **116**: 1436-1446.

Rastetter, W.H., Erickson, T.J., and Venuti, M.C. (1981) Synthesis of iron chelators. Enterobactin, enantioenterobactin, and a chiral analogue. *J. Org. Chem.* **46**, 3579-3590.

Raymond, K.N., and Carrano, C.J. (1979) Coordination chemistry and microbial iron transport. *Acc. Chem. Res.* **12**, 183-190.

Rutz, J.M., Abdullah, T., Singh, S.P., Kalve, V.I. and Klebba, P.E. (1991) Evolution of the ferric enterobactin receptor in gram-negative bacteria. *J. Bacteriol.* **173:** 5964-5974.

Rutz, J.M., Liu, J., Lyons, J.A., Goranson, J., Armstrong, S.K., McIntosh, M.A., Feix, J.B. and Klebba, P.E. (1992) Formation of a gated channel by a ligand-specific transport protein in the bacterial outer membrane. *Science* **258**: 471-475.

Saint, N., Lou, K.L., Widmer, C., Luckey, M., Schirmer, T., and Rosenbusch, J.P. (1996) Structural and functional characterization of OmpF porin mutants selected for larger pore size. II. Functional characterization. *J. Biol. Chem.* 271: 20676-20680.

Sakai, H., and Tsukihara, T. (1998) Structures of membrane proteins determined at atomic resolution. *J. Biochem. (Tokyo)* **124**: 1051-1059.

Sawai, T., Matsuba, K., and Yamagishi, S. (1977) A method for measuring the outer membrane-permeability of beta-lactam antibiotics in gram-negative bacteria. *J Antibiot. (Tokyo)* **30**: 1134-1136.

Samanta, U., Pal, D. , and Chakrabarti. (1999) Packing of aromatic rings against tryptophan residues in proteins. *Acta Cryst.* D**55**: 1421-1427.

Sansom, M.S.P. (1999) Membrane proteins: a tale of barrels and corks. *Current Biology* **9:** R254-R257.

Schiffer, M., Chang, C.H., and Stevens, F.J. (1992) The functions of tryptophan residues in membrane proteins. *Protein Eng.* **5**: 213-214.

Schirmer, T., and Cowan, S.W. (1993) Prediction of membrane-spanning beta-strands and its application to maltoporin. *Protein Sci.* **2**: 1361-1363.

Schirmer, T., Keller, T.A., Wang, Y.-F., and Rosenbusch, J.P. (1995) Structural basis for sugar translocation through maltoporin channels at 3.1A resolution. *Science* **267**: 512-514.

Schramm, E., Mende, J., Braun, V., and Kamp, R.M. (1987) Nucleotide sequence of the colicin B activity gene cba: consensus pentapeptide among TonB-dependent colicins and receptors. *J. Bacteriol.* **169**: 3350-3357.

Schulein, K., Schmid, K., and Benzl, R. (1991) The sugar-specific outer membrane channel ScrY contains functional characteristics of general diffusion pores and substrate-specific porins. *Mol. Microbiol.* **5**: 2233-2241.

Schulz, G.E. (1992) Structure-function relationships in the membrane channel porin as based on a 1.8 Å resolution crystal structure. In *Membrane Proteins: Structures, Interactions and Models.* Edited by Pullman, A. *et al.* Kluwer Academic Publishers, Amsterdam.

Schulz, G.E. (1994) Structure-function relationships in porins as derived from a 1.8 Å resolution crystal structure. In *Bacterail Cell Wall.* Edited by J.-M Ghuysen and R. Hakenbeck. Elsevier Science B.V.

Schulz, G.E. (1996) Porins: general to specific, native to engineered passive pores. *Curr. Opin. Struct. Biol.* 6: 485-490.

Scrutton, N.S., and Raine, A.R. (1996) Cation-pi bonding and amino-aromatic interactions in the biomolecular recognition of substituted ammonium ligands. *Biochem. J.* **319** (Pt 1): 1-8.

Shilton, B.H., Flocco, M.M., Nilsson, M., and Mowbray, S.L. (1996) Conformational changes of three periplasmic receptors for bacterial chemotaxis and transport: the maltose-, glucose/galactose- and ribose-binding proteins. *J. Mol. Biol.* **264**: 350-363.

Sippel, T.O. (1981a) Microfluorometric analysis of protein thiol groups with a coumarinylphenylmaleimide. *J. Histochem. Cytochem.* 29: 1377-1381.

Sippel, T. O. (1981b) New fluorochromes for thiols: maleimide and iodoacetamide derivatives of a 3-phenylcoumarin fluorophore. *J. Histochem. Cytochem.* **29**: 314-316.

Smith, B.S., Kobe, B., Kurumbail, R., Buchanan, S.K., Venkatramani, L., van der Helm, D., and Deisenhofer, J. (1998) Crystallization and preliminary X-ray analysis of ferric enterobactin receptor FepA, an integral membrane protein from *Escherichia coli. Acta Crystallogr.* **54**: 697-699.

Steinhoff, H.J., Mollaaghababa, R., Altenbach, C., Hideg, K., Krebs, M., Khorana, H.G., and Hubbell, W.L. (1994) Time-resolved detection of structural changes during the photocycle of spin-labeled bacteriorhodopsin. *Science* **266**: 105-107.

Stroud, R.M., Reiling, K., Wiener, M., and Freymann, D. (1998) Ion-channel-forming colicins. *Curr. Opin. Struct. Biol.* **8:** 525-533.

Sugawara, E., and Nikaido, H. (1992) Pore-forming activity of OmpA protein of *Escherichia coli. J. Biol. Chem.* **267**: 2507-2511.

Sugawara E, Nikaido H (1994) OmpA protein of Escherichia coli outer membrane occurs in open and closed channel forms. *J. Biol. Chem.* **269**: 17981-17987.

Sun, D.P., Sauer, U., Nicholson, H., and Matthews, B.W. (1991) Contributions of engineered surface salt bridges to the stability of T4 lysozyme determined by directed mutagenesis. *Biochemistry* **30**: 7142-7153.

Szmelcman, S., and Hofnung, M. (1975) Maltose transport in *Escherichia coli* K-12: involvement of the bacteriophage lambda receptor. *J. Bacteriol.* **124**: 112-118.

Thulasiraman, P., Newton, S.M.C., Xu, J., Raymond, K.N., Mai, C., Hall, A., Mantague, M.A., and Klebba, P.E. (1998) Selectivity of ferric enterobactin binding and cooperativity of transport in gram-negative bacteria. *J. Bacteriol.* **180**: 6689-6696.

Timmis, K. (1972) Purification and characterization of colicin D. *J. Bacteriol.* **109**: 12-20.

Tuckman, M., and Osburne, M.S. (1992) *In vivo* inhibition of TonB-dependent processesby a TonB box consensus pentapeptide. *J. Bacteriol.* **174**: 320-323.

Vogel, H., and Jahnig, F. (1986) Models for the structure of outer-membrane proteins of *Escherichia coli* derived from Raman spectroscopy and prediction models. *J. Mol. Biol.* **190**: 191-199.

Wang, C. C. and Newton, A. (1969) Iron transport in *Escherichia coli*: roles of energy-dependent uptake and 2,3-dihydroxybenzoylserine. *J. Bacteriol.* **98**: 1142-1150.

Wang, C., and Smith, R.L. (1975) Lowry determination of protein in the presence of Triton X-100. *Anal. Biochem.* **63**: 414-417.

Wang, Y.-F., Dutzler, R., Rizkallah, P.J., Rosenbusch, J.P., and Schirmer, T. (1997) Channel specificity: structural basis for sugar discrimination and diffusion flux rates in maltoporin. *J. Mol. Biol.* **272**: 56-63.

Wayne, R., and Neilands, J.B. (1975) Evidence for common binding sites for ferrichrome compounds and bacteriophage phi 80 in the cell envelope of Escherichia coli. *J. Bacteriol.* **121**: 497-503.

Wayne, R.R., Frick, K. and Neilands, J.B. (1976) Siderophore protection against colicins M, B, V, and Ia in *Escherichia coli. J. Bacteriol.* **126**: 7-12.

Weiss, M.S., Abele, U., Weckesser, J., Welte, W., Schiltz, E., and Schulz, G.E. (1991a) Molecular architecture and electrostatic properties of a bacterial porin. *Science* **254**: 1627-1630.

Weiss, M.S., Kreusch, A., Schiltz, E., Nestel, U., Welte, W., Weckesser, J., and Schulz, G.E. (1991b) The structure of porin from *Rhodobacter capsulatus* at 1.8 Å resolution. *FEBS Lett.* **280**: 379-382.

Weiss, M.S., and Schulz, G.E. (1992) Structure of porin refined at 1.8 Å resolution. *J. Mol. Biol.* 227: 493-509.

White, J.C., Girolamo, P.M., Fu, M.L., Preston, Y.A., and Bradbeer, C. (1973) Transport of vitamin B12 in *Escherichia coli. J. Biol. Chem.* **218**: 3978-3986.

Wilmot, C.M., and Thornton, J.M. (1988) Analysis and prediction of the different types of β-turn in proteins. *J. Mol. Biol.* **203**: 221-232.

Wiener, M., Freymann, D., Ghosh, P., and Stroud, R.M. (1997) Crystal structure of colicin Ia. *Nature* **385**: 461-464 (see comment in *Nature* (1997) **385**: 390-391).

Wu, J., Hardy, D., and Kaback, H.R. (1999) Site-directed chemical cross-linking demonstrates that helix IV is close to helices VII and XI in the lactose permease. *Biochemistry* **38**: 1715-1720.

Wu, J., Frillingos, S., and Kaback, H.R. (1995) Dynamics of lactose permease of *Escherichia coli* determined by site-directed chemical labeling and fluorescence spectroscopy. *Biochemistry* 34: 8257-8263.

Xia, D., Yu, C.A., Kim, H., Xia, J.Z., Kachurin, A.M., Zhang, L., Yu, L., and Deisenhofer, J. (1997) Crystal structure of the cytochrome bc1 complex from bovine heart mitochondria. *Science* **277**: 60-66.

Zimmermann, W., and Rosselet, A. (1977) Function of the outer membrane of Escherichia coli as a permeability barrier to beta-lactam antibiotics. *Antimicrob. Agents Chemother.* **12**: 368-372.